

INITIATION AND GROWTH OF MICROCRACKS IN HIGH STRENGTH STEEL BUTT WELDS

by

EDWARD OLSEN

B S , Mechanical Engineering
University of South Carolina, 1985

Submitted to the Department of Ocean Engineering
in Partial Fulfillment of the Requirements for the Degrees of

Naval Engineer

and

Master of Science in Mechanical Engineering

at the
Massachusetts Institute of Technology
May 1993

© Edward Olsen, 1993. All rights reserved.

The author hereby grants to MIT permission to reproduce and to
distribute publicly copies of this thesis document in whole or in part.

Professor A Douglas Carmichael, Department of Ocean Engineering
Department Graduate Committee

T260800

INITIATION AND GROWTH OF MICROCRACKS IN HIGH STRENGTH STEEL BUTT WELDS

by

EDWARD OLSEN

Submitted to the Department of Ocean Engineering
on 7 May 1993 in partial fulfillment of the
requirements for the Naval Engineer Degree and
Master of Science in Mechanical Engineering.

ABSTRACT

Early tests such as the explosion bulge test created a preference for overmatched welds (welds which are stronger than the base metal) which eventually became codified for many structural applications. While an overmatched system offers advantages such as the shedding of strain to the base plate, it requires the use of expensive fabrication procedures to avoid cracking. Undermatched welding of some high strength steels may offer reductions in welding costs with little sacrifice in weld performance or low cycle fatigue integrity.

An experimental study was carried out to observe microcrack initiation and growth of overmatched and undermatched butt welded high strength steel samples using globally elastic low cycle fatigue testing. First, 1 inch thick HY-80 and HY-100 base plates were multipass, spray gas metal arc welded (GMAW) with overmatching and undermatching filler metal using a semiautomatic welding machine. Second, 1/4 inch thick MIL-A-46100 high hardness armor plates (HHA) were manually, two pass spray GMAW welded with two grades of undermatching consumables. Weld reinforcements were removed from all HY specimens and six HHA specimens. All specimens had a crack initiator slit machined in the test section. The specimens were fatigue tested by transverse tensile loading with a 12 to 13 Hz tension-tension profile. The loading range was from 10% to 85% of the tensile strength of the HY steel base plate and HHA weld metal respectively. Crack initiation and propagation was observed in situ using a confocal scanning laser microscope.

In the HY 80 tests, the undermatched specimens failed between 14,500 and 16,500 cycles, overmatched specimens failed between 21,000 and 26,500 cycles, and the base plate failed at 20,000 cycles. In the HY 100 tests, undermatched specimens failed between 16,500 and 21,000 cycles, overmatched specimens failed between 17,800 and 21,600 cycles, and the base plate failed at 32,000 cycles. All "as welded" HHA specimens failed between 8,000 and 17,500 cycles. HHA ground 100S-1 welds failed at 10,000 cycles and the 70S-6 welds failed at 17,500 cycles

Thesis Supervisor: Professor Koichi Masubuchi
Title: Kawasaki Professor of Engineering

Acknowledgments

I would like to extend special thanks and gratitude to the people who have helped me in this endeavor.

Professor Koichi Masubuchi for his expertise, guidance and support.

Professor Frank McClintock for his expertise in fracture mechanics and helping me to understand it better.

Captain Osie Combs, USN, for providing the HY plate specimens and the requisite testing.

Tom Melvin of the Army Research Laboratory for providing the HHA material specimens.

Warren Mayott and Bob Pierce of Electric Boat for preparing the HY specimen plates, their NDT, and documentation.

Gene Franke of David Taylor Research Center, Annapolis for allowing me to study their research material and work with the materials group during "Professional Employment".

The Navy for making this MIT graduate program possible and my colleague 13A's for keeping it fun.

My brothers Andy and Greg who provided me with ongoing inspiration and friendly phone calls.

Dr. Sally Boyd who through her love and patience taught me the value of friendship and helped me grow immeasurably.

Finally, to my wife, Kathy R, and daughter, Brooke, thanks for being there throughout these past three years. Your love and devotion have given me strength throughout these trying times.

Table of Contents

Initiation And Growth Of Microcracks In High Strength Steel Butt Welds

Title Page	1
Abstract	2
Acknowledgments	3
Table of Contents	4
List of Tables	6
List of Figures	7
List of Thermal Image Photographs	8
 Chapter 1 Introduction	 9
 Chapter 2 Background	 11
Hot Cracking	12
Cold Cracking	16
Carbon Equivalent	16
Residual Stresses	17
Hydrogen Embrittlement Cracking	19
Stress Corrosion Cracking	21
Stress Concentrations	21
Fatigue Fracture	22
Overmatching and Undermatching of Welds	27
Weld Defects	29
Fracture Mechanics	32
Weld Strength Matching Effects on J_I and ϕ	33
Single Edge Notch Specimens	34
Wide Plate Specimens	37
The Energy Concept of Cracking	42
Submarine High Strength Steel Fatigue search	46
Chemical Compositional Effects of Titanium	47
Nonmetallic Inclusion Effects on Fatigue Life	48
Comparison of Over and Undermatched Welding	48
Crack Initiation of Thick Specimens	50
Fatigue Life versus Yield Strength	51
Temperature Effects on Low Cycle Fatigue	52
Reheating Effects on Multipass Welds	53
Toughness and Tensile Properties in HSLA	53
Weldment Cooling Effects on Strength and Toughness	53
Undermatched Double V Butt Welds	54

Chapter 3	Experimental	57
	Specimen Acquisition	57
	Base Plates	57
	HHA Base Plates	58
	NDT of HY and HHA	59
	Specimen Surface Hardness Testing	59
	Specimen Sizing for Testing	59
	Description of Equipment	61
	Experimental Procedure	63
	Observation with CSLM	64
Chapter 4	Results and Discussion	66
	Crack Growth	66
	Crack Initiation From the EDM Slit	66
	Crack Growth Versus Cycles	68
Chapter 5	Conclusion and Recommendation	69
	Experiment Comments	69
	Conclusions	69
	Recommendations for Future Work in This Field	70
Tables		71
Figures		98
References		131
Appendices		
	A. The Confocal Scanning Laser Microscope (CSLM)	133
	B. HY Steel Welding Data Sheets	138
	C. High Hardness Armor (HHA) Performance Data Sheets	154

List of Tables

<u>No.</u>	<u>Title</u>	<u>Page</u>
1	Effects of Chemical Composition on Properties of Steel	71
2	Mismatch Values for HY Weld Samples	72
3	Mismatch Values for HY Weld Samples	72
4	Selected Welding Parameters for HY Specimen	73
5	Base Plate Material Nominal Chemical Analysis	74
6	HY Base Plate Material Properties	74
7	HY Specimen Sizing Data	75
8	HHA Specimen Sizing Data	75
9	HY 80 O/M-1 Specimen Crack Data	76
10	HY 80 O/M-2 Specimen Crack Data	77
11	HY 80 O/M-3 Specimen Crack Data	78
12	HY 80 O/M-4 Specimen Crack Data	79
13	HY 80 U/M-1 Specimen Crack Data	80
14	HY 80 U/M-2 Specimen Crack Data	81
15	HY 80 U/M-3 Specimen Crack Data	82
16	HY 80 U/M-4 Specimen Crack Data	83
17	HY 80 Virgin Base Plate Specimen Crack Data	84
18	HY 100 O/M-1 Specimen Crack Data	85
19	HY 100 O/M-2 Specimen Crack Data	86
20	HY 100 O/M-3 Specimen Crack Data	87
21	HY 100 O/M-4 Specimen Crack Data	88
22	HY 100 U/M-1 Specimen Crack Data	89
23	HY 100 U/M-2 Specimen Crack Data	90
24	HY 100 U/M-3 Specimen Crack Data	91
25	HY 100 U/M-4 Specimen Crack Data	92
26	HY 100 Virgin Base Plate Specimen Crack Data	93
27	HHA 100 S-1 Specimen Crack Data	94
28	HHA 100 S-2 Specimen Crack Data	94
29	HHA 100 S-4 Specimen Crack Data	95
30	HHA 70 S-1 Specimen Crack Data	95
31	HHA 70 S-2 Specimen Crack Data	95
32	HHA 70 S-4 Specimen Crack Data	96
33	HHA 70 S-5 Specimen Crack Data	96
34	Selected CSLM Operating Parameters and Data	97
35	CSLM Image Display Information	97

List of Figures

<u>No.</u>	<u>Title</u>	<u>Page</u>
1	Residual Stress Distribution In a Butt Weld	98
2	Endurance Limit Versus Ultimate Tensile Strength	99
3	Common Weldment Heat Affected Zone (HAZ) Characteristics	100
4	HY-100 Overmatched Specimen Weld Bead Arrangement	101
5	HY-100 Undermatched Specimen Weld Bead Arrangement	101
6	HY-80 Overmatched Specimen Weld Bead Arrangement	101
7	HY-80 Undermatched Specimen Weld Bead Arrangement	101
8	HY-80 Overmatched Surface Hardness Profile	102
9	HY-80 Undermatched Surface Hardness Profile	102
10	HY-100 Overmatched Surface Hardness Profile	103
11	HY-100 Undermatched Surface Hardness Profile	103
12	HHA 100 S-1 Surface Hardness Profile	104
13	HHA 70 S-6 Surface Hardness Profile	104
14	HY Specimen Dimensions	104
15	HHA Specimen Dimensions	105
16	HY 80 O/M-2 Crack Growth	106
17	HY 80 O/M-3 Crack Growth	107
18	HY 80 O/M-4 Crack Growth	107
19	HY 80 Virgin Base Plate Crack Growth	108
20	HY 80 U/M-1 Crack Growth	108
21	HY 80 U/M-2 Crack Growth	109
22	HY 80 U/M-3 Crack Growth	109
23	HY 80 U/M-4 Crack Growth	110
24	HY 100 O/M-1 Crack Growth	110
25	HY 100 O/M-2 Crack Growth	111
26	HY 100 O/M-3 Crack Growth	111
27	HY 100 O/M-4 Crack Growth	112
28	HY 100 U/M-1 Crack Growth	112
29	HY 100 U/M-2 Crack Growth	113
30	HY 100 U/M-3 Crack Growth	113
31	HY 100 U/M-4 Crack Growth	114
32	HY 100 Virgin Base Plate Crack Growth	115
33	HHA 100 S-1 Crack Growth	116
34	HHA 100 S-2 Crack Growth	116
35	HHA 100 S-4 Crack Growth	117
36	HHA 70 S-2 Crack Growth	118
37	HHA 70 S-4 Crack Growth	118
38	HHA 70 S-5 Crack Growth	119
39	CSLM Optics Arrangement	120
40	HHA 70 and HHA 100 Stress - Strain Diagram	121

List of Thermal Image Photographs

<u>No.</u>	<u>Title</u>	<u>Page</u>
41	Image of 100 O/M-1 Fusion Zone, 100X Objective	122
42	Image of 80 O/M-2 UR Crack at 2,500 Cycles, 40X Objective	122
43	Image of 100 U/M-2 UL Crack at 2,500 Cycles, 40X Objective	123
44	Image of 80 U/M-2 LR Crack at 2,500 Cycles, 40X Objective	123
45	Image of 80 Virgin Base Plate LR, 2,500 Cycles, 100X Objective	124
46	Image of 100 O/M-1 UL Crack at 3,000 Cycles, 20X Objective	124
47	Image of 80 Virgin Base Plate LL, 7,500 Cycles, 20X Objective	125
48	Image of 100 O/M-2 UR Crack at 8,000 Cycles, 100X Objective	125
49	Image of 100 O/M-2 UR Crack at 9,730 Cycles, 10X Objective	126
50	Image of 80 U/M-4 LL Crack at 11,130 Cycles, 10X Objective	126
51	Image of 100 O/M-2 Asperity Profile, 11,730 Cycles, 100X Objective	127
52	Image of 100 O/M-2 Asperity Profile, 11,730 Cycles, 100X Objective	127
53	Image of 100 O/M-3 UL at 17,500 Cycles, 10X Objective	128
54	Image of 100 O/M-3 LL Profile at 10,000 Cycles, 40X Objective	128
55	Image of 80 Virgin LR Plastic Zone at 18,500 Cycles, 10X Objective	129
56	Image of HHA 100 S-4 UL Crack at 2,500 Cycles, 40X Objective	129
57	Image of HHA 100 S-4 UL Profile at 10,000 Cycles, 40X Objective	130
58	Image of HHA 70 S-4 LL Crack Fork, 12,500 Cycles, 40X Objective	130

Chapter 1

Introduction

Many modern structural applications require high strength steels to reduce size and weight. High strength HY steels have been used in the construction of Navy warships and submarines since World War II. These steels are used as both structural hull material and ballistic armor. Submarines have especially led the field in the development and application of high strength steel. Research in the area of relative weld strength in submarine material design during the 1950's by Pellini and Hartblower formed the basis for some of today's structural codes.

An important code that has developed is requiring the weld metal to be relatively stronger than the plate material. A weldment is by its very nature, different from its base metal. Most welds fall into the category of overmatched in terms of weld strength relative to the base plate strength. Unfortunately, with the overmatching comes a reduction in ductility and toughness. Some welds are designed to be undermatched or evenmatched but this is fairly rare. Relative weld metal strength has profound effects on structural behavior, performance under fatigue conditions, and welding costs.

Perhaps the most profound penalty associated with high strength steels is the well documented and researched sensitivity to failure mechanisms that are influenced by the weldment's relative strength. In particular, high strength steels are subject to cracking that is aggravated by hydrogen contamination, inclusions or flaws, environment, and residual

stresses. Crack initiation and propagation properties are also a function of loading and joint geometry. It is important for a designer to understand the effects of relative weld strength on failure mechanisms peculiar to high strength steels.

A particularly dangerous failure endemic to high strength steel is brittle fracture. The failure is usually sudden and catastrophic. This failure is difficult to predict and is not well understood. It is thought that fatigue related failure is closely associated with brittle fracture because the final phase of fatigue failure is usually brittle in nature. The fatigue mechanism reduces the effective stress bearing area until the stress concentration reaches a critical loading and failure is imminent. Crack initiation and propagation are the key to understanding this type of failure.

Crack initiation is sometimes very difficult to identify by normal methods of nondestructive testing (NDT). The cracks are very small and can easily escape even sophisticated radiography techniques. Subsurface cracks require sophisticated X-ray or neutron diffraction techniques which are cost prohibitive and small scale in nature. Neutron diffraction is essentially destructive because the material becomes radioactively activated and unusable. The situation becomes even more difficult when dealing with large scale structures and complex weldments. Efficient NDT may simply be impossible. A simple way to experimentally observe cracks is to use a microscope. The Confocal Scanning Laser Microscope is an ideal tool for high resolution, in situ nondestructive observation of weld specimens.

Chapter 2

Theory and Background

High strength steels show sensitivity to loading with regards to differentiation between crack initiation and growth. In ship building where shock loading such as hull slamming must be taken into account, both crack initiation and propagation properties are important [Masubuchi]. Crack propagation may be inhibited at the production level by using fine grain steels and production quality control to ensure fracture toughness. In-service crack propagation is minimized by designing for loading within acceptable stress levels.

Fracture toughness is important to avoid brittle fracture of welded structures. This is especially true of high strength quenched and tempered steels such as HY-80 and HY-100. These steels have high yield strength and excellent notch toughness that is difficult to match in the weld metal. Fracture initiation may be inhibited by proper material selection, fabrication quality control, and regular inspections.

Fractures are most likely to initiate from a welding defect. Induced thermal stresses during cool down can create a great deal of localized strain. Stress relief occurs when a crack initiates and grows to relieve additional stresses. Local defects such as inclusions also create localized high stresses which can develop into crack sites.

In the most general sense weld metal cracking may be divided into hot cracking and cold cracking. The following sections discuss various types of common cracking experienced by high strength steels

Hot Cracking

Some of the following information was extracted from Iwancowicz, 1992. Hot cracking is intergranular and occurs at or near bulk solidus temperature, approximately 1400° C to 1500° C for steel. The majority of hot cracking is referred to as weld metal solidification cracking and occurs at the initial stages of cooling when the thermal shrinkage is greatest, about 2%-6%. Strains across the liquidus weld metal and fusion zone cause rupturing of the dendritic interfaces with subsequent crack nucleation. Hot cracks have also been observed in the HAZ adjacent to the fusion zone. The HAZ is particularly vulnerable to cracking because of the propensity for microcrack formation along the fusion line. Figure 3 shows the characteristics of a common weldment HAZ.

Hot cracks may be characterized by their formation and location. Dixon classifies hot cracking as either segregation hot cracks or ductility-dip cracking.

Segregation cracking is caused by microsegregation of the liquidus phases into intergranular films having a low melting temperatures. This may occur in the weld metal and in the HAZ.

Ductility-dip hot cracking is the result of the reduction in ductility some alloys exhibit immediately below recrystallization temperature. Ductility-dip regions form near newly formed grain boundaries. This may occur in the weld metal and in the HAZ. The ductility-dip regions do not contain low melting temperature film boundaries and require higher strains to crack than segregation cracking.

Several hot cracking mechanism theories share a common crack initiation site theory. It is generally accepted that the molten weld pool solidifies in a method consistent with heat input and thermal gradient. A high thermal gradient process such as GTAW promotes cellular grain growth while a lower thermal gradient method such as SAW and GMAW promote dendritic growth.

The dendritic crystals growth initiates at the liquid-solid interface and continues into the molten weld pool along crystallographic directions. During cooling, dendritic growth perpendicular to the advancing solidification front become dominant by blocking the growth of other advancing dendrites. Weld metal solute is rejected from the solid-liquid interface. The final product is a non homogeneous grain boundary at the dendrite-liquid interface with a preferential crystallographic orientation. Thermal stresses near the solidification front may cause interdendritic cracking which subsequently serve as initiation sites for the growth of solidification cracks during cooling. These crack sites are initially filled in and "healed" by liquidus weld metal flow from adjacent pockets. This process continues until solidus, then permanent cracks are formed.

Borland proposed a hot cracking mechanism theory involving Dixon's Shrinkage-Brittleness theory and Pellini's Strain theory. Dixon's strain theory claims that cracking does not occur during the "mushy" stage of solidification because shrinkage strains are uniformly distributed across the weld pool. Instead, cracking is caused by low melting temperature liquid films formed between solidified grains.

Dixon's shrinkage-brittleness theory considers the interlocking of dendrites and subsequent rupture caused by ununiform contraction strains. Aforementioned "healing" occurs but eventually ceases. The rupturing and tearing of dendritic boundaries takes place in the "brittle temperature range" (BTR) which covers the temperature range from dendritic interlocking to just below solidus. Contraction strains become uniform when solidus is reached and thermal cracking is minimized and stopped. The relation of BTR to hot cracking is not fully understood but it appears to be directly related to a material's susceptibility to hot cracking.

In Borland's theory the solidification process is divided into four stages:

- ♦ Primary dendrite formation: full dispersion of the solid phases in the liquidus with both phases capable of relative movement.
- ♦ Dendrite interlocking: growth and interlocking of dendrites. Liquid and solid phases are continuous but only the liquid phase is capable of movement.
- ♦ Grain boundary development: initial stage of hot cracking. Dendritic growth continues with healing of fissures. Shrinking strains may create permanent crack initiation sites and possibly cracks. Referred to as critical solidification range (CSR)

by Borland. Material susceptibility is directly related to CSR. Advanced crystal growth and solid bridging across dendrites traps any remaining liquid in pockets.

- ♦ Completion of solidification: solidification of the remaining pockets of liquid.

Borland further states that a wide CSR is insufficient in itself to cause hot cracking. Dispersal of the liquid phase over all the grain surfaces is necessary to maximize shrinkage strains. Borland suggests that the liquid phase distribution is a function of the ratio of liquid-solid interfacial energy and the grain boundary energy. Hot cracking is reduced as the ratio increases above 0.58.

Prokhorov described weld metal cracking as a function of temperature and the strain rate within the solidifying metal. He defined a brittle temperature range (BTR) as the band in which cracking will occur. The BTR has an upper limit corresponding to the temperature where liquid cannot freely circulate around the grains. The lower limit is the temperature just below solidus where the grain boundary strength is sufficient to resist thermally induced shear stresses.

The weld metal is ductile during the BTR and can absorb limited strain. These strains cause localized shearing of ductile intergranular phases. Cracks form when the strain rate becomes great enough to cause grain boundary film rupture.

Hot cracking in the HAZ was investigated by Masubuchi. Because the welding process partially melts surrounding base metal, residual tensile stresses caused by cooling

create high strain across grain boundaries which may develop into small intergranular cracks. Grains are assumed to be surrounded by soft material that has a low critical shear stress. Consequently deformation by sliding occurs at fairly low levels of applied stress.

Experimentation in hot cracking mechanisms has led to suggestions of more advanced modeling techniques [Goodwin, 1990]. It was suggested that better understanding of hot cracking dynamics would result from the use of more accurate analytical models using fractal mathematics and super computers.

Cold Cracking

Cold cracking occurs below 205° C (400° F) and is localized in the HAZ and fusion zone and is transgranular in nature. It is also referred to as delayed cracking, hydrogen delayed cracking, hydrogen assisted cracking. Some authors disregard the hydrogen qualifier and refer to cold cracking in a generic sense as anything other than hot cracking. Cold cracking is further subdivided into short-time cracks and delayed cracks. Short time cracking occurs during the cooling process. Delayed cracking may take any amount of time to initiate after cooling. Most high strength steel structures require delayed NDT to identify these cracks. The U. S. Navy requires seven days delay for checking HY steels.

Carbon Equivalent

Carbon equivalency (CE) is the method by which a steel's constituents can be examined with respect to cold cracking. CE is based on the effects of carbon increasing a

material's susceptibility to cold cracking. Carbon content is a contributing factor in the formation of martensite in the weld metal. There are several versions of CE expressions developed for special purposes. The American Welding Society (AWS) defines the CE for high strength steel as:

$$CE = C + \frac{Mn}{6} + \frac{Ni}{20} + \frac{Cr}{10} + \frac{Cu}{40} - \frac{Mo}{50} - \frac{V}{10}.$$

AWS declares 40 as the upper limit for prevention of underbead cracks. Table 1 lists the relative contributions of some alloying elements and their importance compared to carbon.

Residual Stresses

Residual stresses are the result of welding thermal transients which induce incompatible strains and inelastic stresses. Incompatible strains are plastic strains due to solidification and solid phase transformation of the weld metal. Residual stresses may be reduced through thermal stress relief. Unfortunately, post weld heat treatments are prohibited on high strength quenched and tempered steels. Masubuchi has developed a rational analytical approach for determining residual weldment stresses in practical structures through simulation. Residual stresses are characterized as either:

- ♦ Welding stresses produced in the welding of unrestrained members.
- ♦ Reaction stresses caused by external restraint. Figure 1 shows typical welding stresses associated with a butt weld. σ_x represents stresses parallel to the weld axis and σ_y , stresses perpendicular to the weld axis. In Figure 1 part c, curve 1 shows the relatively low intensity tensile stresses in the center of the plate which taper off and become compressive at the edges. Curve 2 shows the additive effects of restraining lateral contraction. Analytical investigation led to the theory that residual stresses in

constrained butt welded joints are caused by; 1) elastic dislocation due to transverse shrinkage, and 2) incompatible strains produced near the weld due to longitudinal shrinkage of the weld metal and plastic deformation of the base plate.

Magnitude and distribution of residual stresses in weldments are affected by:

- ♦ the temperature distribution in the weldment,
- ♦ the thermal expansion characteristics of the material,
- ♦ the mechanical properties of the material at elevated temperatures.

Computer simulation models and experimentation by Masubuchi have shown that peak residual stresses in the weld center can approach yield stress in some high strength steels. However, experimentation with quench and tempered (HY) steels indicated peak residual stresses below yield stress. In any case, high strength steels exhibit very narrow bands of tensile stresses near the weld which seems to be related to the size of the HAZ.

Specimen size plays an important role in residual stress distribution and magnitude of unrestrained butt welds. Weld length is directly related to the central peak longitudinal stress with a limit of about 18 inches where the stress becomes uniform. Transverse stress remained tensile in the central area and become compressive at the plate edges and were not affected by weld length. Width was negligible as long as overall width was several times the residual stress zone.

Residual stresses are influenced by the thickness of the specimen. Thick specimens require more welding passes and exhibit greater tensile surface longitudinal and transverse stress fields. A problem with experimentation in this area is that interior stress fields

cannot be measured adequately. All stress fields are predicted from destructive tests which allow surface measurements and as such are limited in accuracy.

It is generally accepted that transverse and longitudinal residual stresses become compressive near the center of the weld, a direct result of multipass welding. Residual stresses normal to the weld surface exhibit mostly compressive stresses but some researchers believe the stresses can become tensile in very thick welds. HY specimens used in this experiment were multipass welded, Figures 4 through 7 depict the weld bead arrangements.

Variations in the sequence of multipass welds affect distortion and the residual stress distribution. Transverse residual stress in restrained welds varied with the sequence used. Block sequence butt welds produced the least shrinkage, strain energy, and reaction stresses. Longitudinal stresses did not vary significantly with different weld sequencing. Local surface hardness is affected in the HAZ when multipass welding is used. Figures 8 through 11 show the effects of multipass welded butt joints on surface hardness of 1 inch HY 80 and HY 100. Figures 12 and 13 show surface hardness for 0.25 inch, two pass welded HHA specimens.

Hydrogen Embrittlement Cracking

Hydrogen is one of the most common and serious types of time dependent failure [Masubuchi, 1980]. The presence of hydrogen reduces the ductility of unnotched

specimens and hence reduces tensile strength of notched specimens. Characteristics of

hydrogen cracking include:

- ♦ not being a form of stress corrosion cracking
- ♦ embrittlement resulting from hydrogen greater than the equilibrium solubility limit, about 1 ppm for high strength steels.

Material and weld strength is directly related to its susceptibility to hydrogen cracking. Life of the specimen is significantly reduced as a function of tensile load and hydrogen in solution. A specimen of HY-80 briefly exposed to hydrogen contamination and loaded to 80,000 psi in tension failed after 400 minutes. A specimen of SAE 4340 quenched and tempered steel with a tensile strength of 260,000 psi failed after 15 minutes when loaded in tension to 80,000 psi while hydrogen was being charged to the steel [Masubuchi, 1980].

The affects of hydrogen embrittlement are aggravated by high longitudinal residual stresses. Transverse crack length is uniform in the center of the weld and decrease in length as one moves toward the edge of the plate. There were no cracks at the plate's edge. Typical hydrogen induced cracks were short, transverse and adjacent to the weld. Severe hydrogen embrittlement enhanced extensive cracking while less hydrogen embrittled specimens exhibited short, less predominant and widely spread cracks. A lower limit of embrittlement produced no cracking along with a lower limit on material toughness which indicated no cracking even when highly charged with hydrogen.

Stress Corrosion Cracking

Stress corrosion cracking (SCC) is characterized by its severe localized effects on a structure. The combination of corrosion and tensile stresses can cause a normally ductile material to fail in a brittle manner. SCC does not affect pure metals and seems to be reduced when pure metals are used in alloying steels. Specifically, aluminum, copper, and magnesium based alloys show reduced susceptibility to SCC as the alloying components are reduced. Environments causing SCC vary depending on the base metal. For steels the most detrimental environments are alkalis, nitrates, hydrogen cyanide, hydrogen sulfate, anhydrous liquid ammonia, sodium chloride solutions and marine atmosphere [Masubuchi, 1980]. While SCC can occur without external loading, it is aggravated by the presence of high residual stresses.

Stress Concentrations

Geometric conditions can create zones of stress concentration that can become zones of high strain from which cracks can initiate. Flaws are not required for a stress concentration to occur. Most generally, a stress concentration will occur wherever there is a geometric discontinuity such as sharp edges, slits, notches and even inadvertent arc strikes.

An arc strike is defined as an inadvertent heat affected zone or change in contour of the finished weld or adjacent base metal resulting from an arc or heat generated by the passage of electrical current between the surface of the finished weld or base metal and a

current source [Czyryca, Juers, Werchniak, 1991]. An arc strike may be considered a metallurgical notch from which failures may initiate. During the fraction of a second that it takes an arc strike to occur, a very thin layer of the base metal is melted. This molten base metal is not protected by flux or shield gas, thus it is probably contaminated. Since a small volume of base metal is melted, the large mass of the surrounding conducts the heat away rapidly, causing a very high cooling rate. The rapid quenching can cause a local brittle HAZ which then lies in a field of tensile residual stress caused by thermal gradients and volume changes that accompany metallurgical transformations. Arc strikes may also contain microcracks and porosity .

Fatigue Fracture

Fatigue is a complex phenomena that is not well understood, and difficult if not impossible to predict [Shigley, Mitchell, 1983]. Designs can easily compensate for static load failures but not for fatigue failures. Fatigue failures are usually sudden and catastrophic in nature, hence very dangerous. Fatigue fracture is caused by cyclic stresses. The stress may be classified by its frequency, range and profile with respect to time.

Engineers are generally concerned with two types of fatigue fracture mechanisms:

- ♦ high cycle, low stress loading
- ♦ low cycle, high stress loading

High cycle fatigue must consider the endurance limit which is generally accepted as greater than 10^6 cycles. High cycle fatigue is associated with ship structures near high speed equipment such as the propeller. Low cycle fatigue is more important for ocean

engineering structures because the major loads on the ship's hull girder are (low frequency) wave induced elastic loads. Empirical data for ocean engineering structures and ships is very scarce. Figure 2 shows the variation in endurance limit as a function of material condition and tensile strength.

Fatigue fractures grow slowly and may never actually cause failure of the structure. As the crack propagates through a ductile structure, cross sectional area is slowly reduced to the point where loading exceeds the ultimate tensile stress which results in failure.

Less ductile or brittle materials fail catastrophically when a critical crack length is reached. Brittle failures exhibit strong dependence on temperature and geometry. Ductility tests yield a transition temperature which indicates ductile to brittle failure for a given load.

Fatigue cracks typically exhibit three stages:

- ♦ initiation
- ♦ slow growth
- ♦ onset of unstable fracture

Repeated stress cycles below the ultimate strength (and sometimes even the yield strength) of the material still result in failure. The failure initiates from a point of discontinuity in the material such as a keyway or hole. Less obvious are welding defects that are invisible to the eye but are usually undetectable by NDT also. When the stress at a discontinuity exceeds the elastic limit, plastic strain results. A fatigue fracture occurs with

the presence of cyclic plastic strain. As the crack initiates and continues to grow, so too does the plastic strain field around the crack site. Eventually, stress concentration becomes great enough to cause total failure. The ensuing slow growth of transgranular cracks occurs as a function of cyclic loading. Striations (beach markings or concentric rings) are formed along the crack front and are related to the number of cycles. Other variables such as mixed mode failure and plasticity influence the actual ratio of cycles to striations.

The site of a fatigue failure contains two distinct areas. The first is caused by progressive development of the crack, while the second is due to the sudden fracture. The sudden fracture zone is similar in appearance to the fracture of a brittle material such as cast iron, that has failed in tension.

Cracks propagate in the direction normal to the maximum tensile stress; transverse to the load axis. Finally, the onset of unstable fracture occurs when the nonlinear crack growth reduces cross sectional area. If the area is reduced sufficiently, ultimate strength is exceeded resulting in failure. The plastically failed surface will appear fibrous or crystalline depending on ductile or brittle failure respectively.

Several methods have been developed to portray cyclic failure. The most common is the Wohler or S-N curve where S is the nominal cross sectional stress, and N is the number of cycles. The graph is usually plotted in a log-log format to yield a linear curve.

The overall curve has a constant slope to the endurance limit which for ferrous materials is about 10^6 cycles. For the section of the curve preceding the endurance limit, the general relation for the slope of the S-N curve is:

$$F_n = S (N/n)^k$$

where

F_n is the fatigue strength computed for failure at n cycles

S is the stress loading producing failure in N cycles

k is the slope of the best fit straight line S-N curve [Masubuchi, 1980].

Factors influencing fatigue limit include:

- ♦ Most high strength steels are particularly susceptible to reduced endurance limits caused by sensitivity to microstructure and chemical content. Material effects are illustrated in Figure 3. This condition is strongly influenced by any welding process and the subsequent formation of a HAZ.
- ♦ Stress concentrations will form where ever there is a change in structural continuity such as cracks, holes, welds, and notches. The shape and size of the discontinuity influence the concentration factor. A sharp crack has the highest stress concentrating effect. Weld reinforcements reduce fatigue life considerably and must be ground flush on critical joints. Reinforcement or doubler plates may also suffice.
- ♦ Corrosion fatigue is a highly localized failure that can significantly reduce the life of a structural material. High strength steels and titanium alloys are subject to severe corrosion fatigue in seawater. High stress aggravates the situation.
- ♦ Residual stress significantly affects those phenomena occurring under low applied stress. For instance, stress corrosion cracking and hydrogen induced cracking take place with no applied load, so residual stresses can further reduce the fatigue limit [Masubuchi, 1991]. Residual stress is important in high cycle fatigue since it is characterized by low stress. Some investigators feel that residual stress effects are minimal while others contend that surface compressive residual stresses are beneficial and caused an increase in fatigue life. Evidence suggests that most residual stresses can be eliminated by stress relieving the structure.

Fatigue crack growth rate (da/dN) correlates with stress intensity factor (ΔK). As a fatigue crack grows, da/dN and ΔK increase also. Diagrams of da/dN versus ΔK show the material's relative resistance to crack growth.

Low cycle fatigue failure is generally characterized by high local stress loading which involves plastic deformation. True stress cannot be calculated by elastic theory and plastic theory is not developed enough. Plastic strain causes hysteresis of the loading-unloading curve on a stress strain diagram, therefore total strain must be used as the second variable [Masubuchi, 1980]. However, if the material response to loading remains in the elastic range, stress remains an adequate parameter. Experimentation has indicated that strain is the dominant factor in low cycle fatigue and is independent of the strength or type of material. High cycle fatigue strength varies with strength however. The problem is that there is no clear cutoff between high and low cycle fatigue. Experimentation has also indicated that high yield strength materials may suffer low cycle fatigue failure while being cycled in the elastic region.

Fatigue limits for welded specimens can be estimated to be 0.5 to 0.8 tensile strength loading for 100,000 cycles. Low cycle fatigue is defined as failure below 10,000 cycles. Failure above this value is referred to as high cycle fatigue. The endurance limit for steels is typically 1,000,000 cycles or greater. The significance of the endurance limit is that failure is not anticipated beyond this number of cycles. Interestingly, nonferrous metals and some steels do not have an endurance limit and are classified as having a finite cyclic lifetime.

Marin classified several factors influencing the endurance limit (and hence the failure limit) of practical structures. These include the following: surface factor, size factor, reliability factor, temperature factor, stress concentration factor and a miscellaneous effects factor.

Overmatching and Undermatching of Welds

Cracking of butt welded high strength steel is a complex phenomena that continues to be researched extensively. Important factors in butt welded high strength steels include joint geometry, direction of principal strain axis, and the weldment's strength relative to the base metal.

Joint geometry is important because it determines the moments and forces transmitted from the base plate to the weldment. Principal strain axis direction will effect the relative direction and propagation of failure cracks. Weldment relative strength is categorized as overmatched if the weldment is stronger than the base plate or undermatched if the base plate is stronger than the weldment.

The degree of weldment mismatch is determined from the weld metal and base plate metal respective yield or tensile strengths as follows:

$$\text{Mismatch} = (YS_{\text{weld}} - YS_{\text{plate}}) / YS_{\text{plate}} ,$$

or

$$\text{Mismatch} = (TS_{\text{weld}} - TS_{\text{plate}}) / TS_{\text{plate}} .$$

Mismatch is sometimes indicated as negative for undermatched welds and positive for overmatched welds. Multiplying the mismatch by 100 yields the percent mismatch. It is important to indicate which reference is being used. The percent yield and tensile referenced mismatch for each of the samples is presented in Table 2 and Table 3.

For the past several decades weld overmatching has been the norm. In many instances this policy has been codified in structural applications. The history of the preference for overmatching can be traced back to explosion bulge experimentation with high strength steels with overmatched and undermatched welds in the 1950's [Kirk, 1991]. The topic of overmatched versus undermatched weld joints has been the focus of recent experimentation and analytical research, perhaps driven in part by the economics of welding manufacturing. Kirk has researched the affects of overmatched and undermatched welds, some of the following information is taken from his paper.

Overmatching has technical and economic penalties. Overmatch welded high strength steels usually require preheating to avoid hydrogen cracking. Satoh demonstrated that preheat requirements could be halved when welding HT-80 (113 ksi nominal tensile strength) steel with an undermatched electrode (AWS E9016G, 90 ksi nominal tensile strength) rather than with an overmatched electrode (AWS E1106G, 110 ksi nominal tensile strength). This resulted in a reduction of energy costs and increased production. Increased production is the result of the reduced preheat allowing a greater welding duty cycle. Undermatched welding of HY steels in the 80 to 130 ksi range has a deposition rate

greater than overmatched welding. Lack of fusion and lack of penetration defects are reduced because of the higher heat input. Residual stresses are reduced and weld metal toughness is increased. Since the hydrogen embrittlement problem is reduced, the electrodes do not require the same degree of preheating and special storage resulting in a further savings in energy.

The welding process has many uncontrolled variables that effect the characteristics of the solidified weld and surrounding heat affected zone (HAZ). Toughness of the weldment and HAZ must be considered along with weld defects which can serve as crack initiators.

Analytical and experimental results indicate that transversely loaded weldment plastic strains concentrate in the material with the lower yield strength. An overmatched weld sheds strains to the plate where there is better fracture toughness and less defects. An undermatched weld concentrates strains in the weldment.

Weld Defects

Weld defects can be categorized as planar / crack-like (cold cracking, lack of fusion, hot tearing, lack of penetration, or undercut) or volumetric (porosity, slag inclusion). These defects may not be detectable using economical methods of nondestructive testing (NDT). The most important defects are those that provide initiation sites for cracking during service.

Overmatching welds on high strength steels have an increased probability of weld defects which increase considerably with base metal and weldment strength. While high quality undermatched welding may be easier to perform on high strength steel structures, there remains the problem of contending with the concentrated weldment strains that could cause premature failure.

Historical preference for overmatching came about as the result of empirical studies of weld metal deformation. In 1951, Pellini and Hartblower performed explosion bulge tests to study deformation and fracture behavior of weldments in high-rate, multiaxial loading. The test results indicated that overmatched welds experienced local strains that were less than the global plate strain while undermatched welds exhibited the opposite effect. The ability of overmatched welds to shed strain to the base plate was influenced by both the geometry of the weld and the relative strength (not absolute) of the weld over the strength of the base metal.

Pellini and Hartblower's experiments further bolstered overmatching by indicating that overmatched welds absorbed more energy than undermatched welds. Overmatched samples exhibited a greater ability to thin without fracture for a given temperature.

Weldment cracking propagated perpendicular to the principal strain axis, therefore cracking initiated and propagated parallel to the weld axis in undermatched samples while in overmatched samples, cracks propagated perpendicular to the weld axis into the plate

where they were arrested. Since weldments are subject to defects, the arresting feature of the overmatched welds was highly desirable. The base metal became the major contributor in governing fracture resistance of the overmatched structure. This was a very important discovery since metallurgical controls for plate fabrication are easier to control than the welding process. Consequently, undermatching was not considered as a realistic alternative in high strength steel structures.

Experiments by Satoh and Toyoda investigated strength and ductility of undermatch butt welded wide plate in tension. The feasibility of reducing or eliminating the preheat when welding HY-80 was investigated. Results showed that the weldment ultimate strength approached that of the plate as joint thickness decreased, indicating that joint strength is a function of joint geometry and flow properties. An increase in the weldment's strength resulted from the higher strength base metal constricting plastic flow in the joint. Reduction in ductility was characterized by a reduction of both ultimate strain to failure and strain at maximum load. Finally, experimentation with combinations of undermatching double-V and double-U groove joints typically used in industry were performed. These tests indicated that a 10% undermatched weld could achieve the ultimate strength of a slightly overmatched weld. Undermatching effected ultimate ductility of the weldment much more than its ultimate strength. A 34% undermatched weld retained 94% of the ultimate strength of an overmatched weld but only 29% of its ultimate ductility. A major obstacle facing the use of undermatching welds is the reduced ductility of the weldment.

Tensile tests performed by Patchett and Bellow in 1983 indicated that the weldment thickness of undermatched submerged arc welded pressure vessels was indirectly related to the ultimate strength of the weld. The weld's yield strength was unaffected. Plastic flow dependent failure, a function of yield strength, is independent of weld thickness.

Undermatched welds are still an attractive alternative because it can alleviate special needs such as, the need to reduce hydrogen cracking by preheating, or the need for residual stress relief. Overmatched and undermatched weldments must also be examined with respect to crack initiation and propagation.

Fracture Mechanics

Fracture toughness and the fracture driving force of a material can be quantified by a crack tip characterizing parameter. Stress intensity factor, K_I is used when linear elastic conditions prevail. If the crack tip is not vanishingly small compared to other dimensions, then the nonlinear fracture mechanics (NLFM) term of crack tip opening displacement (CTOD), δ or the J-integral, J_I , are used.

When conditions of linear elastic loading exist, the three parameters are related. For post yield loads, δ and J_I are related by material flow properties and a geometry factor. Intensity of the crack deformation field with some geometry independence can be

measured by the crack characterizing parameter. NLFM provides a framework to predict maximum safe load of a flawed structure.

Experimental procedures are well established for computing values of K_I , δ , and J_I for homogeneous specimens. No guidelines have been established for welded specimens. Currently there is research on the effects of mismatch on J_I , δ , and critical fracture toughness.

Weld Strength Matching Effects on J_I and δ

Experimentation and analytical finite element modeling of test pieces has been performed by numerous investigators. Single edge notched specimens in tension SE(T), and single edge notched specimens in bending SE(B) have been used to estimate fracture toughness of the material. Tension loaded wide plate specimens are used as a structural scale proof test because the loading and relative crack size more closely model a structure than an SE(T) or SE(B) specimen.

In the following section, the test pieces were treated as a bi-material consisting of a weldment and a base metal where the values of J_I and δ did not vary significantly from the finite element estimations. The elastic modulus of the weldment and base plate were held equal while the post yield flow properties were allowed to differ. The heat affected zone (HAZ) of the weld vicinity is an important issue because the bi-material treatment of the specimen can break down. Figure 3 shows the region of a typical HAZ.

The HAZ is an area of large gradient of change in constitutive properties between the weldment and base plate with the size of the HAZ relative to the dimensions of the plate and weldment being the critical parameter. Thin plate or narrow weld specimens therefore will not behave according to the bi-material treatment making analysis very difficult. Thick plate (on the order of 3/4 inch to 2 inch) that has been multipass welded has a large HAZ but it is relatively small compared to the plate and weldment dimensions so bi-material modeling is acceptable. A thick plate specimen HAZ is far away from the center of the notched weldment where the crack will initiate and propagate. This prevents the crack from encountering the HAZ where applied J_I varies.

Single Edge Notch Specimens

Fracture toughness of a material can be determined using the SE(T) and SE(B) tests. SE(B) tests have the advantage of requiring less loading and simpler equipment to perform the experimentation, therefore it is the most common test. Values of applied load, displacement, and crack edge separation or crack tip opening displacement (CTOD) are typically monitored during the experiment. Loading progresses to the point of crack initiation by either cleavage (brittle fracture) or microvoid coalescence (ductile failure). These data can be used to calculate the critical fracture toughness, J_{IC} and/or δ_c using equations for unwelded specimens as cited in ASTM testing standards. It is important to determine if J_{IC} or δ_c are influenced by the presence of a weld and if so, by what amount.

The effect of weld geometry for 15% undermatched 0.1 a/W (ratio of crack depth, a, to test piece width, W) SE(B) specimens was investigated by Bleackley. The plot of applied J_I versus load point displacement indicated an initial parabolic curve that was a function of linear elastic response and therefore not influenced by weldment matching or joint geometry. The curve continues to a linear portion that is indicative of gross section yielding, the slope of which varies directly with the severity of fracture. Gross section yielding is a function of both weld metal matching and joint geometry. Undermatched welds exhibited a large slope and overmatched welds had a small slope. Bleackley's data showed that experimentally measured values and crack tip driving force, J_I , varied with joint geometry. The single-V and square groove welds agreed with values for a monolithic weld metal specimen. Double-V groove welds showed less applied J_I than predicted by the previous model. The reduction of J_I occurred because the width of the weld joint caused high strains to concentrate inside the weld along the metal-plate fusion line, but these strains did not spread to engulf the crack tip.

The effects of matching ratio and crack depth to specimen width ratio on SE(B) double-V groove specimens was studied by Cray, Luxmoore and Sumpter. It was determined that no correspondence of J_I for a given load existed between the homogeneous and welded specimens. The welds exhibited trends that were consistent with weld deformation behavior of uncracked weld joints. The undermatched weldment concentrated the strain and increased the applied J_I while the overmatched weld reduced the applied J_I by shedding the strain to the base plate.

Investigation of SE(B) specimens revealed the following:

- ♦ Shallow Cracks: accurate J_I estimates that take into account weld mismatch and nonhomogeneity of the specimen do not exist for welded plates.
- ♦ Deep Cracks: a reasonably accurate value of J_I may be experimentally determined if the weldment is treated as a monolithic specimen. The model is constrained to plastic deformation of the weldment only.

Similar experiments with SE(T) specimens indicate that applied J_I , relative to plain plate general yielding, is reduced in both under and overmatched welds. The greatest reduction in J_I is by the undermatched weld because in tension the width of the joint allows high strains to concentrate into slip bands along the weld-plate fusion line. Since crack tip strains were kept low, the applied J_I was reduced.

Finite element analysis of four a/W ratios (0.05 to 0.2) was performed by Cray. In bending, overmatched welds needed less toughness than an undermatched weld to resist fracture for a shallow crack. Increasing crack depth mitigates this feature. Tension testing results were inconclusive and enforced the dependence of applied J_I on the mismatched weld-plate fusion line deformation concentration.

Dong and Gordon investigated the effects on J_I of SE(B) specimens. Monolithic bend specimens made of entirely of weld metal and base metal were compared to overmatched square groove welded samples. Results for a 0.1 a/W qualitatively agreed with Cray's double-V results and indicated no correspondence. A deep crack specimen with a 0.5 a/W showed good correspondence with the homogeneous weld metal case.

This is probably the result of the deep crack yielding being confined to the intact weld metal, the net ligament. This suggests that accurate estimates of J_I for a deeply cracked undermatched weld is possible by this procedure. Undermatching and bending load concentrate deformation strains in the weldment. The limit of the homogeneous model occurs when the weldment has a very narrow ligament such as a narrow groove weld or a double-V weld with a small bevel angle. In these cases the yielded zone of the ligament can exceed the width of the weld causing a breakdown of the model.

Wide Plate Specimens

Wide plate specimens typically contain semi-elliptical surface cracks that are comparable to those found in structural service, making them ideal for scale testing. Specimens are modeled as either having a through crack or a semi-elliptical surface crack. Only one analytical model exists for the semi-elliptical surface crack while there are several variations of the through crack. Both crack models use a symmetrically located crack on the centerline of the weld and loading perpendicular to the weld axis.

Reed and Petrovski estimated J_I of semi-elliptical surface flaws for a double-V butt welded HSLA-80 plate. Three matching ratios ranging from 37% undermatched to 17% overmatched and two crack depth to plate (a/t) ratios, 0.2 and 0.4 were used. Undermatched welds with small cracks experienced a rapid increase of J_I , especially when strain exceeded 1.5 times the yield strain. The overmatched weld with small cracks reached a plateau and remained constant for strains of 1.5 times the yield strain. Deep

crack specimens (a/t of 0.4) of under and overmatched welds both indicated a high J_I regardless of weld metal matching. Overmatched welds shield shallow cracks but this advantage disappears as crack depth increases.

Weidian performed finite element analysis of 37% overmatched wide plate with a square groove joint containing a middle crack severing 20% of the plate width. Effects of varying the weld layer width or distance between the plates on J_I were studied. J_I was found to react inversely with weldment width. This is apparently because the wider weldment removes the highly strained lower strength plate material from the crack tip.

Dong and Gordon performed finite element analysis of wide plates having the same weld/crack geometry as Weidian but with a wider range of conditions. Specimens having cracks with an a/W of 0.05 and 0.2 were studied. Undermatched weldments experienced a slightly higher applied J_I in the weld compared to overmatched welds. A panel of base plate material was found to closely approximate applied J_I for all weldments studied. The ratio of the weld layer thickness to crack length ($2h/2a$) did not significantly effect J_I for the range studied. The last two results were explained by an earlier detailed analytical study performed by Zhang, whom studied the effects of strength and strain hardening mismatch on applied J_I .

Zhang performed finite element analysis of wide plates with square butt welds containing cracks that were 40% of the panel width. The concept of equivalent yield

stress and equivalent strain hardening exponent were introduced. These values were defined as those that produce the same applied J_I in a monolithic wide plate having the equivalent constitutive properties as in the welded plate. If the weld layer thickness exceeds 1.5 times the crack length then the equivalent yield strength nearly equals the weld metal yield strength. In the limit, equivalent yield stress approaches the base metal yield stress as the ratio of weld layer thickness to crack length ($2h/2a$) approaches zero. This data agrees qualitatively with that of Dong and Gordon for estimations of J_I from weldments with $2h/2a < 0.3$ and the J_I for a monolithic wide plate with base metal properties.

The Ramberg-Osgood strain hardening exponent, n , approaches 1 for linear elasticity and infinity for perfect plasticity. When the weld layer thickness exceeds 1.5 times the crack length the equivalent hardening exponent will approach the value of the weld metal. Conversely, in the limit, the equivalent hardening exponent will approach the value of the base metal. This is especially true of undermatched welds where the equivalent hardening exponent changes at a greater rate than the overmatched case. Barsom and Rolfe have said that a wide variety of martensitic steels exhibit strain hardening rates that is inverse to the yield strength. This leads to the notion that the strength of an undermatched weld is overmatched with respect to strain hardening. The same analogy holds true for overmatched welds.

Some limitations of the concept of equivalent yield stress and equivalent strain hardening exponent were cited by Read and Petrovski. Experimentation with shallow cracks in welded panels indicated that under certain conditions J_I did not increase as anticipated with increased strain because of the accumulation of strains at the fusion boundary. This condition precludes the use of the equivalent yield stress and equivalent strain hardening exponent concept because the applied J_I in the monolithic panel will not reach a plateau for the same reason. The accumulation of strains at the fusion boundary of the welded panels causes J_I to plateau because of asymmetric in plane yielding that occurs between net and gross section yield. This poses a restriction on the application of Zhang's concept to cases where J_I has yet to plateau or cannot reach plateau. Thus, models are limited to either having cracks of adequate depth to prevent plateauing, or, shallow cracks at loads not much above the limit load.

Analytical and experimental results indicate the concentration of strain will occur in the material of lowest material strength in a transversely loaded weldment. Remote bending and tension tests indicate that the driving force for fracture, J_I , in an undermatched weld increases at a much faster rate with increasing plastic strain than for a crack in an overmatched weldment. The effects of this phenomena are augmented by the crack's geometry and location in the weldment. The most important of these include cracks that are either shallow with respect to the specimen thickness (less than 30% of thickness) or small with respect to gross load bearing cross section (less than 4% to 21% area reduction).

Experiments studying the effects of weld strength mismatch on weld metal toughness have produced data that shows no significant toughness variation with strength matching ratio. If this is correct, then undermatched welds could reduce the factor of safety against fracture for a structure. This area needs more research since plate material typically exhibits toughness that is inversely related to strength.

Overmatched weldments generally require less weld metal toughness than undermatched welds to prevent crack initiation. The equivalent yield stress and strain hardening exponent appears valid provided J_1 cannot plateau with increasing strain. Since cracks in structures are fairly shallow, the use of this concept in structural safety assessments is limited.

Investigation of wide plate tension specimens have indicated the following:

- ♦ **Small or Shallow Cracks:** cracks in welds are shielded from high applied J_1 . Overmatched weldments reach a plateau at a certain plastic strain level after which no appreciable change in J_1 occurs. Undermatched weldments do not exhibit a plateau. If cracks in a structure can be kept small then overmatched welds require less toughness to prevent failure than undermatched welds. If simplified schemes for J_1 existed, it would be reasonable to select a toughness greater than the J_1 plateau for the largest expected crack size in a structure.
- ♦ **Deep or Large Cracks:** The rate of increase of J_1 with increasing plastic strain is less rapid for cracks in overmatched welds than in undermatched welds. A J_1 plateau does not occur in this case. J_1 can be estimated by treating the weldment as a monolithic plate with an equivalent yield stress and strain hardening exponent (Zhang, et al). The equivalent properties become those of the plate as the plate thickness becomes small compared to the crack length. Conversely, the equivalent properties become those of the weldment when the weld thickness becomes large compared to the crack length.

The Energy Concept of Cracking

Fracture toughness, the ability to withstand plastic deformation without fracture even in the presence of a flaw, is a function of the material's response to local stress and the geometry of the flaw producing the high localized stresses [Flinn, Trojan, 1981]. Material fracture that occurs with local yielding has an energy balance: energy input (work) to produce fracture \geq surface energy (γ_s) of fracture surfaces + energy of plastic deformation (γ_p). γ_s is the surface energy per unit surface area (J/m^2) and may be considered to be the energy required to break the atomic bonds and create the new surfaces. γ_p is the energy of plastic deformation per unit volume (J/m^3). The energy input is the difference between external work supplied and the stored elastic energy at the onset of fracture. Work is the area under the true stress - true strain curve. Energy required for fracture is the sum of γ_s multiplied by fracture surface area and γ_p multiplied by the volume of plastic deformation. Typically, $\gamma_s \sim \gamma_p / 10^4$ so fracture toughness is essentially proportional to γ_p , the ability to undergo plastic deformation before failure.

Stress concentration is the result of geometry effects such as flaws and drillings. The concentration is analytically modeled by a stress concentration factor, K_σ . As a flaw approaches the geometry of a sharp crack, the concept of stress concentration breaks down and methods of fracture mechanics are required.

Fracture mechanics takes into account the difficulty in accurately measuring the energy required for plastic deformation of the crack tip. The material's fracture toughness

is proportional to the crack tip plastic deformation energy. Stress intensity factor, K_I is used to determine the fracture toughness of most materials. It is similar to the stress concentration factor K_σ , but the two are not equivalent. For a given material, catastrophic failure occurs when the stress intensity factor reaches a critical value, K_{IC} . This value of K_{IC} is called the fracture toughness. K_{IC} and K_I are related in a manner similar to the relation of stress and tensile strength: K_I represents the level of stress intensity at the crack tip (stress dependent) and K_{IC} represents the highest value of stress intensity without fracturing (material dependent).

An expression that relates fracture toughness, crack size and fracture stress is :

$$\sigma_f = K_{IC} / Y \sqrt{\pi a} ,$$

where σ_f is nominal fracture stress, K_{IC} is fracture toughness, Y is a geometry constant and a is crack length. Crack size is measured differently depending on whether or not it cuts a free surface. An edge crack has a length of a while a center crack has a length of $2a$.

The previous equation may be rearranged to form an expression for stress intensity as follows:

$$K_I = Y \sigma \sqrt{\pi a} ,$$

where σ is the nominal applied stress. Stress is linearly related to the stress intensity factor. Y does not account for the geometrical parameter of thickness. Thickness is important because it determines if a specimen is in plane stress or plane strain. Thin specimens are typically in plane stress and yield a higher value of fracture toughness, K_{IC} .

This is because of a large plastic zone at the crack tip. Thick specimens are typically in plane strain and exhibit a lower fracture toughness which approaches a minimum value referred to as plane strain fracture toughness, K_{IC} . The transition from plane stress to plane strain fracture toughness is a function of the material's yield strength. Empirical results show that plane strain conditions prevail when:

$$t \geq 2.5 \left(\frac{K_{IC}}{\sigma_{YS}} \right)^2,$$

where t is thickness and σ_{YS} is yield stress. This relationship must be satisfied to ensure accurate calculation of K_{IC} , especially for a specimen of unknown fracture toughness. If the sample is tested and calculated K_{IC} does not satisfy the previous expression, then thicker test samples must be used and the experiment repeated.

Fracture toughness is inversely related to yield strength. High strength steels used to minimize component size and weight are highly stressed and thus have increasingly smaller tolerance for flaws.

Cyclic stress loading can cause premature failure of a component. Small flaws are initiated and grow until the critical crack size is reached, then rapid failure occurs. This type of rapid failure after a time in service is at worst, dangerous and at best, detrimental to consumer confidence. Critical crack size is directly related to K_{IC} or inversely related to yield stress. Crack detection (with normal nondestructive testing methods) becomes very difficult with high strength steels.

S-N diagrams depicting nominal stress loading versus the number of cycles can be interpreted as having two separate parts. The first part would plot crack initiation versus number of cycles and the second part would plot crack growth versus number of cycles. Cracks may initiate from flaw-free regions or from defects such as inclusions. The variation in initiation is usually responsible for data scatter for failure as a function of cycles.

In a defect free region, cracks may initiate from minute stress concentrators caused by localized plastic deformation on particular slip bands. After repeated cycling small cracks appear at the intersections of the local deformation bands. Minute imperfections such as surface scratches may greatly shorten or even eliminate the crack initiation phase. Surface finish is therefore an important factor in total fatigue life of an item.

Internal defects simply shorten the number of cycles required to initiate cracking. As the crack grows, crack propagation is categorized by its direction of travel. Early stages of propagation are dependent on the orientation of the grain and is referred to as stage I cracking. The cracks propagate on specific crystallographic planes and subsequently, tend to change directions quickly. As the crack grows it becomes independent of grain orientation and travels normal to the applied stress, even through grain boundaries. This is referred to as stage II cracking and is predominant during propagation life. Stage II crack growth is often indicated by distinct surface markings called fatigue striations.

It is generally accepted that the rate of crack propagation is a function of the stress intensity factor, K_I . For most engineering alloys, the rate of propagation da/dN can be expressed as function of the range of the stress intensity, ΔK_I , that is experienced by the crack during the stress cycle:

$$\frac{da}{dN} = C \times \Delta K_I^m,$$

where C and m are material dependent constants. ΔK_I is calculated using

$$\Delta K_I = \Delta K_{I \max} - \Delta K_{I \min} = (s_{\max} - s_{\min}) Y \sqrt{\pi a},$$

where it can be seen that ΔK_I is not a constant value but varies with crack length, a .

Submarine High Strength Steel Fatigue Research

High strength steels used in submarine pressure hulls are required to endure high stress, low cycle fatigue. Several new high strength alloys were compared to HY-80 steel in the cycle-life range of 10,000 to 100,000 cycles [Rolfe, Haak, Imhof, 1964]. Candidate fatigue strengths, the strain range necessary to cause failure, were compared and found to vary as a function of the number of cycles, composition, and yield strength of the steel. The investigators state that a high strength steel's resistance to fatigue failure should be proportional to the yield strength of the steel in order to reduce susceptibility to cracking.

Experimental results showed significant differences in fatigue strength for plain base plate and GMAW welded plate. Generally, the welded plate exhibited fatigue strength better than plain base plate above 10,000 cycles to the maximum of interest, 100,000 cycles. Fatigue analysis was conducted and compared using predictions

developed by Morrow, Langer and Manson. Langer and Manson's fatigue predictions are based largely on monotonic tensile properties and did not predict failure as well as Morrow. Morrow's methods best agreed with experimental results because his equations were both empirically derived and they take into account the material's cyclic stress-strain properties such as hardening or softening. Morrow defined total strain as the sum of elastic and plastic strain. He showed that while the plastic and elastic strain versus cycles log-log plots were linear, the total strain versus cycles log-log plot was not. Plastic strain fatigue loading has a much greater effect on the reduction of fatigue life. The slope of the plastic strain versus cycles log-log plot for HY-80 is three to four times the elastic strain versus cycles log-log slope.

Chemical Compositional Effects of Titanium

Transition temperature is a function of cleavage fracture stress. Cleavage fracture initiation is associated with the population of titanium bearing, nonmetallic inclusions located in the region of coarse cleavage facets [DeLoach, Franke, 1989]. Inclusion initiated fracture occurred at the sites on the order of 0.5 μm to 1.0 μm . Titanium content as little as 0.01 % weight resulted in inclusion fracture sites. A increase of 0.004% titanium increased inclusion size by 0.05 μm . Several cases of inclusion initiated cleavage fracture in crack opening displacement and Charpy vee notch specimens. Previous studies had identified lath pocket size as the controlling feature for martensitic and bainitic steels and weldments. DeLoach and Franke have found that packet size alone can cause

dislocation pile-ups. Packet size is proportional to the effective grain size of the microstructure and hence promotes microcrack initiation through dislocation pile-up.

Nonmetallic Inclusion Effects on Fatigue Life

Experiments with SMAW, GMAW, ESW, and ES butt welded joints indicated low cycle fatigue life is indirectly related to the volume fraction of nonmetallic inclusions in the weldment [Dziubinski, Adamiec, Brunne, 1987]. The inclusions can act as stress concentrators. The microstructure was also found to influence fatigue life but to a lesser degree. SMAW as deposited weldments displayed the lowest cyclic plasticity and the highest volume percent of nonmetallic inclusions; 0.56%. Interestingly, the ES welds which had the least favorable deposited microstructure displayed the greatest cyclic plasticity. This can be attributed to the very low (0.15%) nonmetallic inclusions which was less than the base plate.

A Comparison of Over and Undermatched Welding

Low cycle fatigue tests of full section beam specimens of HY-130 steel GMAW and SMAW butt joint with undermatching and overmatching weld metal yield strength: Overmatching of base metal is done through tradition with little or no experimental data to support the requirement [Czyryca, Werchniak, 1991]. Overmatching of high strength steels results in decreased toughness and increased propensity for weld metal cracking. Welding of higher strength steels becomes difficult because the narrowing in range of welding parameters that dictates yield strength and toughness. In particular, weld metal cooling rate is proportional to yield strength but inverse to toughness. Undermatched

welds allow for maximum heat input which results in high deposition rates. Fabrication, rework and repair costs are reduced because the higher heat input yields better fusion, reducing sidewall and interbead fusion defects. Overmatched systems must use low heat input in order to attain the required cooldown rates for higher yield weld metal.

Undermatched welding systems could increase producibility and efficiency through:

- ♦ expanded welding parameters
- ♦ increased weld deposition rates
- ♦ increased selection of weld filler metals.

Weld metal matching is defined in terms of 0.2% offset yield strengths of base plate and weld metal. Low cycle fatigue experimental results with overmatched and undermatched HY-130 plates indicated crack initiation and propagation occurring in the parent material and not the weld. This result held true for SMAW and GMAW welds, in as-welded and flush ground reinforcements. Similar experiments with HY-100 also indicated no preferential site for crack initiation.

Extensive high cycle fatigue testing of construction steels by the American Welding Society has indicated that fatigue properties may not be dependent on the yield strength of the base metal or weld metal. Instead, structural joint performance was related to joint design and the quality of welding workmanship. Undermatched samples with the weld reinforcement removed exhibited fatigue lives approximately identical to equivalent overmatched beams. Stress concentrations, residual stresses, and alignment of pieces were

the dominant factors, not yield strength. Local stress concentrations caused by fabrication defects, joint geometry, and metallurgical flaws are most likely to occur in the vicinity of a weld, namely the HAZ or fusion zone. Residual stresses influenced the crack growth path of undermatched specimens. Crack growth did not propagate perpendicular to the applied bending stress but instead deviated toward the HAZ.

Crack Initiation of Thick Specimens

Empirically plotted low cycle fatigue growth rate of large through thickness cracks and small surface cracks as a straight line against logarithmic ΔJ , the cyclic J integral and ΔK_e , the strain intensity factor [Hatanaka, Fujimitsu, 1988]. The relation was relatively independent of material in both cases. Accurate predictions of specimen fatigue lives were found to be slightly conservative, especially as N became large, about 10,000 cycles.

Crack initiation to failure ratio, N_i / N_f , is about 0.15 ~ 0.20 and is material independent.

In low strength, high ductility steels fatigue cracks nucleate at or near the grain boundary in response to lines of intense slip deformation impinging ferrite grains. In quench and tempered high strength steels the crack initiates at an inclusion site with very little evidence of slip lines. This difference in crack initiation behavior makes microcracks easier to detect in the quench and tempered steels.

Log da/dN versus log ΔJ plots of high strength, low ductility steels indicate through thickness cracks have a greater slope than surface cracks. Therefore the system tends to minimize the potential energy required for a given change in crack length.

Fatigue Life versus Yield Strength

Empirical results with transversely loaded butt welds indicated that fatigue life decreased with the increase in material yield strength when the estimated mean stress exceeded the yield strength of the base metal [Ohta, Maeda, Suzuki, 1992]. Mean stress is defined as the sum of the applied stress and the residual stress. Residual stresses as high as σ_y exist in large scale structures, thereby reducing the usable applied stress loading.

Increased fatigue strength may be attained through development of 1) TMCP steels with yield to tensile stress ratios near one, and 2) welding consumables with lower transformation temperatures. TMCP steels offer high tensile strength with relatively lower yield strength. The authors cite an example of structural application where tensile strength is the determining factor in material design strength. Fatigue strength requirements then dictate that yield strength be minimized. Low transformation weld consumables reduce residual stress by allowing weldment expansion during cooling.

Temperature Effects on Low Cycle Fatigue

Constant strain low cycle fatigue tests were conducted on butt welded joints at 20°C and 350°C [Gregor, 1987]. The low temperature case required less cycles to crack initiation, N_i , and less cycles to failure, N_f , than the high temperature case. However, the

difference in cycles, $\Delta N = N_f - N_p$, was less for the high temperature case. The rate of crack growth, $\Delta a/\Delta N$, was greatest for the high temperature case.

Reheating Effects on Multipass Welds

Primary factors that determine a weld metal's microstructure and mechanical strength are cooling rate and chemical composition [Oldland, Ramsay, Matlock, Olson, 1988]. The complexity of multipass welds is caused by subsequent passes of weldment causing reheating and thermal cycles which change the weld's microstructure and mechanical properties significantly. Heat input and cooling rate can be controlled and monitored to produce the weldment's desired strength and ductility. Experimentation by Krantz indicated significant losses in weldment strength caused by the presence of increased volume fractions of lower strength microconstituents like bainite and ferrite after partial reaustenization of the weldment. Further reheating of the weldment produced a further reduction in strength.

Experimentation by Strunck investigated the detrimental effects of increased heat input on toughness of a multipass weld. Strunck suggests that toughness can be improved in multipass welds by controlling weld variables that increases the fraction of reheated weldment above A_1 by subsequent weld passes, thereby decreasing the fraction of as-deposited weld metal. Lower heat inputs, causing faster cooling rates, increased weld toughness by reducing the amount of proeutectoid ferrite in the weld metal. Other researchers believe the increased toughness is the result of weld metal microstructure refinement and tempering.

HAZ Toughness and Tensile Properties in HSLA

Welding thermal cycle simulations and detailed microstructural study of instrumented single pass weldments of HSLA-80 were conducted [Scoonover, 1988]. Heat input had different affects on the various HAZ microstructures but in general heat input was inverse to the strength of the weld metal.

The HAZ can be broken down into six zones by their microstructure. Moving from the unaffected base plate to the fusion line are the following regions:

- ◆ inner and outer subcritical or tempered
- ◆ inner and outer intercritical or partially transformed
- ◆ grain refined
- ◆ grain coarsened

Four of the six zones had Charpy transition temperatures higher than the base plate. Three zones, outer subcritical, intercritical, and grain-coarsened, had toughness inferior to the base plate. The grain-coarsened zone had a transition temperature above specification and was described as a local brittle zone (LBZ). The investigators likened the HAZ to a composite material where the mechanical properties of each region are influenced by those of the surrounding regions and by its own and their relative sizes. Undermatched welds were criticized because concentration of strain in the HAZ can cause low strain fracture unless the microstructure at the crack tip exhibits high toughness. The intercritical HAZ microstructure in HSLA-80 had the lowest strength in the HAZ and a toughness lower than the base plate.

Weldment Cooling Effects on Strength and Toughness

Cooling rate of weld metal is a major influence on the microstructure and mechanical properties of the weldment [Blackburn, Franke, 1992]. Heat input, interpass

and preheat temperature, and consumables can be controlled to yield (within reason) the desired weldment strength and toughness. Heat input also effects the size and microstructure of the HAZ. The investigators pointed out some shortfalls of traditional cooling rate calculations used for thick, high strength steel plate that should be considered.

Specific points not covered in the cooling rate equation include the following:

- ♦ Multipass welding is a special case of three dimensional cooling with a constantly changing heat sink. The mass of weld metal and joint geometry change with each pass.
- ♦ Weld metal deposition rate (lb of weld metal / inches of travel) is affected by wire diameter, travel speed and current. For a given current, thinner weld wire has a greater deposition rate than large diameter wire.
- ♦ Weld joint configuration (type of intersection and dimensions) and position of welding other than bead on plate and butt welds.
- ♦ Use of backing bars on single side butt welds act as a heat sink and increase cooling rate.

The authors further state that cooling rate data and weld metal properties are very case specific. Accurate extrapolation of data is not possible. Cooling rate calculations should only be considered a tool to establish trends when all other variables are held constant.

Undermatched Double V Butt Welds

Experiments with undermatched double v butt welds in the elastic-plastic range were performed to investigate the weld metal's behavior during loading [Lee, Luxmoore, 1990]. A defect was simulated with a slit machined across the weld and transverse to the

loading. Undermatched double v welds experience stress concentration when loading reaches the weld's plastic strain limit. Under tensile loading, the weldment initially reaches yield. Continued loading causes strain concentrations at the center of the weld because the base plate acts like a rigid body. The effects of the strain concentrations on a defect cannot be predicted accurately. Small edge cracks that may escape NDT can become the initiation site for failure. The enhanced yield strength of the HAZ may be responsible for locally increased strain concentrations. The authors chose to use crack tip opening displacement (CTOD) because it was easiest to measure experimentally. CTOD is related to the strain concentration at an elastic-plastic crack tip. During tensile testing the parent plates rotated as rigid bodies, symmetrically about the crack plane during the phase of constant CTOD. An in-plane slip line field was apparent as additional plastic regions formed in the base plate areas adjacent to the weld. The CTOD increased rapidly once the plastic zone reached the far boundary opposite the crack, indicating that the main mechanism for large crack openings was the formation of conventional in-plane slip line fields.

5% undermatched specimens displayed virtually no effect on CTOD during tensile loading. There was no significant transition in CTOD behavior as weld metal net section yielding gave way to gross yielding. The overall was similar to homogeneous edge cracked specimens.

A 26% undermatched specimen showed significant impact on CTOD behavior during tensile and bend testing. Net section yielding of the weld was reached well before yielding of the base plate occurred. Rigid body rotation of the base plate under restraint and the joint geometry created a concentrated transverse stress field. In tension, yielding begins in the center of the plate and extends outward, forming a triangular shaped crack tip slip band. In bending high strain occurs in the weld metal near the fusion zone and low strains occur at the base plate just after weld yielding. which at the fusion area and cause local yielding of the base plate. High shear strains contribute to gross yielding of the base plate.

For highly undermatched specimens in both tension and bending, testing indicated a temporary shielding effect on the deformation of weld metal at the notch. Gradual strain build up and yielding of the base metal was found to be the cause. The shielding effect temporarily reduces the CTOD until the base plate reaches gross section yield. CTOD will then increase and the specimen one again behaves as a homogeneous material because crack geometry has become the dominant feature.

Chapter 3

Experimental

Specimen Acquisition

HY-80 and HY-100 steel base plates were obtained from General Dynamics, Electric Boat (EB) Division of New London, Connecticut. EB performed the fitup, welding, tensile testing and nondestructive testing (NDT). All machine work was performed by Custom Machine, Inc. of Woburn, Massachusetts.

The High Hardness Armor (HHA) was obtained from the Army Research Laboratory (ARL) of Watertown, Massachusetts. ARL performed the fitup, welding and initial specimen shaping into 1.5 x 12 inch rectangles by water jetting. All subsequent machining of the HHA specimens was performed by Custom Machine, Inc. of Woburn, Massachusetts.

HY Base Plates

Four HY plates, two of HY-100 and two of HY-80 were welded using undermatched and overmatched weld metal. The base plates were multipass welded by semiautomatic gas metal arc welding (GMAW) process. The torch speed, rate of torch oscillation and wire feed rate were manually set and then automatically controlled while the arc length was manually adjusted throughout the process. Preheat and interpass temperature controls were used. Regulation of the interpass temperature and cooldown rates established the final tensile characteristics of the weldments. The HY-100

overmatched weldment required two twelve hour soaks at 350° F. Appendix B contains photocopied data sheets used to record the welding parameters during the process. Table 4 lists selected welding data from the process. Weld bead configurations are indicated in Figures 4 through 7. Nominal base plate metallurgical compositions are listed in Table 5 and are enclosed in Appendix B.

The final dimensions of each of the four welded HY plates were 30 inches long, 16 inches wide and 1 inch thick. The single vee weld bead was along the 30 inch length. Backing plates and run-on / run-off tabs were used on the plates and removed before delivery. Transverse and longitudinal (relative to rolling direction) tensile specimens were taken from each of the two types of base plate. This data is presented in Table 6. Ten inches of welded length was removed and machined into all weld metal tensile specimens. This specimen data is presented in Table 6. Figure 14 shows the final dimensions of the HY specimens.

HHA Base Plates

The HHA specimens were welded using the manual downhand GMAW process. Each specimen consists of a single vee with lands welded with two passes. A total of fifteen plates was provided by ARL, five each of undermatched and overmatched plates, two plain base plates, and one plate with an arc strike. Figure 15 shows the final dimensions of the HHA specimens.

NDT of HY and HHA

Radiographic NDT was performed on both the HY and HHA weldments. All plates passed standard examination by qualified inspectors at Electric Boat and ARL respectively.

Specimen Surface Hardness Testing

Rockwell C scale surface hardness testing of the base metal, heat affected zone and weld metal was performed on samples of each specimen. The weld reinforcement was machined away and the surface polished to reduce the variance of the readings. The results are shown in Figures 12 and 13.

The HHA exhibited some deviation from the advertised value of Rockwell C-52. During conversations with ARL it was discovered that surface hardness is not normally performed on HHA. The HAZ is subject to decarburization which reduces hardness significantly. ARL recommended machining away 0.030 inch of thickness in order to reach the RC-52 hardness. This was not performed because a qualitative study of the hardness profile was desired, not to mention the impracticality of machining such a hard material.

Specimen Sizing for Testing

The criteria used for sizing of the specimens were as follows:

- ◆ test section loading must be within the capacity of the test machine
- ◆ specimen should fail in a reasonable time, say 10,000 - 100,000 cycles
- ◆ specimen must fit in the hydraulic chuck

- ♦ test the full thickness of the weld, therefore only width is variable
- ♦ elastic loading of the weldment
- ♦ avoid stress concentrators such as pin mounting holes

Estimation of the endurance limit for the welded specimens was accomplished by reviewing experimental data of high strength steel fatigue experiments and generic textbook information. The endurance limit for steels below 200 ksi are about 0.5 tensile strength. Other data suggests that the endurance limit for martensitic microstructural steels range from 0.23 to 0.47 tensile strength. This lower value suggests martensite's brittleness and sensitivity to cyclic stress loading. The mean endurance limit corresponding to steels with a tensile strength not exceeding 200 ksi is about 0.45 tensile strength. The conservative approach then is to design the specimens for loading exceeding the higher loading of 0.5 tensile strength.

Figures 14 and 15 shows the HY and HHA specimen design and dimensions. All specimens were sized to reflect the maximum hydraulic chuck load of 50,000 pounds force. Empirical data from high strength steel fatigue testing indicated a loading of 80% to 90% of tensile strength produced failure in 10,000 to 100,000 cycles. This translates to 16.7 minutes and 2.7 hours respectively at 10 cycles per second (cps). Tables 7 and 8 show the sizing data and tensile specimen results used in computing the 80% and 90% tensile strength load window for the HY and HHA specimens, respectively.

Weld reinforcements were machined off all HY specimens to allow proper use of the CSLM. The irregular surface of the reinforcement would not permit positioning the

objective lens close enough to the specimen. The weld surface was then smoothed with 600 grit wet/dry silicon carbide and then polished with a commercial polishing compound and buffing wheel. Two of each type of HHA sample were tested with intact weld beads. The welds were such that the microscope could be used even over the uneven surface. Reinforcements were removed from all other welded HHA specimens and the test areas polished as described for the HY plates.

All samples had a crack starter slit electrical discharge machined (EDM) into the test area to initiate crack growth through stress concentration. The slit was machined transverse to the loading and centered across the weld or test area. The slit dimensions were selected by examining fatigue experimental data using crack starters. The selected depth of the slit was 5% of the thickness, length was twice the depth, and width was 0.020 inches as this was the minimum reasonably attainable by the EDM process. Figures 14 and 15 show drawings of the EDM slits used on the HHA and HY specimens.

Description of Equipment

A computer controlled electro-hydraulic MTS tensile testing machine was used to fatigue test the welded specimens. The machine has a 100,000 pound load capacity but this is limited by the hydraulic chuck's 50,000 pound force maximum load when in the cyclic fatigue mode.

The pulsating tension loading profile was used. This loading function is sinusoidal and ideally ranges from a minimum stress of zero to the maximum stress. Operational constraints prevented the zero stress minimum, therefore a "tension-tension" loading resulted. The minimum attainable load is approximately 10% of the total range. The mean load is the average of the minimum and maximum loads. Maximum load is the sum of the minimum load (MTS "setpoint") and load range (MTS "span"). Setpoint and span were input at potentiometers mounted in the load drawer of the cabinet. The span setting required using the potentiometer dial while the setpoint and maximum load forces are displayed as linear voltage signals. The maximum signal is 10 volts. For example, a 50,000 pound maximum load corresponds to 10.0 volts. The 10% minimum or setpoint is 5,000 pounds force corresponding to a 1.0 volt signal. The span is the difference of maximum and setpoint and is therefore 45,000 pounds which is a 9 volt signal.

The cyclic loading frequency is adjustable and is indirectly related to the load range. A high frequency is desirable in order to reduce testing time but it must not be allowed to over range the hydraulic system. The 50,000 pound load range restricted the frequency to a maximum of about 15 cycles per second. A frequency of 12 Hz was selected because the machine exhibited better load control. A counter drawer in the computer control system recorded the number of completed cycles and stopped the machine when a set number of cycles had been completed. This allowed for precise control and accounting of the number of cycles between observations.

A stroke sensor also stopped the machine if the specimen separated. This interlock had to be overridden each time a new specimen was loaded or the hydraulic pumps would trip off line. A stroke controller potentiometer had to be zeroed to indicate the new null position of the chuck for each test.

Experimental Procedure

The hydraulic pump and control cabinet were energized and allowed to run and warm up for 15 minutes prior to testing. Each piece was marked for consistent mounting in the hydraulic chucks. Pieces were first centered and mounted squarely in the upper chuck using a square. The upper cross head was then unlocked and lowered until the specimen engaged the lower chuck. The lower chuck was raised at least one inch above its bottom stop to ensure freedom of movement during cycling. Once the specimen was aligned in the lower chuck, it was hydraulically locked in place.

Test parameters such as cycle frequency, load span, and load setpoint were set for the specimen. The counter drawer's preset number of cycles was set to the desired number of cycles. The stroke potentiometer zeroed and the machine started. Peak load is then monitored and fine adjusted using the setpoint potentiometer.

Initially, four HY specimens (one of each category) were tested "as is" to verify the integrity of the specimens and the procedure. Subsequently, the same four HY specimens were slotted by EDM process on a trial basis and retested to determine the range of cycles

to crack initiation and failure. The HY-80 overmatched specimen was cycled to failure to verify timely fatigue life. Based on this performance, all HY samples were EDM slotted using the original dimensions of the slit and tested at low cycle, high stress loading. HHA samples were EDM slotted straight away using the 5% depth guideline. HHA testing commenced without any trial period. Tables 9 through 33 lists cycle information, crack growth, and video mapping for each specimen.

HHA specimen tensile testing was performed using the MTS test machine. A moderate strain rate was used and the results plotted for the HHA 70 and 100 series specimens. This was necessary to ascertain the proper load window during testing. Elastic loading of the specimen required the use of the weld tensile strength vice the base material. Figure 42 shows the tensile test stress - strain plots.

Observation With the CSLM

All specimens were examined at regular intervals under the CSLM. The examination consisted of the following steps:

- ♦ visually inspect the specimen for overall condition and cracking outside of the EDM slit test area
- ♦ load and setup video cassette tape for the specific specimen
- ♦ scan the specimen with low power setting (10X and 20X) to ascertain global crack locations
- ♦ position the slide to observe the lower right corner of the EDM slit
- ♦ start the video recorder
- ♦ scan with low and higher powers to identify cracks, look for shadows and use the pencil beam 40X lens to pinpoint highlight small areas of interest
- ♦ when a crack is identified allow the video recorder time to record it, pause the recorder and measure crack length
- ♦ if desired use thermal imager for "photographs"
- ♦ if desired use surface profilometry for crack plate level changes

- ♦ use direct on screen linear measurement or if the crack is too long use stage coordinates, note magnification setting for conversion to microns
- ♦ restart video recorder and scan for more cracks, examine corners in a counterclockwise fashion
- ♦ pause video recorder and remove specimen, record video counter
- ♦ insert next specimen for examination and repeat steps

Cracks were measured in one of two ways. Once identified, short crack length was measured directly using the CSLM's measuring function. Unfortunately, this method is only for dimensions "less than the size of the monitor" because cross hairs marking the desired length can only be moved within the confines of the monitor's field of view. The second method used for the longer cracks involved traversing the length of the crack and recording the coordinates displayed by the stage position indicator. Crack length was determined by assuming a linear profile and applying the Pathagorean theorem. The conversion for stage units to microns is $1.0 \mu\text{m} = 0.001$ stage units. The stage position display indicated seven significant digits, four of which were to the right of the decimal.

Chapter 4

Results and Discussion

Crack Growth

HY EDM slit virgin base plates were tested to compare their crack growth characteristics with the welded specimens. Tables 17 and 26 list the crack length as a function of cycles and Figures 24 and 33 show the crack growth for the HY virgin base plate specimens

All welded HY and HHA specimen crack growth data is shown in Tables 9 through 33. All crack growth as a function of cycles is shown in Figures 16 through 40.

Crack Initiation From the EDM Slit

All HY specimens exhibited EDM slit crack initiation. The HHA specimens with the reinforcement intact showed no cracking. HHA specimens with the reinforcement removed were similar to the HY specimens.

All cracks initiating in the EDM slit occurred near the corner and on the side of the slit running parallel with the axis of loading, in other words, the short sides of the slit. The EDM slit corners were not perfectly square but instead had a small radius. Cracks appeared to form where the radius met the straight edge of the slit, a stress concentration area. The cracks propagated at approximately 30 to 45 degrees off the horizontal. As the cracks propagated, the plastic zone grew. Eventually, the crack fanned out into many branches which would either continue to propagate as a separate branch crack or simply

arrest. The majority of branches arrested after a short distance. Generally, each specimen had two very long cracks formed on either side of the slit. The cracks propagated at about the same rate and reached the specimen's edges approximately together. Two smaller cracks at the opposite corners propagated for a short distance and then arrested as the strain release by the larger cracks became dominant.

Mixed failure modes were indicated by a change in elevation across the crack's width. Elevation change was apparent by shadows when scanning across the crack and then by detailed profilometry which indicated mean elevation changes of three to five microns. Figure 54 shows the profilometry function and the corresponding change in mean elevation across a crack.

The small width of the specimens prevented the cracks from reaching the fusion line. No observations were made concerning overmatched weld crack arresting properties or undermatched weld's propensity to crack along the fusion line.

The HY specimens taken to total failure all indicated fatigue striations with a slight reduction in area around the ductile failure area which had the cup-cone shape. The HHA specimens failed dramatically with little reduction of area and exhibited signs of brittle fracture. Three of four HHA specimens with the weld reinforcement intact failed after a short number of cycles and in a brittle manner. No cracking was detected during the testing prior to failure. All the HHA failures occurred along the weld fusion line with no

assistance from the EDM slit. HHA specimens with weld reinforcement removed and polished exhibited modest crack propagation properties.

Crack Growth Versus Cycles

Cracks were measured at discrete steps in the number of cycles. Crack growth data versus cycles for all specimens is shown in Tables 9 through 26. All cracks were measured linearly from origin to tip. It became impractical to measure true crack length especially as the crack propagated and meandered. Definite measurement also became difficult as the plastic zone grew and the crack tip became less definite as the result of fanning out.

Elevation changes and mixed modes of failure were evident. Slip and cleavage were apparent and caused the downstream load side of the crack to drop in elevation. The elevational gradient was directly related to the number of cycles and the proximity to the initiation point of the crack. The gradient decayed to zero at the crack tip. The area behind the crack tip was comprised of a plastic zone that grew in size with the number of cycles. Figure 43 shows a small, low cycle, sharp crack tip propagation. Figures 51 and 56 show a large high cycle plastic zone and tip branching.

The overmatched HY-100 specimens showed evidence of hard protrusions pushing above the surface as cycles increased. Figures 52 and 53 show the profilometry and views of two of the asperities. These may be very hard weld inclusions but this was not verified.

Chapter 5

Conclusions and Recommendations

Conclusions

- ♦ In the HY 80 tests, undermatched specimens failed between 14,500 and 16,500 cycles, overmatched specimens failed between 21,000 and 26,500 cycles, and the base plate failed at 20,000 cycles. In the HY 100 tests, undermatched specimens failed between 16,500 and 21,000 cycles, the overmatched specimens failed between 17,800 and 21,600 cycles and the base plate failed at 32,000 cycles. All "as welded" HHA specimens failed between 8,000 and 17,500 cycles. HHA ground 100S-1 welds failed at 10,000 cycles and the 70S-6 welds failed at 17,500 cycles.
- ♦ Ground HY 80 base plate had a crack growth rate less than the undermatched specimens but greater than the overmatched specimens. The ground HY 100 base plate had a crack growth rate less than both the undermatched and overmatched specimens.
- ♦ All HY specimens exhibited the cycles to initiation to cycles to failure ratio, $N_i / N_f \sim 0.1 - 0.2$. Ground HHA specimens required many more cycles than the HY steel to initiate cracking and then failed quickly. HHA "as welded" specimens showed sudden brittle failure after only 2,000 cycles, showing the importance of flush grinding weldments to reduce stress concentrations.
- ♦ All HY specimens exhibited the anticipated initial linear crack growth rate followed by a nonlinear increasing growth rate. All specimens formed four cracks, two of which propagated to the edges and ultimately caused failure. These dominant cracks were on opposite sides of the slit and grew at a similar rate. The smaller cracks were essentially arrested as the dominant cracks strain release exceeded the strain energy needed for propagation.
- ♦ The tremendous undermatching of the HHA specimens allowed the base metal act as an elastic member and the weldment as an plastic body. Crack initiation occurred between 2,500 and 7,500 cycles for the 100S-1 and 70S-6 welds respectively. The 70S-6 welded specimens exhibited the least crack growth rate. This is most likely because of the higher toughness compared to the 100S-1 consumable.
- ♦ HHA crack growth rate was generally erratic but demonstrated an initial linear growth with subsequent nonlinear growth rate.

- ♦ 85% tensile loading was correct for this low cycle experiment. All specimens failed in a reasonable number of cycles, the maximum being 32,500 cycles required by the HY 100 base plate. This load was globally elastic but stress concentration at the machined slit produced plastic strain which led to cracking in a very low number of cycles. Crack initiation was observed at 2,000 cycles in the HY 80 specimens.
- ♦ The confocal scanning laser microscope was a valuable tool for this research and should be continued to be explored as a tool for other experiments. In situ examination increased productivity with no loss of resolution or accuracy. Video recordings and still shots taken during the examination process can be used for reexamination or teaching purposes.

Experiment Comments

- ♦ More specimens should be run to allow a meaningful statistical treatment of the data. A small population of samples, while sufficient for this experiment, is not adequate for global conclusions.
- ♦ Surface preparation of the specimens is very important. Little in the way of fatigue crack growth was gleaned from the HHA specimens that were left with intact weld reinforcements (as welded). All other specimens that were ground flush and polished performed well in regards to observing cracks. Another method worth consideration is etching of the test section to allow easier observation.
- ♦ A drawback of the confocal scanning microscope (CSLM) is the limited depth of field available during real time viewing. Specimens with an uneven surface are very difficult to read because the laser illumination can only scan a small section at a time (several hundred square microns depending on the magnification) and the illumination is oblique to the surface, making it difficult to examine irregular surfaces. Memory scan is a viable option but it is time consuming, requiring on the order of one to two minutes per viewing.

Recommendations for Future Work in This Field

- ♦ Use the CSLM for in situ examination of fatigue crack growth in an in-service ship hull girder. A long term study could detect and track cracking over the life of a ship outfitted with a designated test area that was equipped with telemetry to monitor and record data such as strain and load frequency . This experiment could provide valuable information before catastrophic fatigue cracking of the hull.

Elements	Major Function	Ultimate Tensile Strength	Elongation	Notch Toughness	Hot Cracking	Cold Cracking
Carbon	Increase strength and hardenability	Higher 1	Lower 1	Lower Ductile-Brittle 1	Lower	Lower
Manganese	Increase hardenability	Higher 0.2	Lower 0.1	Higher 0.4	Higher (from MnS)	Lower 0.15
Silicon	Deoxidizer	Higher 0.15	Lower 0.8	-	Lower 0.4	-
Phosphorous	Impurity	-	-	Lower 4	Lower 0.3	-
Sulfur	Impurity	-	-	-	Lower 3	-
Aluminum	Deoxidizer	-	-	Higher	-	-
Chromium	Increase oxidation resistance, corrosion resistance	Higher 0.1	Lower 0.25	-	-	Lower 0.1
Nickel	Increase toughness, corrosion resistance	Higher 0.05	Lower 0.05	Higher 0.3	-	Lower 0.05
Molybdenum	Strong carbide former, increase hardenability	Higher 0.5	-	Lower 1.3	-	Higher 0.02
Notes: 1) Effects are for increases in respective element 2) Numbers indicate effect relative to carbon						

Table 1: Chemical Composition Effects On Properties Of Steel [Masubuchi, 1991]

Material / Parameter	Weld Yield Strength (ksi)	Weld Tensile Strength (ksi)	Tensile Mismatch ($\Delta\%$)	Yield Mismatch ($\Delta\%$)
HY-80 Overmatched	99	105	1.9	13.8
HY-80 Undermatched	83	95	7.8	4.6
HY-100 Overmatched	122	127	7.6	14.0
HY-100 Undermatched	91	99	16.1	14.9

Table 2: Mismatch Values for HY Specimens

Material / Parameter	Approximate Weld Yield Strength (ksi)	Approximate Weld Tensile Strength (ksi)	Yield Mismatch ($\Delta\%$)	Tensile Mismatch ($\Delta\%$)
HHA 70 S-6 Specimens	16.25	20.5	1,130.7	1,119.5
HHA 100 S-1 Specimens	21.5	27.0	830.2	825.9

Table 3: Mismatch Values for HHA Specimens

Parameter	HY-100 Undermatched	HY-100 Overmatched	HY-80 Undermatched	HY-80 Overmatched
Type of Weld	GMAW	GMAW	GMAW	GMAW
Shield Gas	95%Ar, 5%CO ₂	95%Ar, 5%CO ₂	95%Ar, 5%CO ₂	95%Ar, 5%CO ₂
Shield Gas Flowrate (scfh)	45	35	45	42
Number of Passes	17	27	13	26
Wire Type	100 S-1	120 S-1	100 S-1	100 S-1
Wire Diameter (in)	0.05	0.045	0.06	0.045
Polarity	DCRP	DCRP	DCRP	DCRP
Interpass Temperature (F)	300	200	400	225
Preheat Temperature (F)	275	200	400	200
Average Wire Feed Speed (ips)	300	320	175	310
Weld Current (Amps)	280	280	340	280
Weld Voltage (Volts)	25.5	25	25.5	25.5
Torch Travel Speed (ips)	6.55	13.98	4.75	11.20
Average Heat Input (kJ/in)	65.39	30.45	109.5	38.5
Torch Oscillation Width (in)	0.5	0	0.625	0
Note: HY-100 Overmatched plate soaked at 350° F for 12 hours.				

Table 4: Selected Welding Parameters for HY Specimens

Composition (% weight)	HY-80	HY-100	HHA
C	0.17	0.20	0.31
Cr	1.16	1.5	0.52
Mn	0.30	0.1 - 0.4	0.96
Mo	0.24	0.4	0.55
Ni	2.92	3.2	1.10
P	0.018	0.025	0.015
S	0.023	0.25	0.003
Si	0.19	0.25	0.39
Al	-	-	0.025

Table 5: Base Plate Nominal Material Chemical Composition

Sample Material	Relative Direction	Tensile Strength (PSI)	Yield Strength (PSI)
HY-80	Transverse	101,000	87,000
HY-80	Longitudinal	103,000	90,000
HY-100	Transverse	119,000	107,000
HY-100	Longitudinal	118,000	105,000

Table 6: HY Base Plate Material Properties

Base Metal Material / Property	HY-80	HY-100
Tensile Strength (ksi)	102	118
80 % Tensile Strength Load (ksi)	81.6	94.4
Maximum Test Area (in ²)	0.61	0.53
90% Tensile Strength Load (ksi)	91.8	106.2
Maximum Test Area (in ²)	0.55	0.47
Notes: 1) MTS Hydraulic Chuck Capacity is 50,000 Pounds 2) Set HY Test Area to 0.5 in ²		
80 % Tensile Strength Load (kp)	40.8	47.2
90% Tensile Strength Load (kp)	45.9	53.1

Table 7: HY Specimen Sizing and Loading Data

Weld Material / Property	HHA 70S-6	HHA 100S-1
Approximate Weld Tensile Strength (ksi)	20.5	27.0
80 % Weld Tensile Strength Load (ksi)	16.4	21.6
Maximum Test Area for 80% (in ²)	0.328	0.43
90% Weld Tensile Strength Load (ksi)	18.45	24.3
Maximum Test Area for 90% (in ²)	0.37	0.48
Notes: 1) MTS Hydraulic Chuck Capacity is 50,000 Pounds 2) Set HHA Test Area to 0.1875 in ²		
80 % Weld Tensile Strength Load (kp)	3.08	4.05
90% Weld Tensile Strength Load (kp)	3.46	4.55

Table 8: HHA Specimen Sizing and Loading Data

Sample Number: HY-80 Overmatched - 1				
Number Cycles	Video Counter	Crack Position (UR, LR,UL,LL)	Crack Length (µm)	Comments
8,000	-	UR UL	-	Cracks visible, 10X mag glass
20,000	-	UR UL	-	7/64" 7/64"
22,000	-	UR UL	-	9/64" 1/8"
24,000	-	UR UL	-	11/64" 9/64"
25,000	-	UR UL	-	At edge, turning corner
26,000	-	UR UL	-	1/8" up respective side
26,460	-	UR UL	-	Failure
26,460	000-142	LL LR #1 LR #2	170 86 70	Post failure
Note: All cracks propagated 45 degrees off horizontal				

Table 9: HY 80 O/M-1 Specimen Crack Data

Sample Number: HY-80 Overmatched -2				
Number Cycles	Video Counter	Crack Position (UR, LR,UL,LL)	Crack Length (µm)	Comments
1,500	142-432	-	-	UL Initiating
2,500	432-1256	UR UL	22.3 48.9	Picture, 40X
3,500	2201-2614	UR UL	22.4 85.6	
4,500	4103-4357	LR UR UL	41.4 82.5 102.4	
6,000	5824-5959	LR UR UL	167.7 124.7 132.4	
6,000	6332-6517	LR UR UL	222.7 240.2 169.1	
11,000	6848-7129	LR UR UL LL	381.5 317.6 186.1 550.3	
13,500	7606-7813	LR UR UL LL	842.1 351.4 191.0 946.8	
18,500	8224-8544	LR UR UL LL	1968.3 356.2 191.0 1133.4	
23,500	Not Used	LR UR UL LL	4301.1 361.1 190.1 4110.5	

Table 10: HY 80 O/M-2 Specimen Crack Data

Sample Number: HY-80 Overmatched -3				
Number Cycles	Video Counter	Crack Position (UR, LR,UL,LL)	Crack Length (µm)	Comments
2,000	1256-1736	-	-	-
3,000	2614-3330	UR UL LL	43.0 33.9 36.4	
3,000	4357-5304	LR UR UL LL	110.6 50.7 34.5 70.0	
5,500	5959-6224	LR UR UL LL	195.2 88.0 90.3 136.9	
8,000	6517-6717	LR UR UL LL	247.6 119.4 277.5 234.4	
10,500	7129-7404	LR UR UL LL	363.4 181.9 280.8 433.3	
13,000	7813-8021	LR UR UL LL	599.1 182.8 281.1 747.4	
13,000	8544-8908	LR UR UL LL	1672.8 193.9 283.0 1693.7	
23,000	Not Used	LR UR UL LL	3261.4 195.0 285.0 3252.6	

Table 11: HY 80 O/M-3 Specimen Crack Data

Sample Number: HY-80 Overmatched -4				
Number Cycles	Video Counter	Crack Position (UR, LR,UL,LL)	Crack Length (μm)	Comments
2,000	1736-2201	UR #1 UR #2	8.5 8.5	
3,000	3330-4103	LR UR #1 UR #2 LL	33.4 67.0 75.5 58.2	
4,000	5304-5824	LR UR LL	78.7 106.5 81.9	UR #1 and UR #2 merged
5,500	6224-6332	LR UR LL	84.8 113.7 82.2	
8,000	6717-6848	LR UR LL	93.0 309.0 92.6	
10,500	7404-7606	LR UR UL LL	150.1 666.8 731.0 109.3	
13,000	8021-8224	LR UR UL LL	150.1 1093.3 1161.7 114.5	
18,000	8908-9305	LR UR UL LL	155.0 2438.8 2506.2 114.5	
21,000	Not Used	LR UR UL LL	158.1 3887.0 3962.7 116.3	

Table 12: HY 80 O/M-4 Specimen Crack Data

Sample Number: HY-80 Undermatched -1				
Number Cycles	Video Counter	Crack Position (UR, LR,UL,LL)	Crack Length (µm)	Comments
1,500	000-400	-	-	-
2,500	1623-2111	LR UR UL	16.6 100.9 49.7	LL Initiating
3,500	3633-4533	LR UR UL LL	37.3 210.4 257.1 15.1	
4,500	6138-6746	LR UR UL LL	61.4 320.8 343.0 79.5	
8,000	8649-8904	LR UR UL LL	108.1 381.1 345.7 115.9	
8,000	9642-9911	LR UR UL LL	261.3 507.5 465.6 122.4	
10,500	10709-11021	LR UR UL LL	551.5 1114.4 550.5 126.4	
13,000	11519-11719	LR UR UL LL	694.2 1626.9 1495.2 129.0	
15,000	12436-12617	LR UR UL LL	694.2 2072.0 2209.2 129.0	
16,500	Not Used	LR UR UL LL	694.2 3090.5 3868.4 129.0	

Table 13: HY 80 U/M-1 Specimen Crack Data

Sample Number: HY-80 Undermatched -2				
Number Cycles	Video Counter	Crack Position (UR, LR,UL,LL)	Crack Length (μm)	Comments
1,500	400-707	-	-	-
2,500	2111-2748	LR UR UL LL	51.7 57.9 44.1 44.0	Picture, 40X
3,500	4533-5141	LR UR UL LL	160.5 200.1 83.6 50.2	
4,500	6746-7700	LR UR UL LL	219.1 246.6 194.2 155.2	
5,500	9044-9323	LR UR UL LL #1 LL #2	349.2 270.2 243.0 178.9 66.1	
8,000	9911-10157	LR UR UL LL #1 LL #2	539.1 273.4 751.1 182.0 68.3	
10,500	11021-11201	LR UR UL LL #1 LL #2	1700.3 376.9 1216.9 207.5 119.4	
13,000	11719-12132	LR UR UL LL	2952.8 384.3 2509.8 268.7	LL#1 and LL#2 merge
14,550	-	-	-	Failure

Table 14: HY 80 U/M-2 Specimen Crack Data

Sample Number: HY-80 Undermatched -3				
Number Cycles	Video Counter	Crack Position (UR, LR,UL,LL)	Crack Length (μm)	Comments
1,500	707-915	-	-	-
2,500	2748-3254	-	-	-
3,500	5141-5741	LR UR #1 UR #2 UL	175.5 30.9 61.3 69.7	
4,500	7700-8117	LR #1 LR #2 UR #1 UR #2 UL LL	204.9 43.5 60.7 66.0 170.8 105.2	
5,500	8904-9044	LR #1 LR #2 UR #1 UR #2 UL LL	568.2 45.1 90.9 151.7 184.5 190.9	LR #1 and #2 merge
8,000	10157-10501	LR UR #1 UR #2 UL LL	796.9 91.7 160.0 339.1 492.8	
10,500	11201-11350	LR UR #1 UR #2 UL LL	1349.5 102.5 171.8 429.5 628.0	
13,000	12132-12326	LR UR #1 UR #2 UL LL	2073.8 102.1 195.7 491.7 1236.0	
15,000	12617-12803	LR UR #1 UR #2 UL LL	2662.5 179.4 296.7 499.2 1963.4	

Table 15: HY 80 U/M-3 Specimen Crack Data

Sample Number: HY-80 Undermatched -4				
Number Cycles	Video Counter	Crack Position (UR, LR,UL,LL)	Crack Length (µm)	Comments
10,130	915-1623	UR LL	255.9 306.2	
11,130	3254-3633	LR UR UL LL	137.2 1308.5 166.6 1256.7	Picture: plastic zone 20X
12,130	5741-6138	LR UR UL LL	252.5 1749.8 174.2 1455.1	
13,130	8117-8649	LR UR UL LL	260.4 2043.1 177.3 1716.0	Weld toe crack formed Branching
14,130	9323-9642	LR UR UL LL	263.9 2490.7 177.7 2106.3	
16,350	-	-	-	Failure UR LL Cracks reached edge at 16,000 cycles.

Table 16: HY 80 U/M-4 Specimen Crack Data

Sample Number: HY-80 Virgin Base Plate				
Number Cycles	Video Counter	Crack Position (UR, LR,UL,LL)	Crack Length (μm)	Comments
2,500	10501-10709	LR UR UL LL	31.9 26.5 50.5 33.7	Picture, 100X
5,000	11350-11519	LR UR UL LL	86.5 125.5 136.2 64.9	Large plastic zone
7,500	12326-12436	LR UR UL LL	363.9 183.8 281.6 144.0	Picture, 20X
12,500	12803-12948	LR UR UL LL	1260.7 196.9 1133.9 171.7	
18,500	Not Used	LR UR UL LL	3109.6 197.8 3069.5 182.5	
20,000	Not Used	LR UR UL LL	4750.7 199.5 4624.3 189.6	

Table 17: HY 80 Virgin Base Plate Specimen Crack Data

Sample Number: HY-100 Overmatched -1				
Number Cycles	Video Counter	Crack Position (UR, LR,UL,LL)	Crack Length (μm)	Comments
160	-	-	-	
1,500	000-145	-	-	
3,000	531-836	UL	78.8	Picture 40X
4,500	2118-2943	UL	149.4	
6,000	4905-5708	LR UR UL LL	119.2 124.0 197.4 149.3	
7,500	7945-8137	LR UR UL LL	355.1 124.0 223.3 242.9	
10,000	8529-8745	LR UR UL LL	700.2 216.2 325.4 524.1	
12,500	9705-10159	LR UR UL LL	1246.4 217.1 338.3 985.5	
17,500	10859-11107	LR UR UL LL	2681.8 218.1 351.4 1090.7	
20,500	11615-11947	LR UR UL LL	3992.0 221.9 351.5 3400.2	
21,500	Not Used	LR UR UL LL	5295.0 226.8 351.7 4121.9	LR crack reached edge Failure imminent

Table 18: HY 100 O/M-1 Specimen Crack Data

Sample Number: HY-100 Overmatched -2				
Number Cycles	Video Counter	Crack Position (UR, LR,UL,LL)	Crack Length (μm)	Comments
8,230	145-348	-	-	-
9,730	836-1221	LR UR UL	438.9 320.0 747.5	Picture, 10X
11,230	2943-3627	LR UR UL	776.5 335.9 1096.1	UR UL large plastic tip zones
12,730	5708-7300	LR UR UL	1018.6 338.1 1434.2	Picture: asperities along lower edge, 100X
14,230	8137-8406	LR UR UL	1114.3 364.4 1646.6	
16,730	8845-9141	LR UR UL	1672.6 372.3 2721.2	
19,230	10159-10446	LR UR UL LL	3299.3 376.6 3602.7 50.1	
21,630	-	-	-	Failure

Table 19: HY 100 O/M-2 Specimen Crack Data

Sample Number: HY-100 Overmatched -3				
Number Cycles	Video Counter	Crack Position (UR, LR,UL,LL)	Crack Length (µm)	Comments
1,500	348-531	-	-	-
3,000	1221-1730	UL LL	12.5 14.8	
4,500	3627-4146	LR UR UL LL	94.8 84.3 71.1 65.8	
6,000	7300-7635	LR UR UL LL	195.2 160.8 137.4 71.5	
7,500	8406-8535	LR UR UL LL	338.9 201.3 233.1 89.7	
10,000	9357-9705	LR UR UL LL	594.2 209.2 482.3 106.4	
10,000	10446-10624	LR UR UL LL	1003.7 219.3 874.0 106.4	
17,500	11107-11319	LR UR UL LL	2355.4 219.3 2169.9 113.6	Picture, 10X
20,500	11947-12301	LR UR UL LL	3697.2 223.2 3601.1 113.6	
21,500	Not Used	LR UR UL LL	4060.3 246.1 5022.6 113.6	UL crack reached edge Failure imminent

Table 20: HY 100 O/M-3 Specimen Crack Data

Sample Number: HY-100 Overmatched -4				
Number Cycles	Video Counter	Crack Position (UR, LR, UL, LL)	Crack Length (μm)	Comments
1,500	1730-2118	UR LL	54.4 77.4	
3,000	4146-4905	UR LL	55.7 83.4	
4,500	7635-7945	UR UL LL	63.5 302.9 85.6	
6,000	8535-8529	UR UL LL	468.6 513.8 94.0	
8,500	9141-9357	UR UL LL	1047.9 981.1 95.4	
11,000	10624-10859	UR UL LL	1717.8 1682.8 95.8	
16,000	11319-11615	UR UL LL	4026.9 4067.7 98.4	
17,840	-	-	-	Failure

Table 21: HY 100 O/M-4 Specimen Crack Data

Sample Number: HY-100 Undermatched -1				
Number Cycles	Video Counter	Crack Position (UR, LR,UL,LL)	Crack Length (µm)	Comments
1,500	000-255	-	-	-
3,000	1005-1331	UL LL	96.9 25.7	
4,000	2805-3500	LR UR UL LL #1 LL #2	179.2 156.6 107.1 47.9 50.5	
5,000	4456-4915	LR UR UL LL #1 LL #2	226.4 236.9 277.1 60.6 64.5	
6,500	5956-6127	LR UR UL LL #1 LL #2	232.2 375.5 323.2 70.5 66.0	
9,000	6922-7205	LR UR UL LL #1 LL #2	302.1 755.7 796.9 80.7 106.7	
11,500	7901-8155	LR UR UL LL #1 LL #2	365.1 1274.4 1195.6 81.3 122.0	
16,500	9251-9521	LR UR UL LL #1 LL #2	365.4 - - 83.9 125.0	Failure imminent: UR and UL cracks reached edges. Weld toe crack forms.

Table 22: HY 100 U/M-1 Specimen Crack Data

Sample Number: HY-100 Undermatched -2				
Number Cycles	Video Counter	Crack Position (UR, LR,UL,LL)	Crack Length (μm)	Comments
1,500	255-503	-	-	
2,500	1331-1810	UL	55.6	Picture 40X
3,500	3500-3426	LR UL LL	65.7 90.0 87.7	
4,500	4915-5259	LR UR UL LL	133.0 66.9 156.3 90.1	
6,000	6127-6256	LR UR UL LL	245.7 112.3 217.4 219.8	
8,500	7205-7432	LR UR UL LL	477.5 250.3 348.9 489.3	
11,000	8155-8441	LR UR UL LL	1022.4 261.0 384.7 981.1	
16,000	9521-9806	LR UR UL LL	2552.9 261.0 385.9 2307.4	
16,500	10446-10845	LR UR UL LL	2712.3 261.0 415.5 2609.9	
18,500	Not Used	LR UR UL LL	4452.1 261.1 431.1 4256.6	LR crack at edge

Table 23: HY 100 U/M-2 Specimen Crack Data

Sample Number: HY-100 Undermatched -3				
Number Cycles	Video Counter	Crack Position (UR, LR, UL, LL)	Crack Length (μm)	Comments
1,500	503-823	-	-	
2,500	1810-2217	UR UL LL	97.3 63.5 86.1	
3,500	3426-4002	UR UL LL	103.6 89.7 86.9	
4,500	5259-5633	UR UL LL	121.0 153.8 165.5	LL branching
6,000	6256-6431	LR UR UL LL	145.2 169.5 171.5 168.4	
8,500	7432-7703	LR UR UL LL	292.1 311.8 187.4 653.6	
11,000	8441-8804	LR UR UL LL	831.0 420.3 211.6 1362.4	
13,500	9806-10014	LR UR UL LL	1590.8 459.9 212.9 2042.0	
16,000	10845-11209	LR UR UL LL	2555.8 461.6 214.8 2600.4	
19,000	Not Used	LR UR UL LL	5102.5 468.7 197.6 5431.8	LL at edge

Table 24: HY 100 U/M-3 Specimen Crack Data

Sample Number: HY-100 Undermatched -4				
Number Cycles	Video Counter	Crack Position (UR, LR,UL,LL)	Crack Length (µm)	Comments
1,500	823-1005	-	-	-
2,500	2217-2805	LR UR UL	51.5 39.3 56.7	
4,500	4002-4456	LR UR UL LL	82.4 131.3 96.5 84.4	
5,500	5633-5956	LR UR UL LL	123.2 172.4 142.6 106.9	
4,500	6431-6556	LR UR UL LL	222.6 292.8 233.0 129.9	
4,500	7703-7901	LR UR UL LL	280.0 466.4 488.4 153.6	
12,000	8804-9007	LR UR UL LL	334.3 700.0 727.3 158.8	
16,000	10014-10325	LR UR UL LL	1012.6 1175.1 1711.2 164.7	
18,000	11209-11557	LR UR UL LL	1267.7 1206.9 2316.8 166.5	
21,000	Not Used	LR UR UL LL	2820.7 1370.5 4629.4 169.1	

Table 25: HY 100 U/M-4 Specimen Crack Data

Sample Number: HY-100 Virgin Base Plate				
Number Cycles	Video Counter	Crack Position (UR, LR,UL,LL)	Crack Length (μm)	Comments
2,500	6556-6920	LR	48.0	
5,000	9007-9251	LR UL	108.4 40.0	
7,500	10325-10446	LR UL LL	153.8 90.2 60.2	
12,500	11557-11653	LR UL LL	211.0 275.3 66.2	
17,500	Not Used	LR UR UL LL	382.1 23.5 452.2 120.3	
22,500	11653-11853	LR UR UL LL	974.4 201.9 831.6 244.6	
27500	11853-12053	LR UR UL LL	1772.7 260.7 1868.2 249.4	
32500	12053-12253	LR UR UL LL	3015.9 260.7 2873.4 249.4	

Table 26: HY 100 Virgin Base Plate Crack Data

Sample Number: HHA 100 S-1				
Number Cycles	Video Counter	Crack Position (UR, LR,UL,LL)	Crack Length (µm)	Comments
2,000	00-131	LL	4.2	
7,000	935 - 1243	LL	27.2	
8,080	-	-	-	Brittle failure along lower weld fusion line

Table 27: HHA 100 S-1 Specimen Crack Data

Sample Number: HHA 100 S-2				
Number Cycles	Video Counter	Crack Position (UR, LR,UL,LL)	Crack Length (µm)	Comments
5,000	131 - 438	LR	68.2	
		UR	97.3	
		UL	130.4	
		LL	454.1	
10,000	1243 - 1643	LR	75.0	
		UR	145.1	
		UL	131.1	
		LL	450.0	
10,880	-	-	-	Brittle failure along lower weld fusion line

Table 28: HHA 100 S-2 Specimen Crack Data

Sample Number: HHA 100 S-4				
Number Cycles	Video Counter	Crack Position (UR, LR,UL,LL)	Crack Length (μm)	Comments
2,500	438 - 551	UR UL	17.7 45.6	
7,500	1643 - 1910	LR UR UL LL	98.3 345.6 452.0 82.1	
10,000	1910 - 2347	LR UR UL LL	105.6 846.9 1112.7 85.0	Picture 40X

Table 29: HHA 100 S-4 Specimen Crack Data

Sample Number: HHA 70 S-1				
Number Cycles	Video Counter	Crack Position (UR, LR,UL,LL)	Crack Length (μm)	Comments
5,000	00 - 403	None	-	
10,000	935 - 1225	None	-	
10,620	-	-	-	Brittle failure along upper weld fusion line

Table 30: HHA 70 S-1 Specimen Crack Data

Sample Number: HHA 70 S-2				
Number Cycles	Video Counter	Crack Position (UR, LR,UL,LL)	Crack Length (μm)	Comments
7,500	403 -630	UR	35.1	
12,500	1225 - 1500	UR	50.8	
17,500	1829 - 2110	LR UR	35.5 80.8	

Table 31: HHA 70 S-2 Specimen Crack Data

Sample Number: HHA 70 S-4				
Number Cycles	Video Counter	Crack Position (UR, LR,UL,LL)	Crack Length (µm)	Comments
5,000	630 - 757	UL	16	
12,500	525 - 704	LR UR UL LL	125.3 54.4 44.9 198.9	Picture 40X
17,500	241 - 454	LR UR UL LL	383.7 85.6 61.4 623.9	

Table 32: HHA 70 S-4 Specimen Crack Data

Sample Number: HHA 70 S-5				
Number Cycles	Video Counter	Crack Position (UR, LR,UL,LL)	Crack Length (µm)	Comments
7,500	757 -933	None	-	
12,500	1639 - 1829	UR UL LL	145.4 114.0 84.0	UR forking
17,500	2323 - 2740	LR UR UL LL	21.1 335.2 333.2 98.5	

Table 33: HHA 70 S-5 Specimen Crack Data

Category	Parameter / Data
Manufacturer / Model	Lasertec Corporation Model 1LM11 Scanning Laser Microscope
Resolution	0.25 mm with Nikon Optiphot 100x 0.95NA Objective
He-Ne Laser Wavelength	6328 Angstroms
Laser Output Power	1.50 mW at laser body 0.14 mW at exit of 5x 0.1NA objective
Scanning Frequency	Vertical: 60 Hz Horizontal: 15730 Hz Interlace: 2:1
Minimum Measurement Unit	0.01 mm
Measurement Repeatability	+/- .03 mm (3s)

Table 34: Selected CSLM Operating Parameters and Data

Objective Lens Magnification	Magnification on Video Monitor	Field of View (μm)	Scan Line Density ($\mu\text{m}/\text{line}$)
10	600	410 x 325	0.68
20	1,200	205 x 163	0.34
30	2,400	125 x 82	0.17
50	3,000	82 x 65	0.14
80	6,000	51 x 41	0.08
100	6,000	41 x 32	0.07

Table 35: CSLM Image Display Information

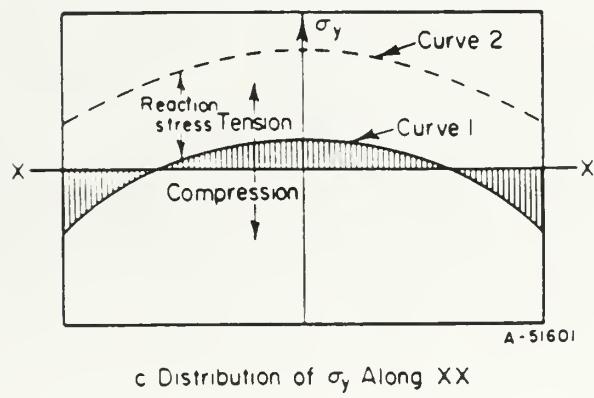
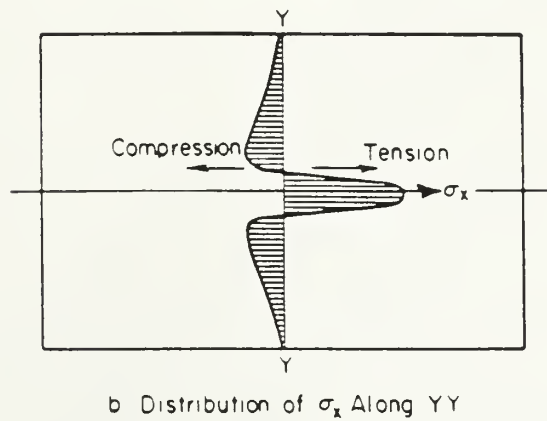
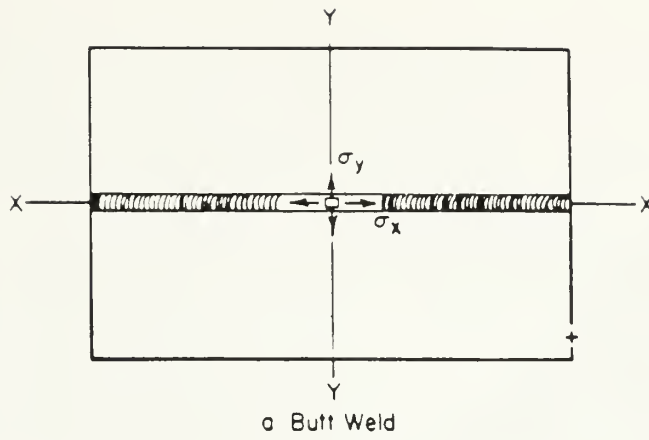


Figure 1: Residual Stress Distribution in a Butt Weld

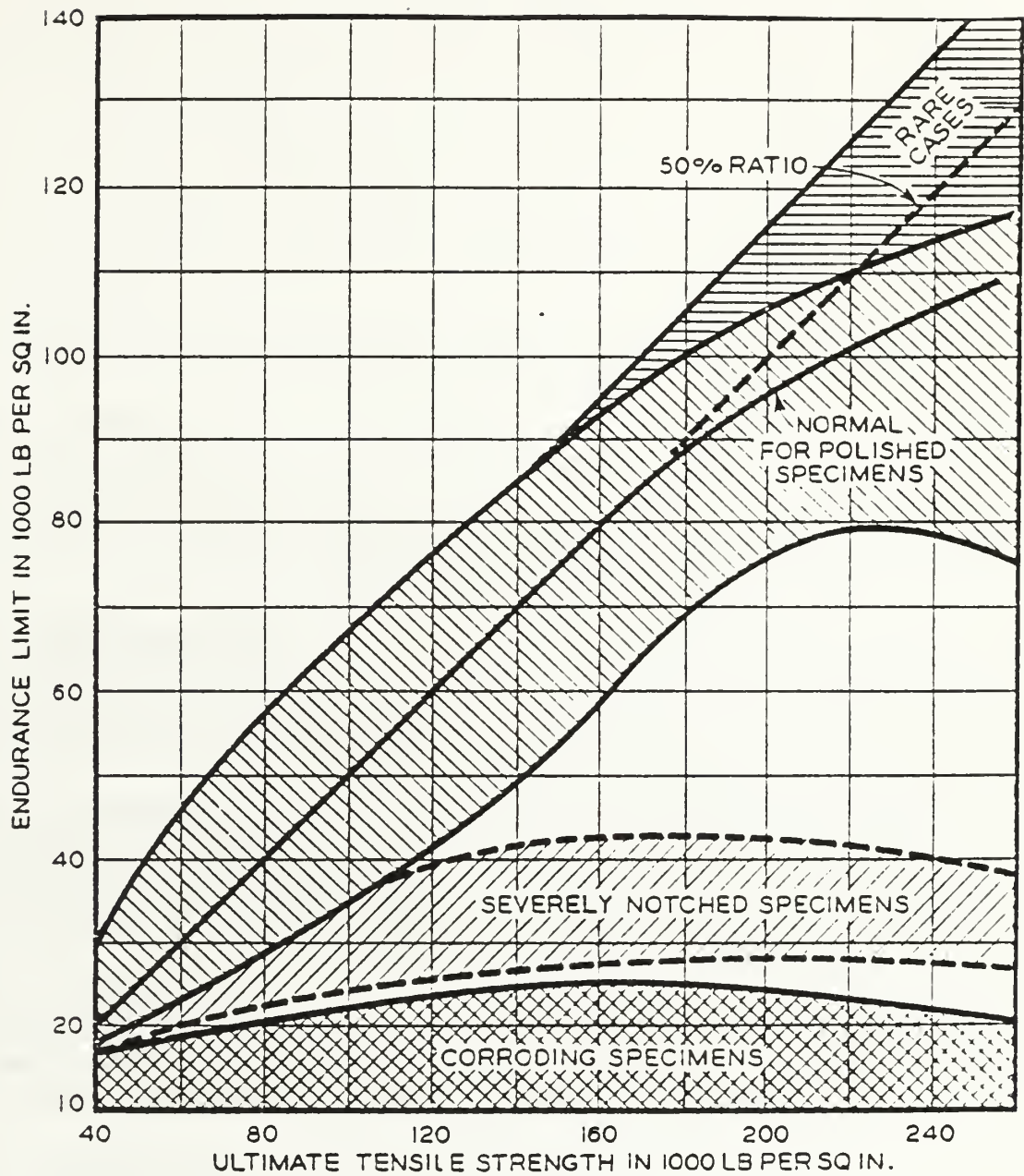


Figure 2: Endurance Limit Versus Ultimate Tensile Strength

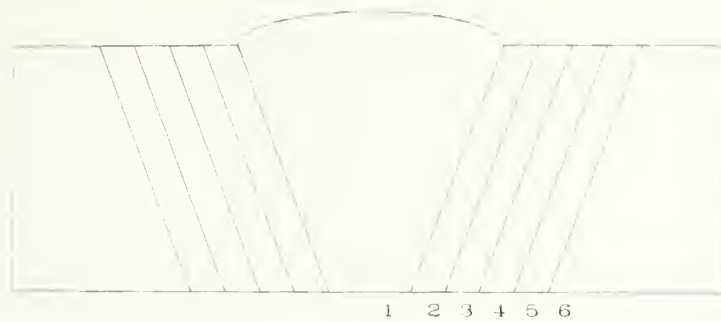


Figure 3: Common Weldment Heat Affected Zone (HAZ) Characteristics.

Zone 1: Weld Metal

- ♦ as-cast microstructure
- ♦ peak temperature above 1650 C
- ♦ toughness is situationally dependent. Microstructurally inferior to the plate but may have better toughness through enriched chemistry

Zone 2: Grain Coarsened HAZ

- ♦ large prior austenite grains
- ♦ peak temperature above 1100 C
- ♦ toughness is much worse than plate

Zone 3: Grain Refined HAZ

- ♦ small prior austenite grains
- ♦ peak temperature above 900 C
- ♦ toughness close to or better than plate

Zone 4: Intercritical HAZ

- ♦ duplex microstructure
- ♦ peak temperature above 700 C
- ♦ toughness depends on grain size and microstructural constituents

Zone 5: Subcritical HAZ

- ♦ spherodized, or microstructurally identical to plate
- ♦ peak temperature between 600 C and 700 C
- ♦ toughness depends on plate initial microstructure:
 - a. embrittlement in rimmed or semi-killed plate caused by strain aging
 - b. tempering in martensitic plate
 - c. spherodized in fully killed plate

Zone 6: Base Plate

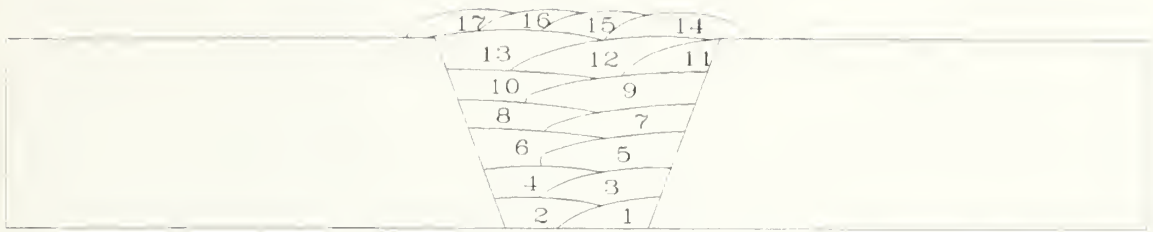


Figure 4: HY-100 Undermatched Specimen Weld Bead Arrangement

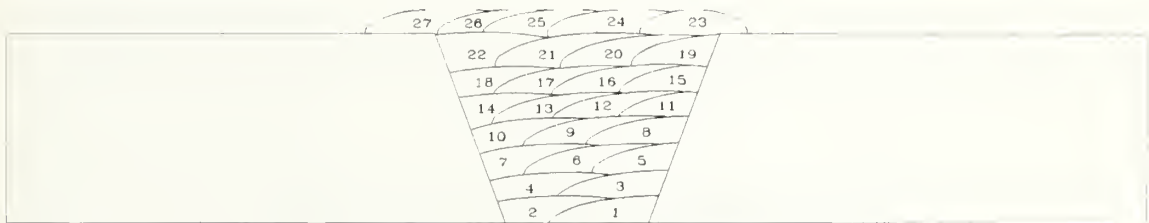


Figure 5: HY-100 Overmatched Specimen Weld Bead Arrangement

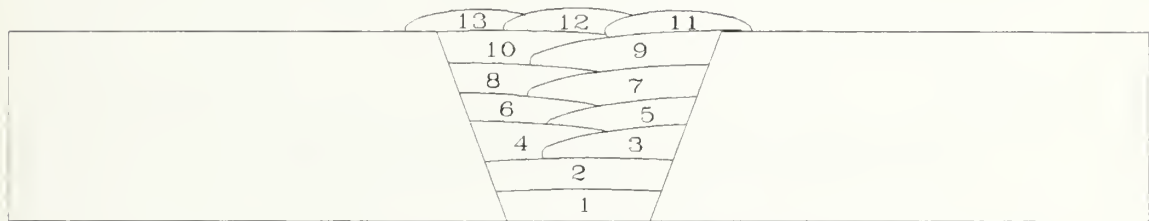


Figure 6: HY-80 Undermatched Specimen Weld Bead Arrangement

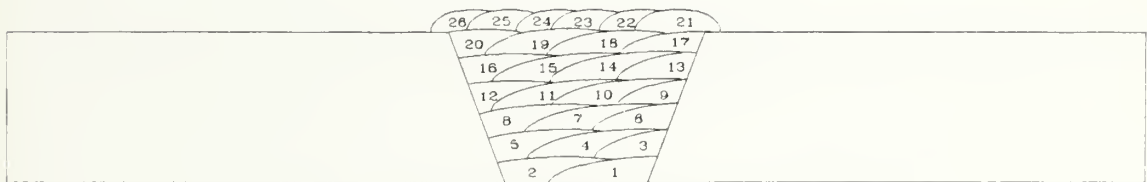


Figure 7: HY-80 Overmatched Specimen Weld Bead Arrangement

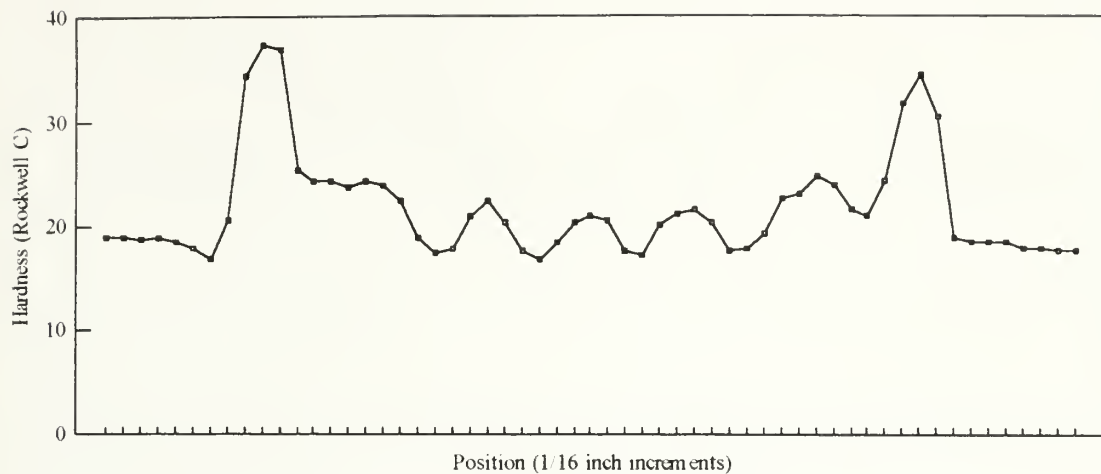


Figure 8: HY-80 Overmatched Hardness Profile

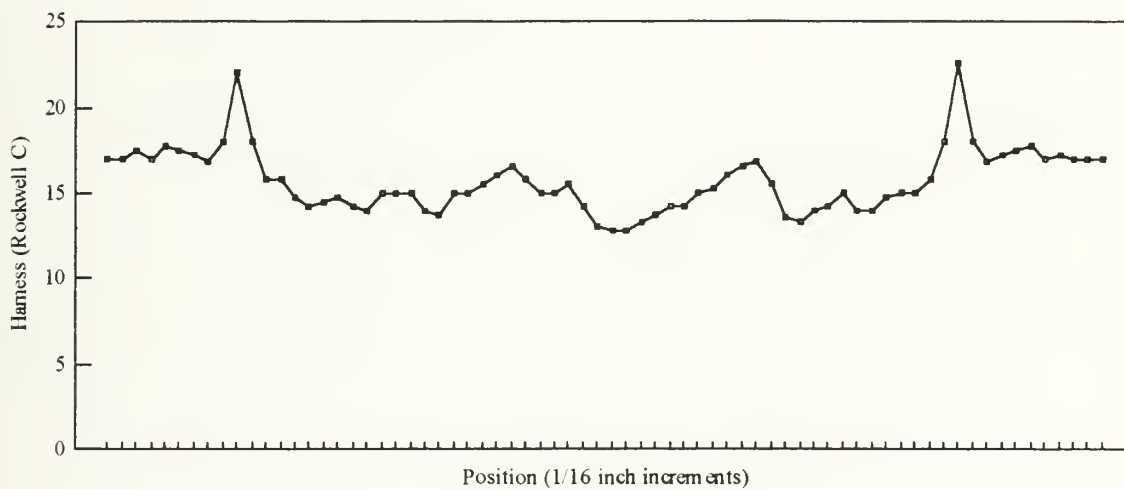


Figure 9: HY-80 Undermatched Hardness Profile

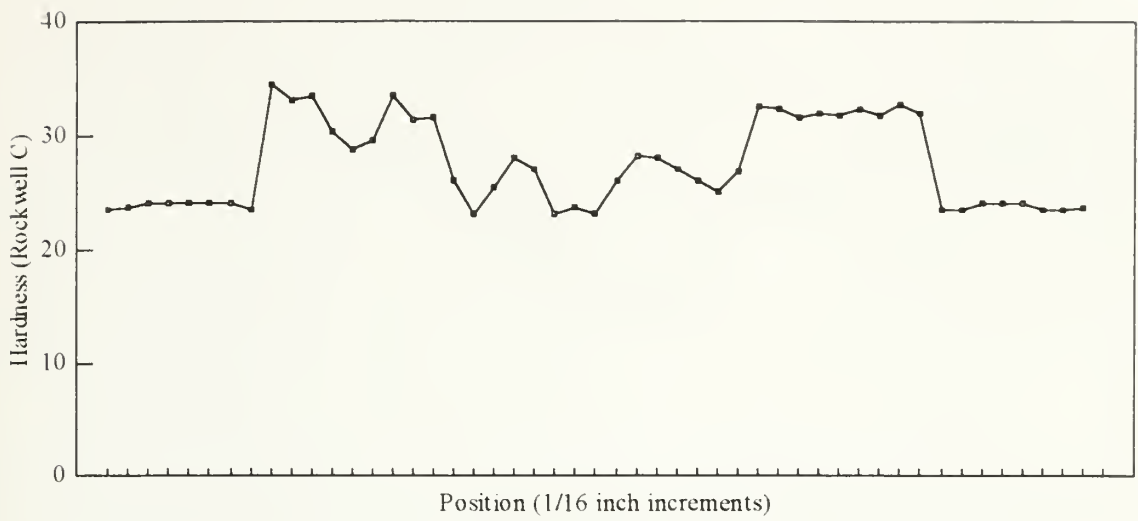


Figure 10: HY-100 Overmatched Hardness Profile

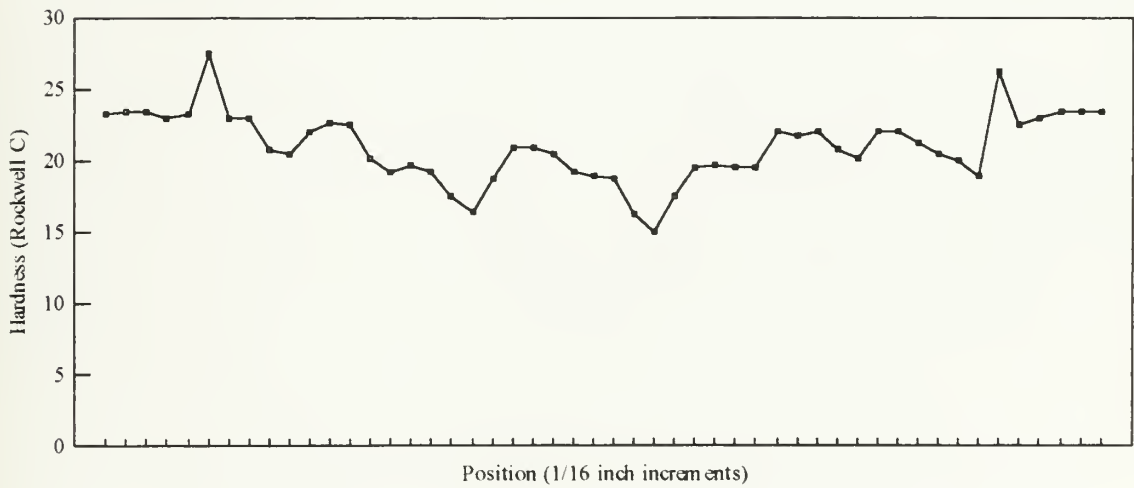


Figure 11: HY-100 Undermatched Hardness Profile

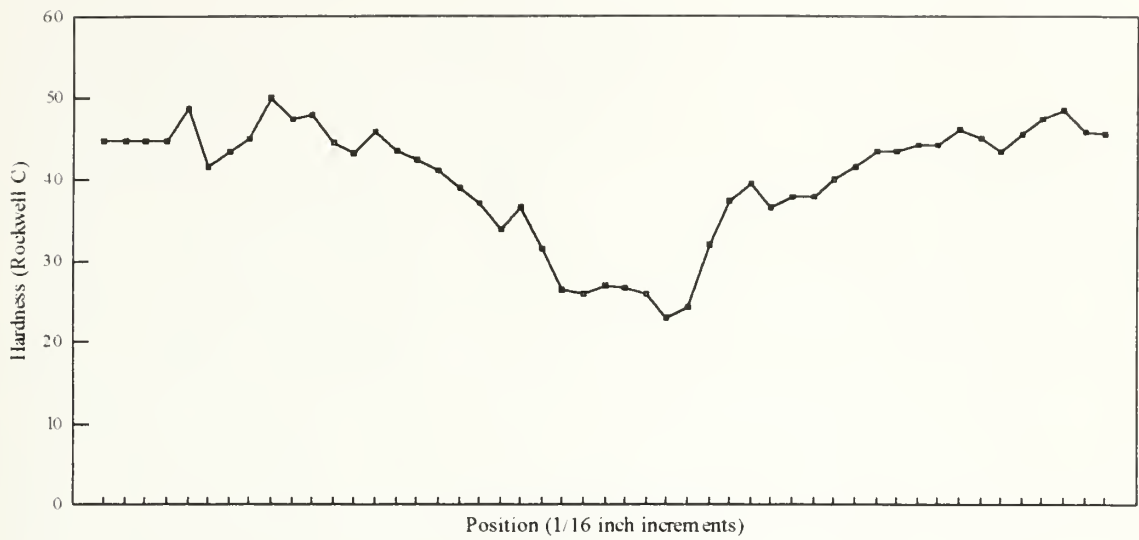


Figure 12: Hardness Profile of HHA With ER100S-1 Consumable

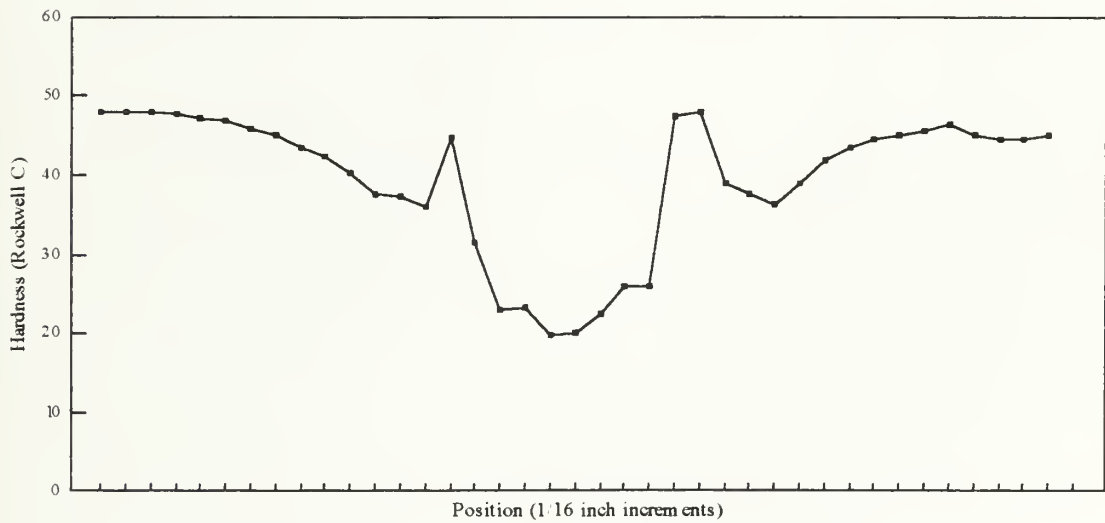


Figure 13: Hardness Profile of HHA With ER70S-6 Consumable

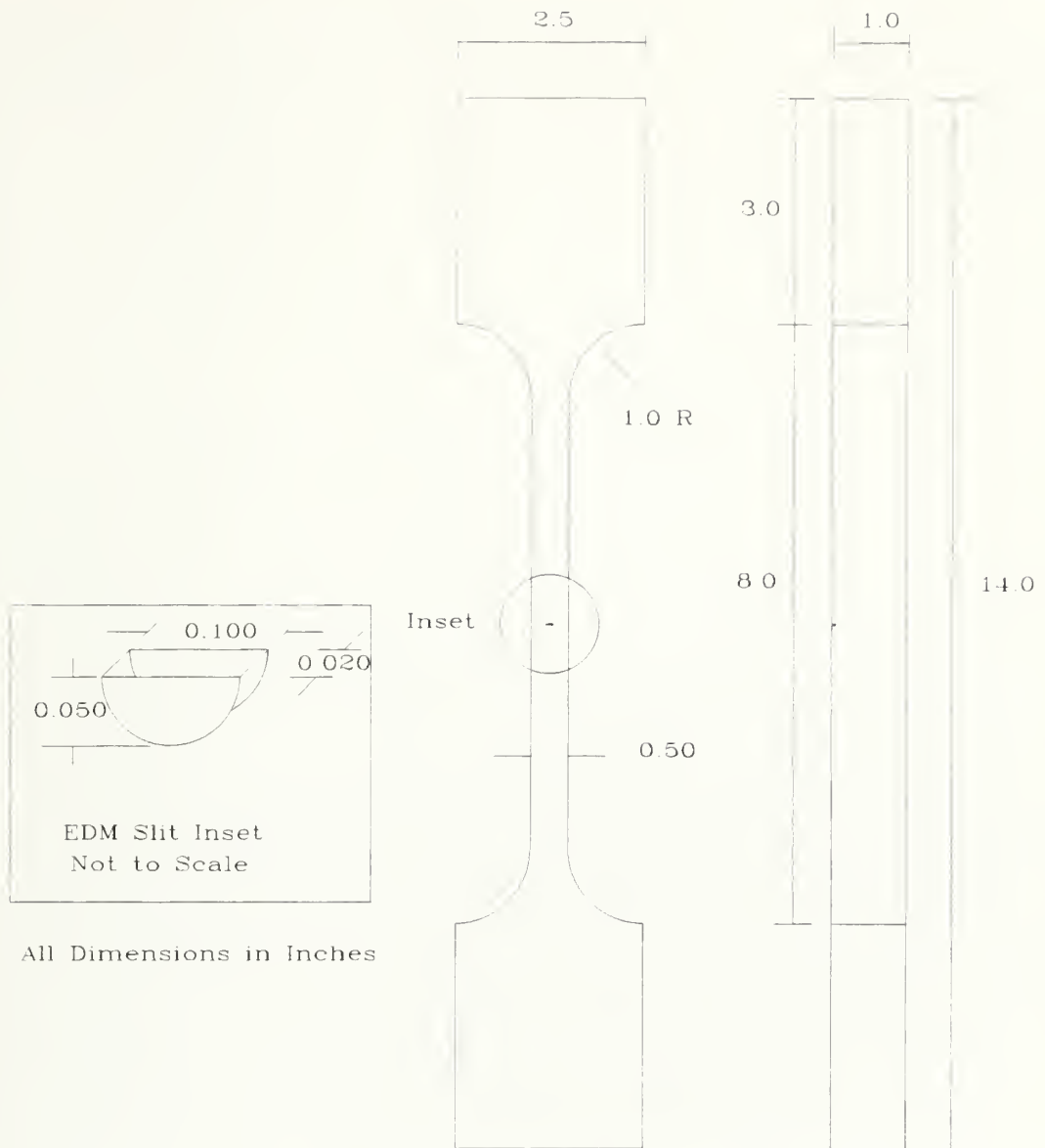


Figure 14: HY Specimen Design

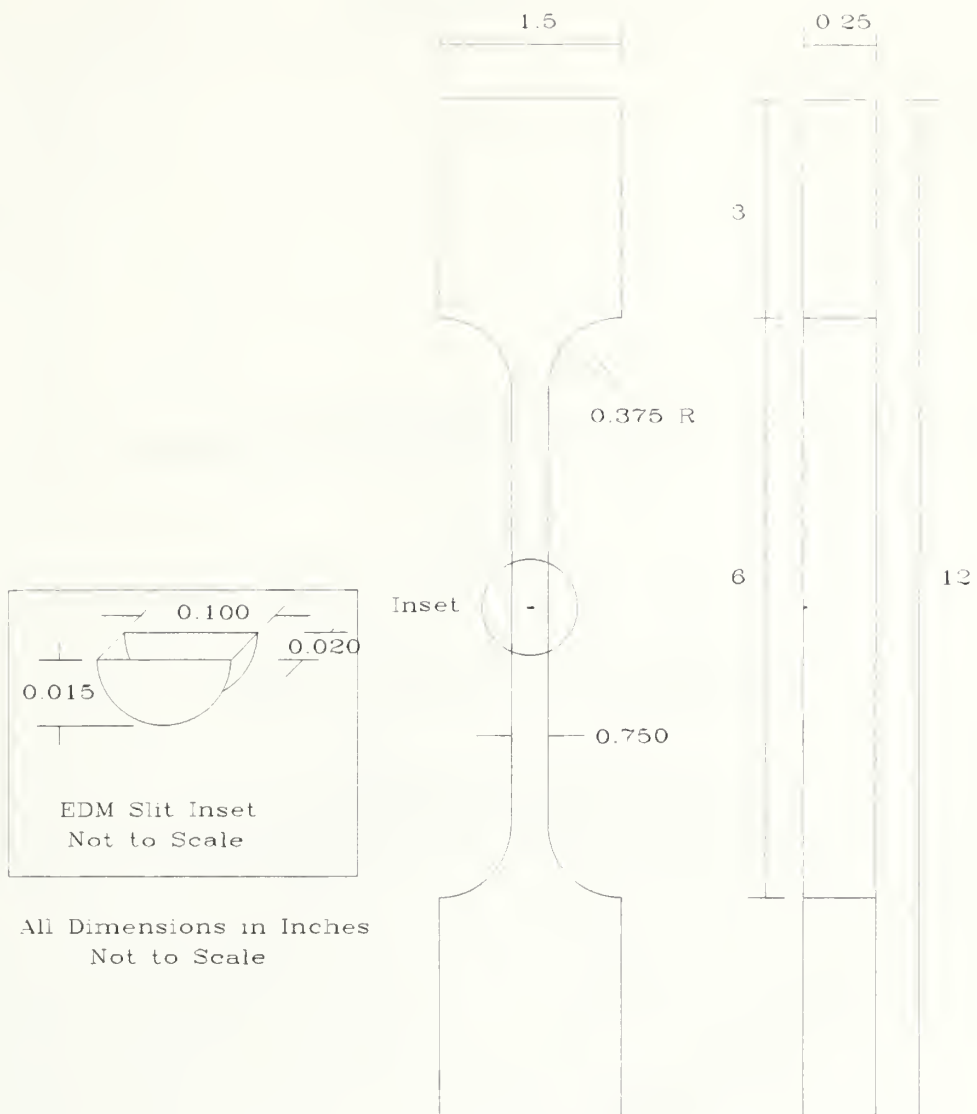


Figure 15: HHA Specimen Dimensions

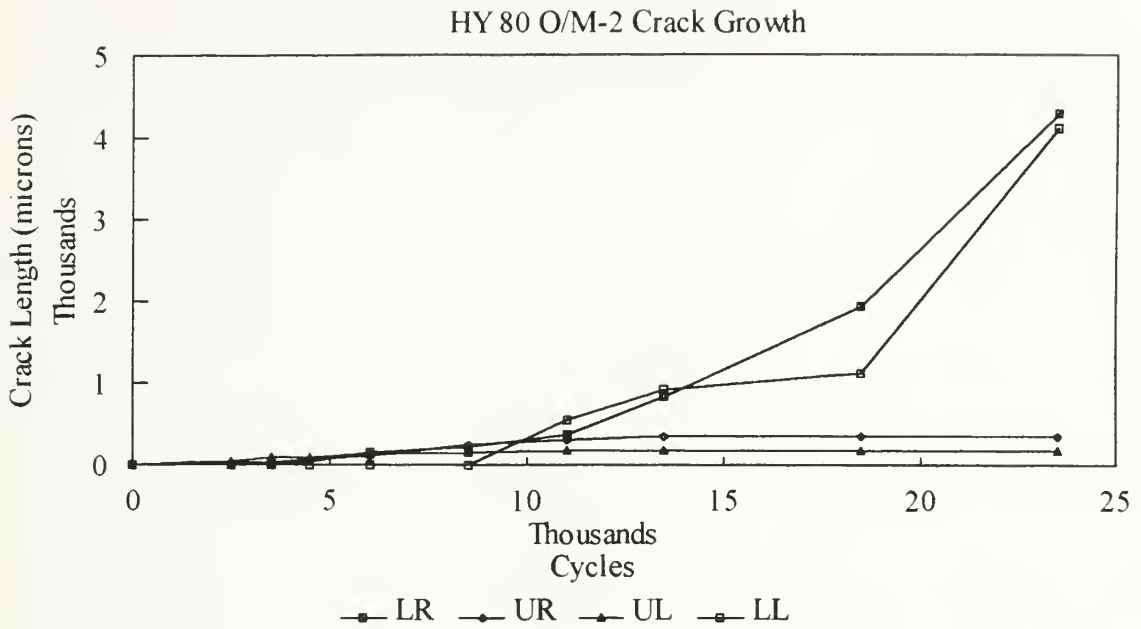


Figure 16: HY 80 O/M -2 Crack Growth

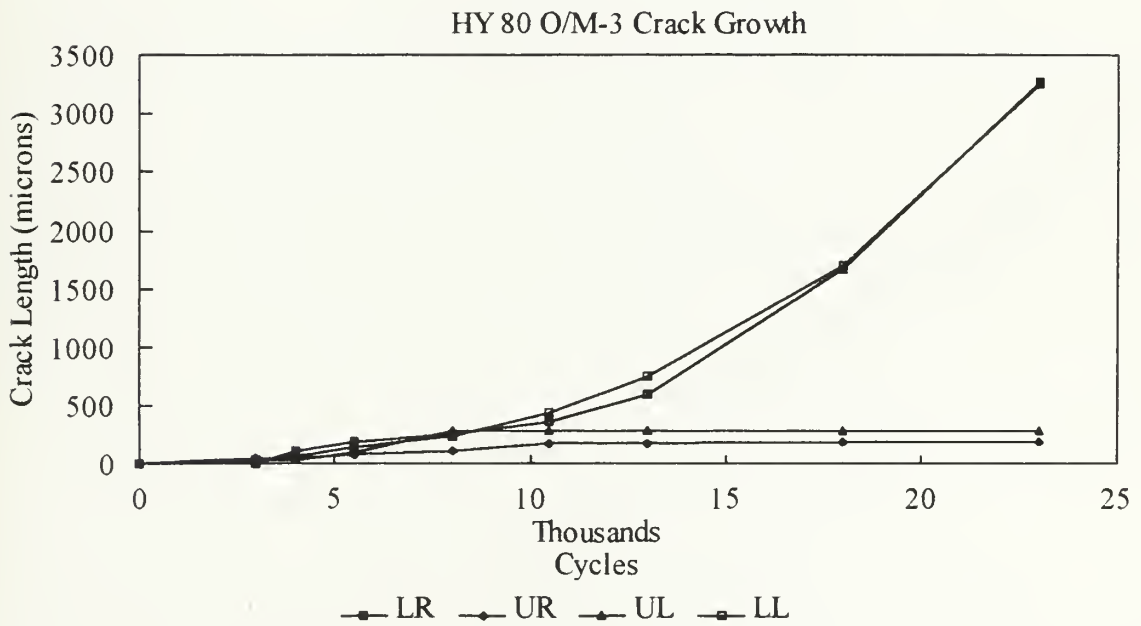


Figure 17: HY 80 O/M-3 Crack Growth

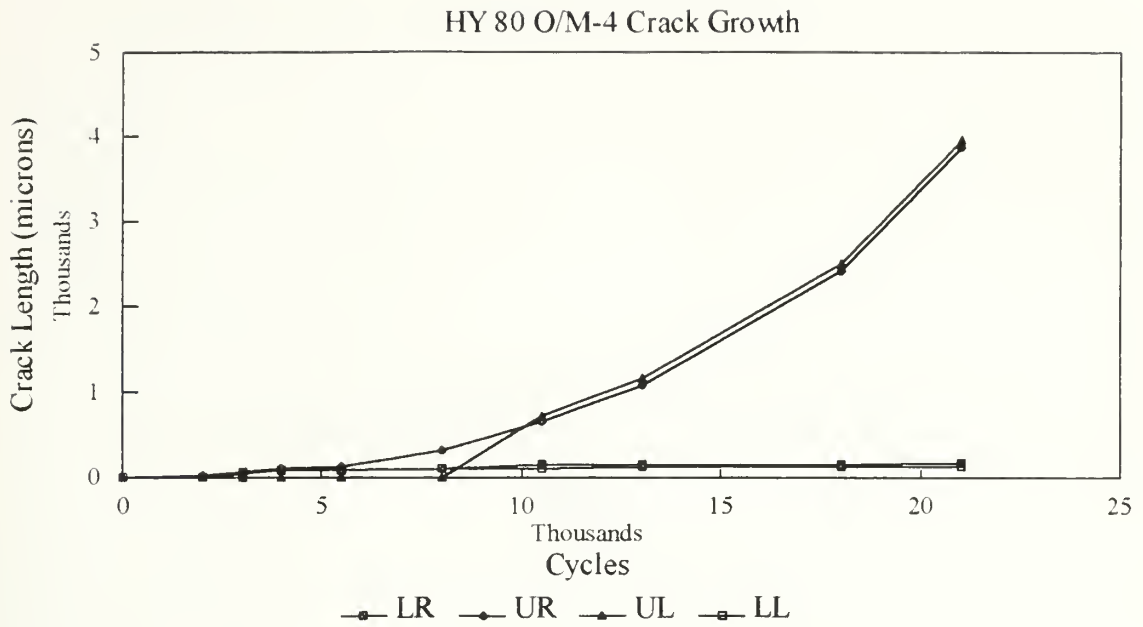


Figure 18: HY 80 O/M-4 Crack Growth

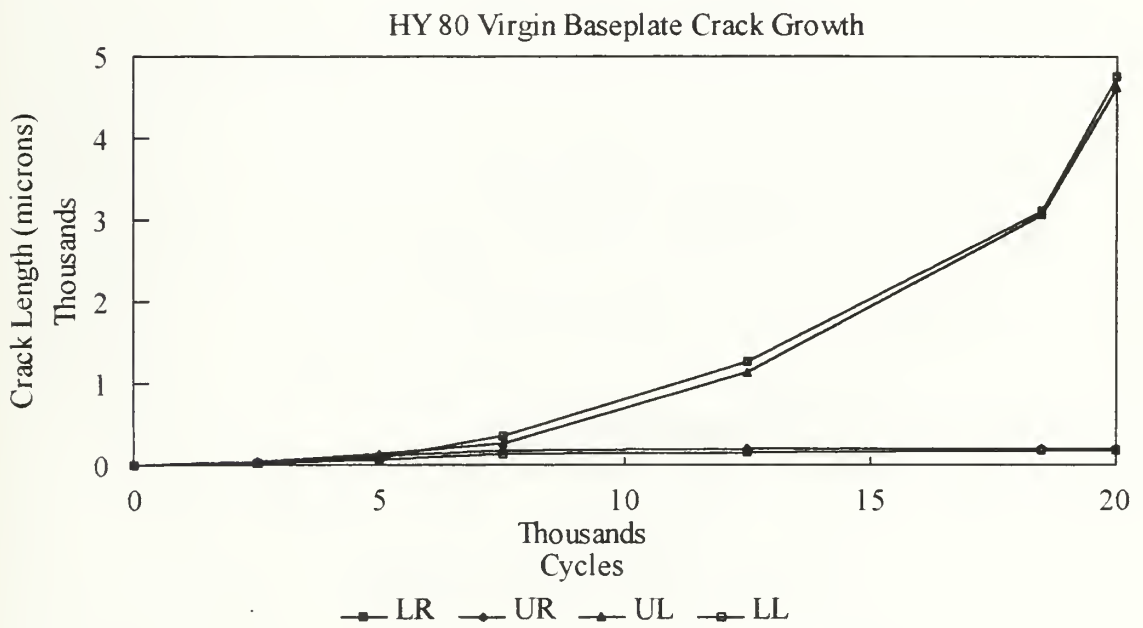


Figure 19: HY 80 Virgin Base Plate Crack Growth

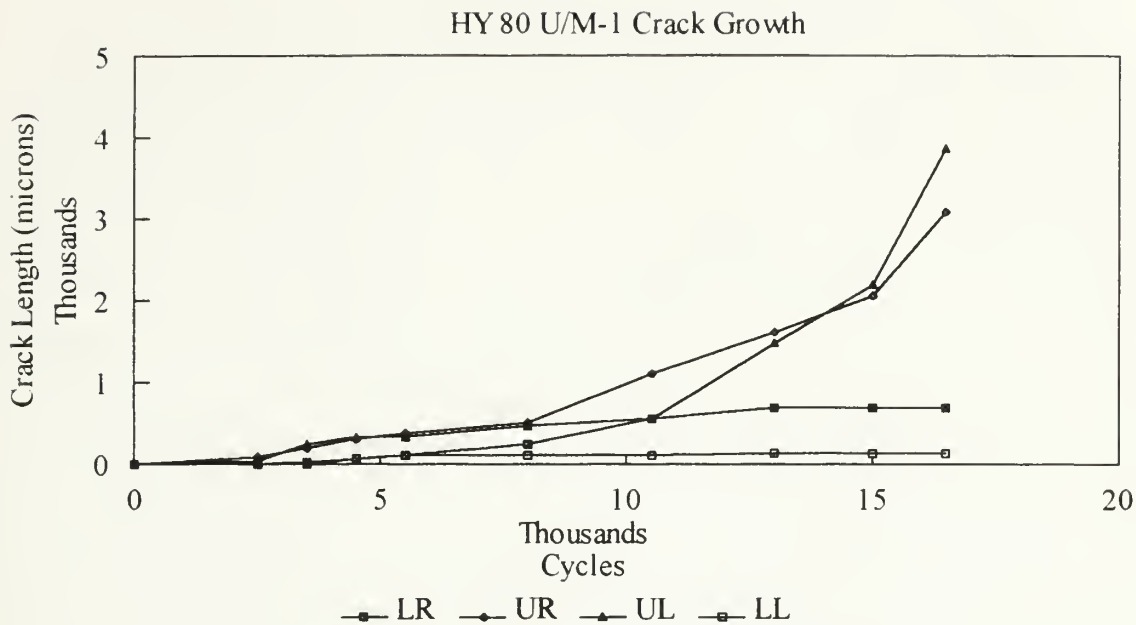


Figure 20: HY 80 U/M-1 Crack Growth

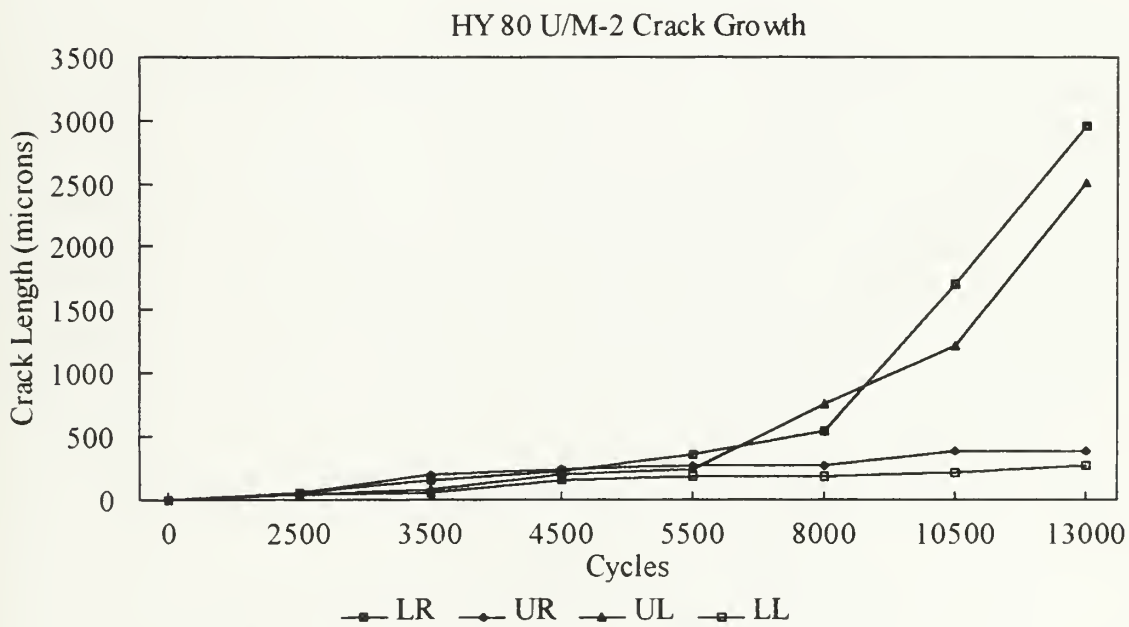


Figure 21: HY 80 U/M-2 Crack Growth

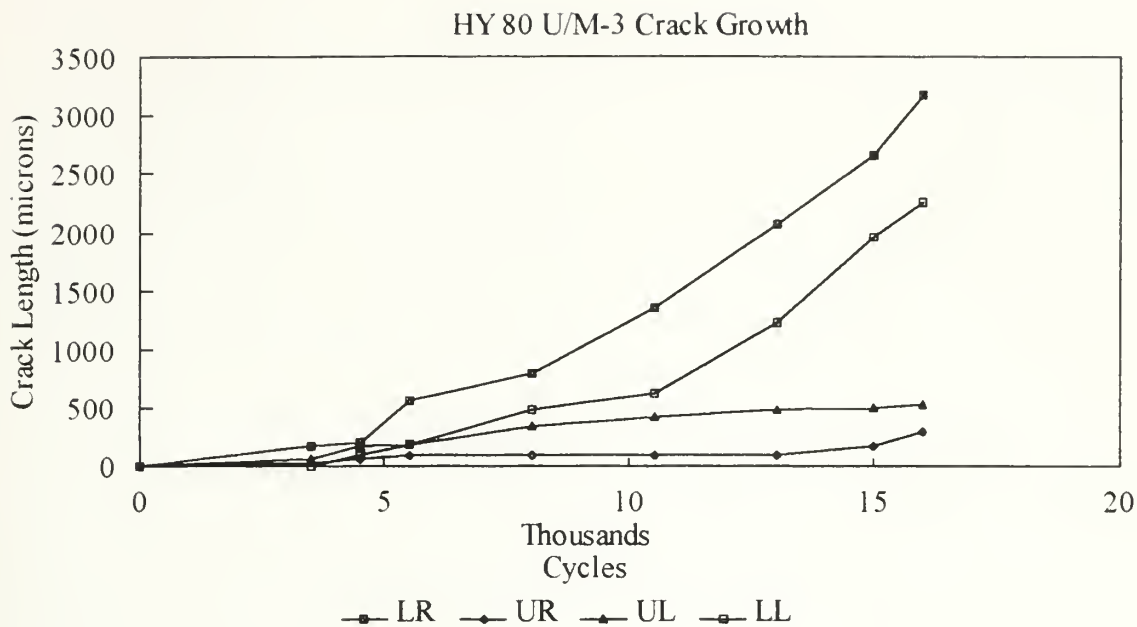


Figure 22: HY 80 U/M-3 Crack Growth

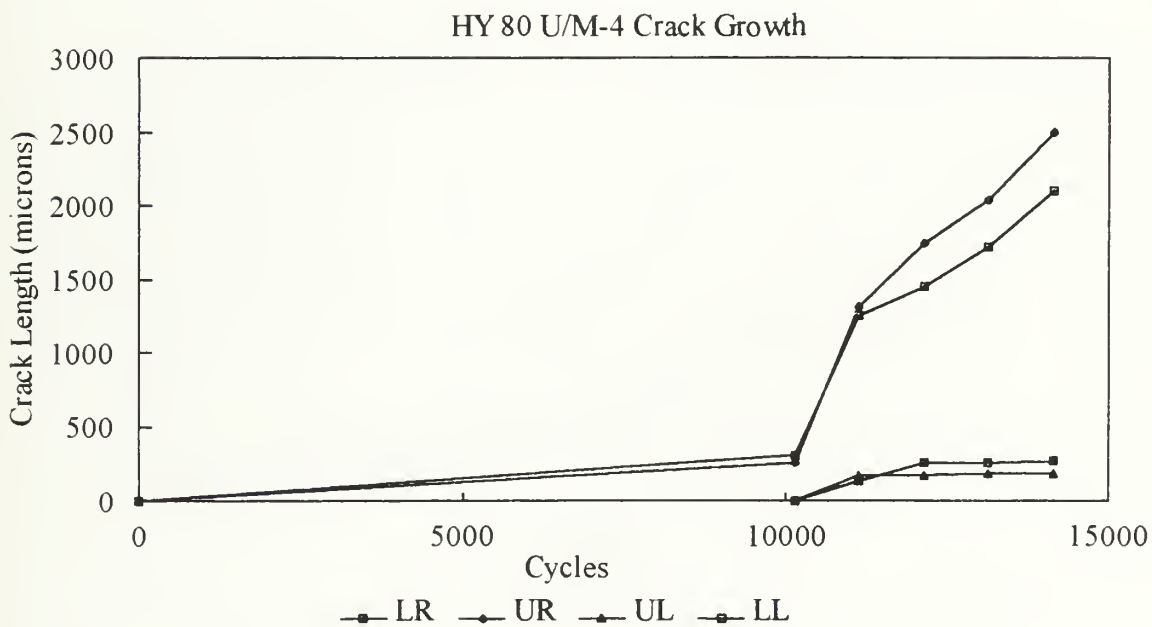


Figure 23: HY 80 U/M-4 Crack Growth

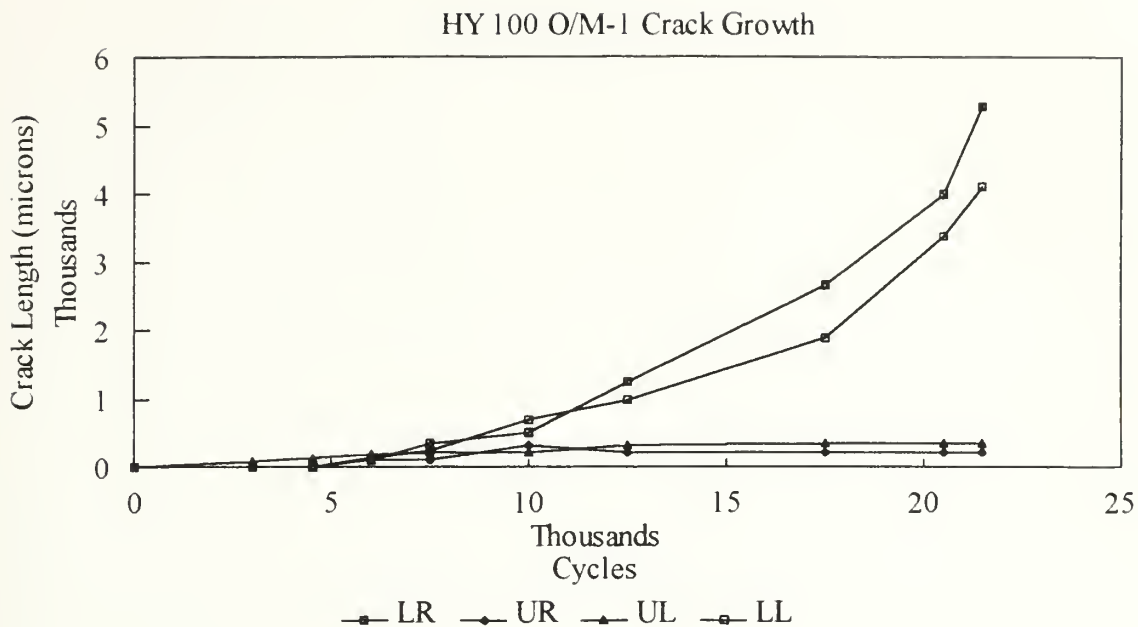


Figure 24: HY 100 O/M-1 Crack Growth

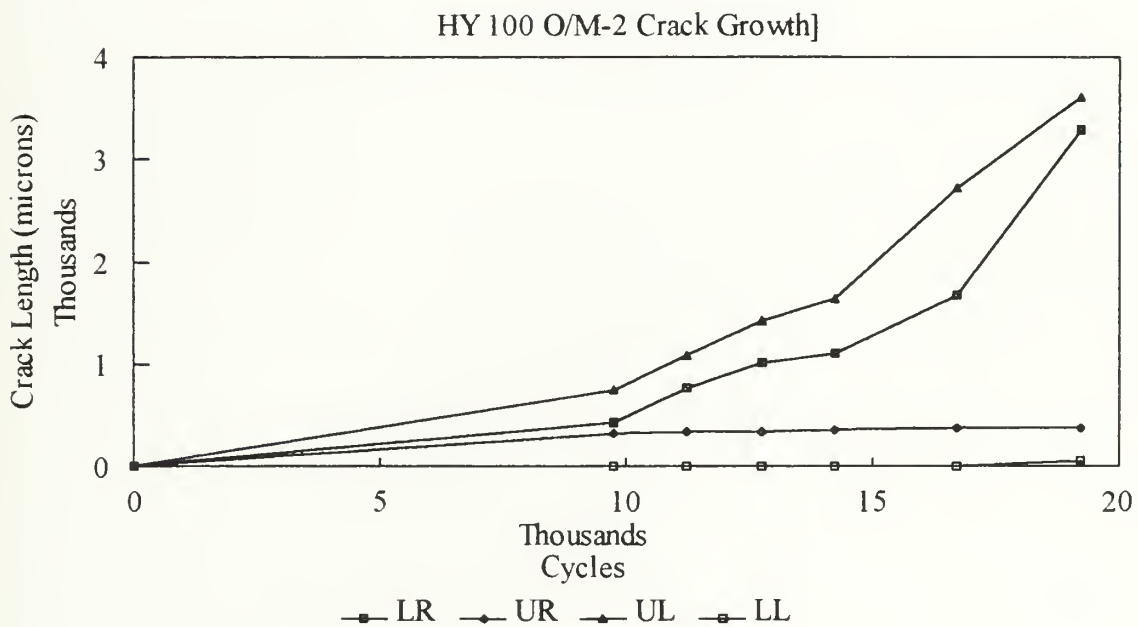


Figure 25: HY 100 O/M-2 Crack Growth

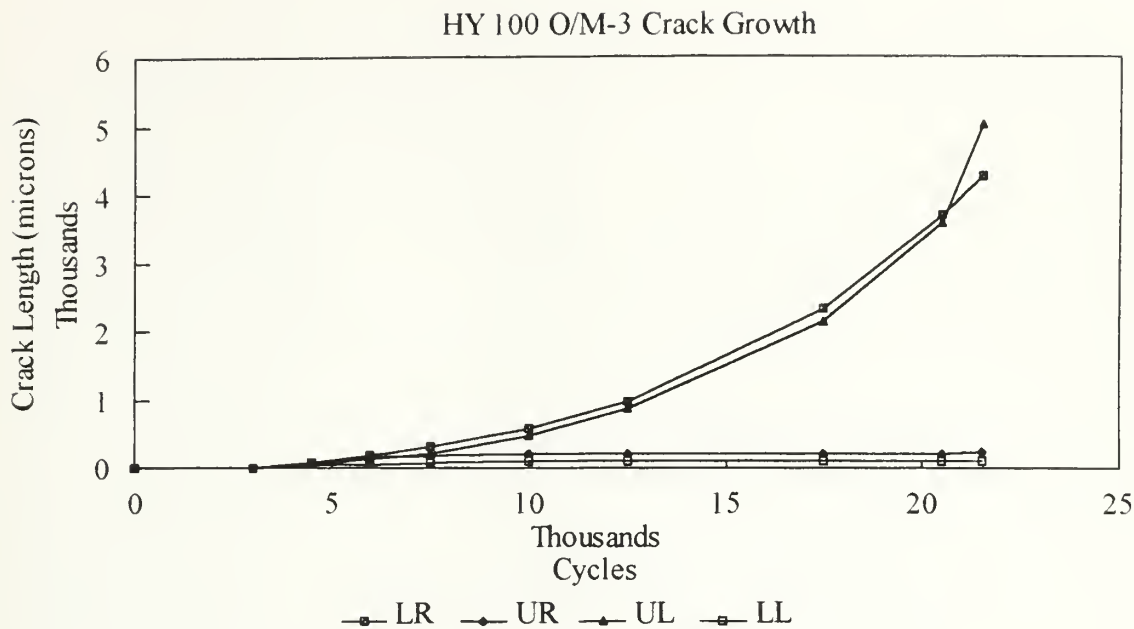


Figure 26: HY 100 O/M-3 Crack Growth

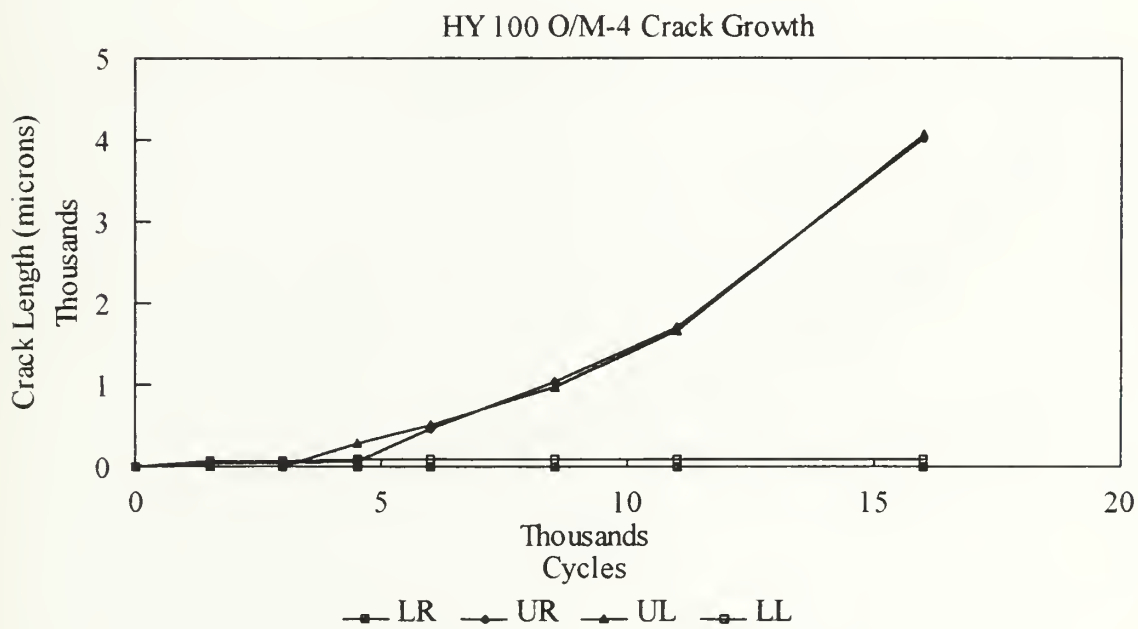


Figure 27: HY 100 O/M-4 Crack Growth

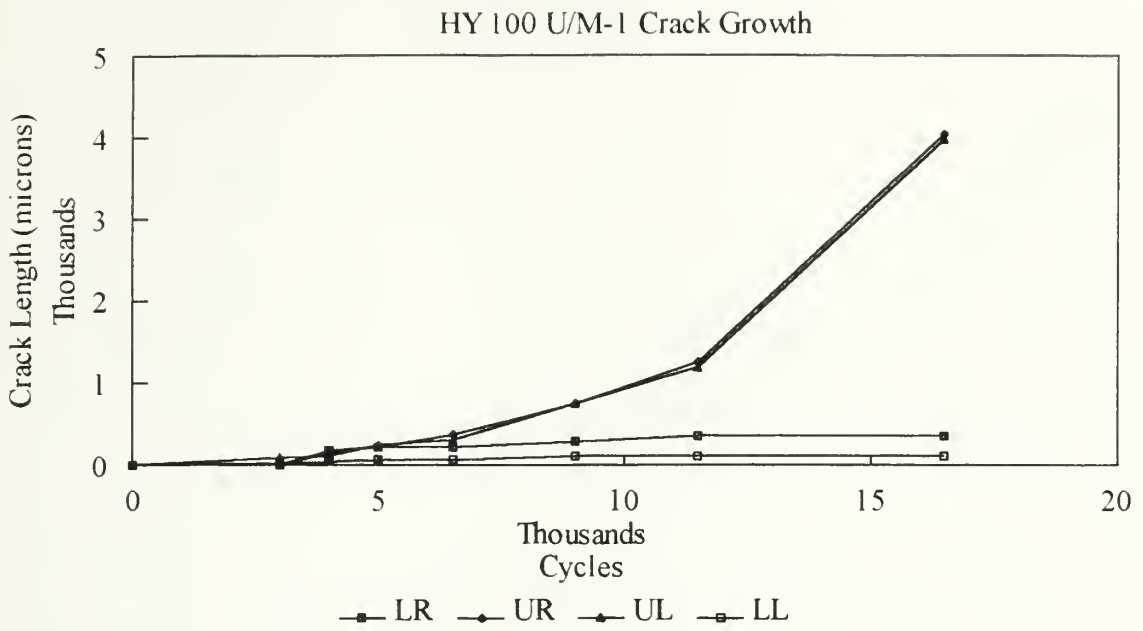


Figure 28: HY 100 U/M-1 Crack Growth

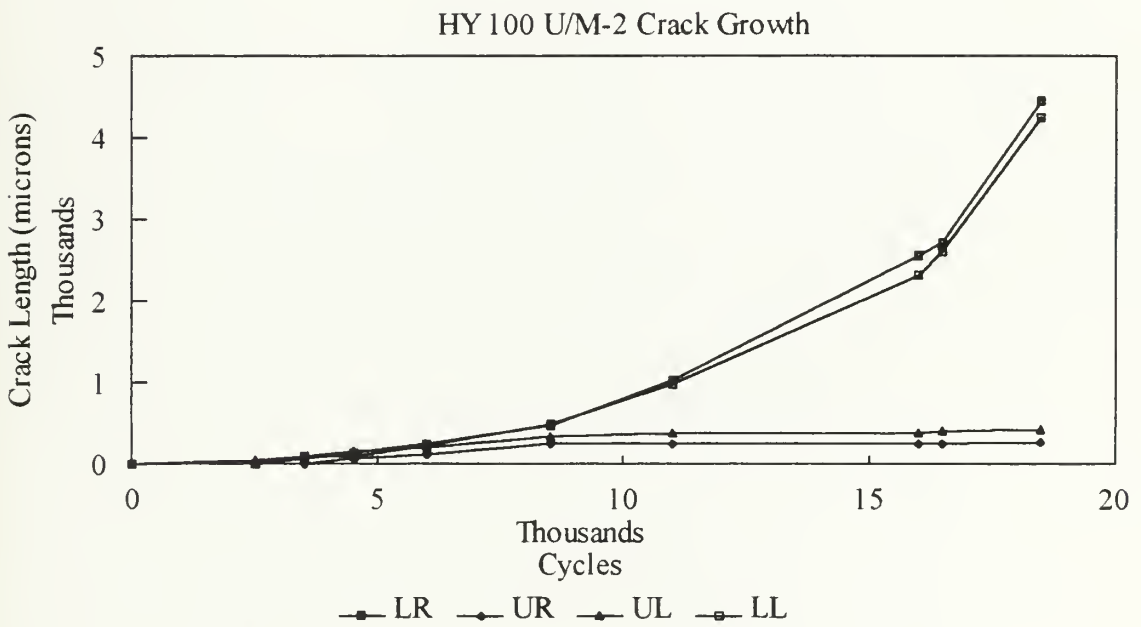


Figure 29: HY 100 U/M-2 Crack Growth

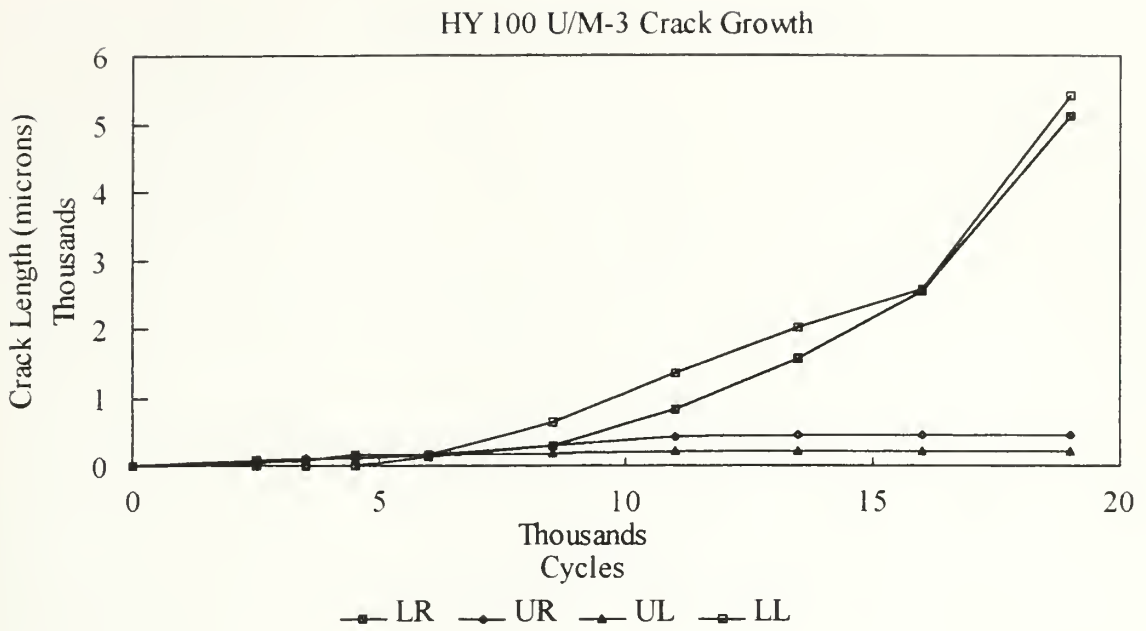


Figure 30: HY 100 U/M-3 Crack Growth

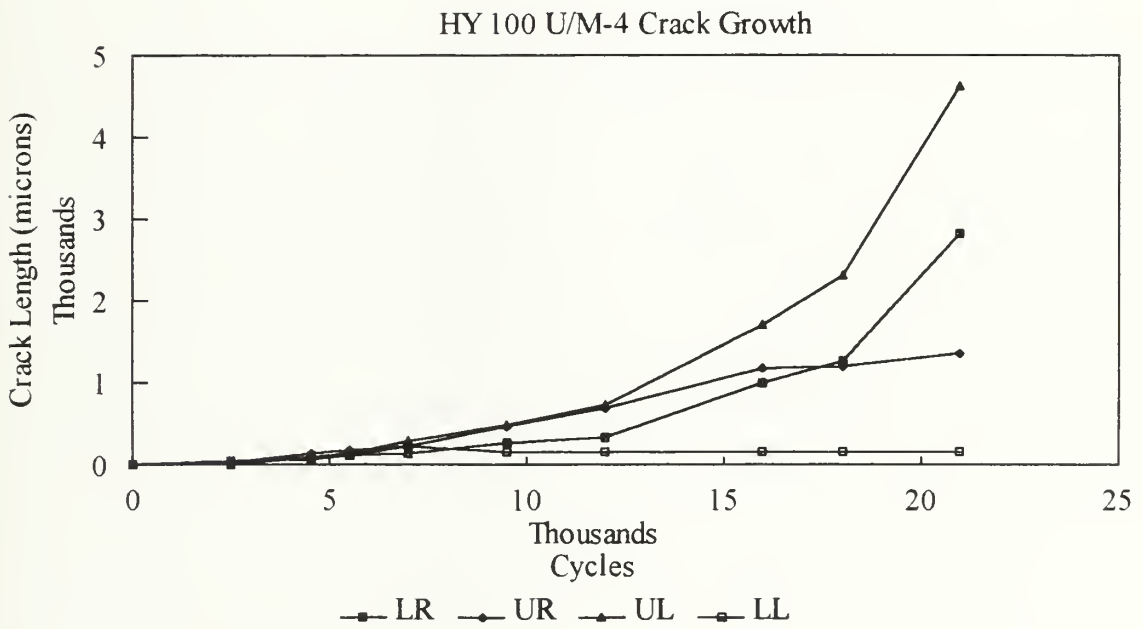


Figure 31: HY 100 U/M-4 Crack Growth

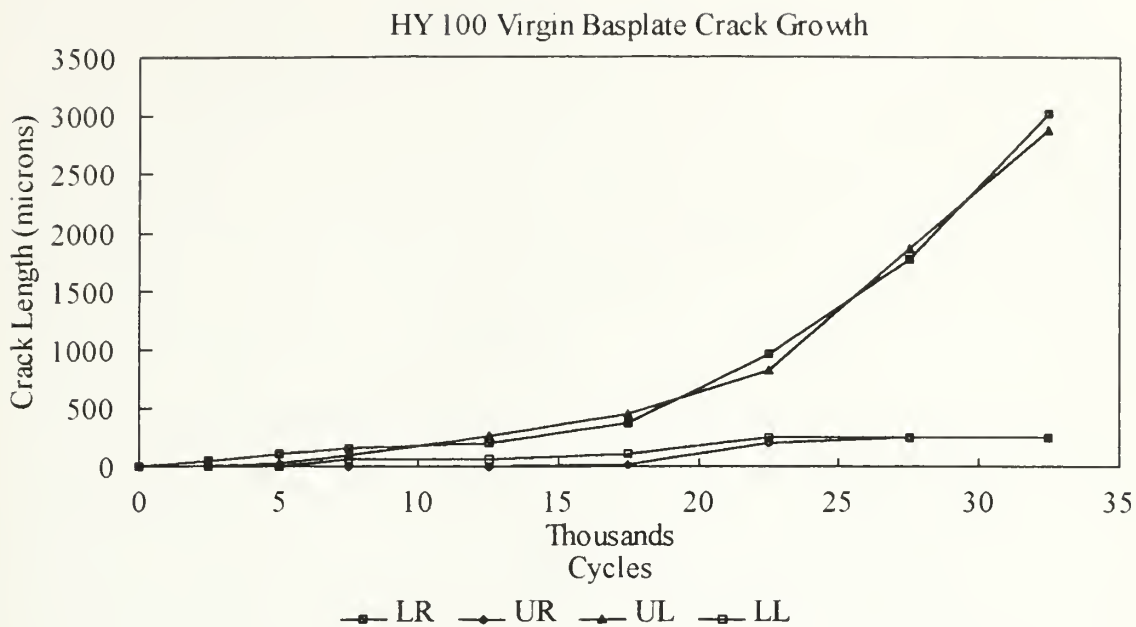


Figure 32: HY 100 Virgin Base Plate Crack Growth

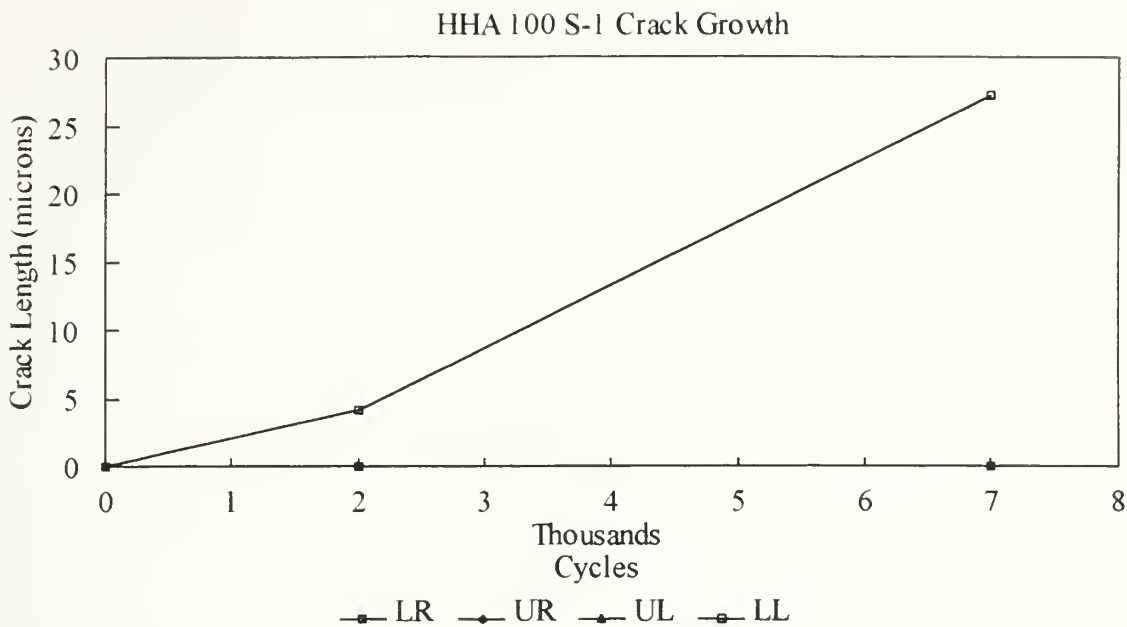


Figure 33: HHA 100 S-1 Crack Growth

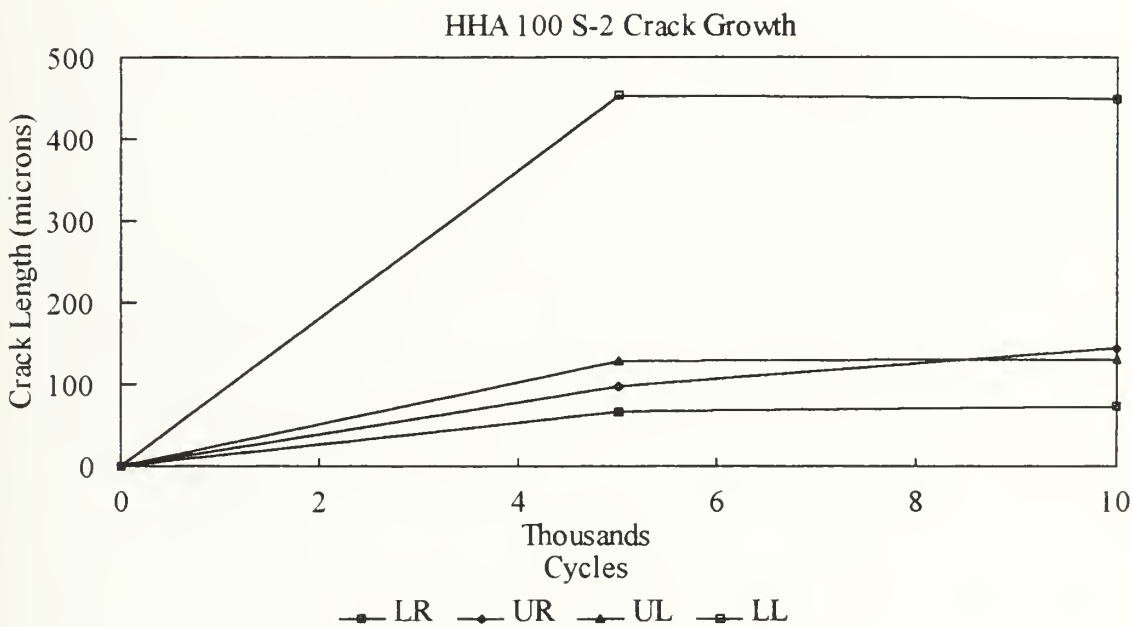


Figure 34: HHA 100 S-2 Crack Growth

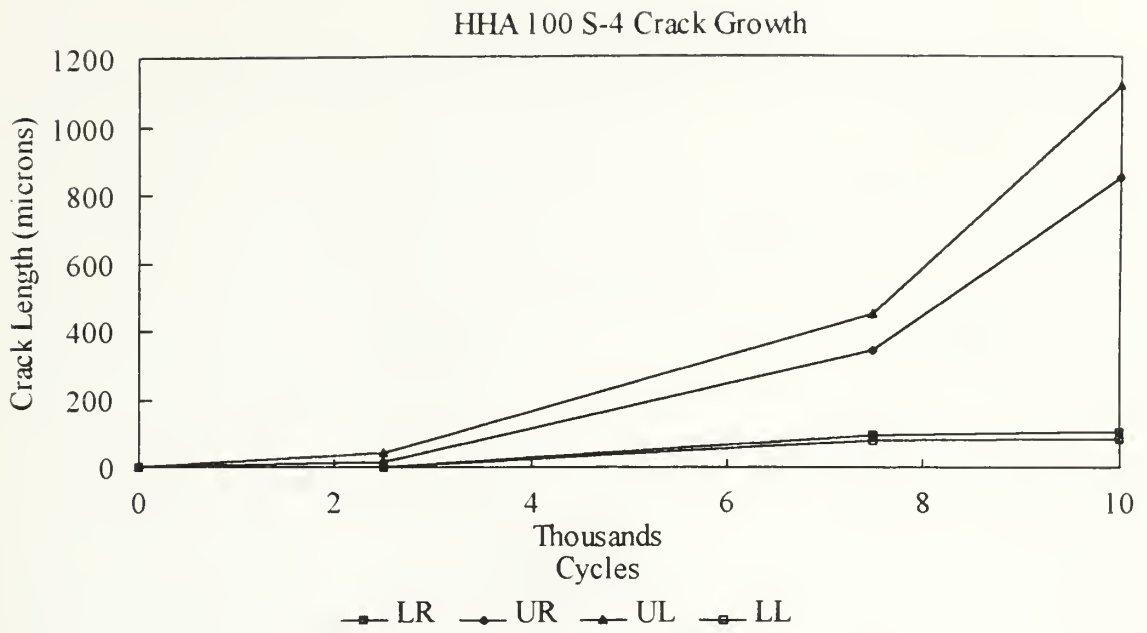


Figure 35: HHA 100 S-4 Crack Growth

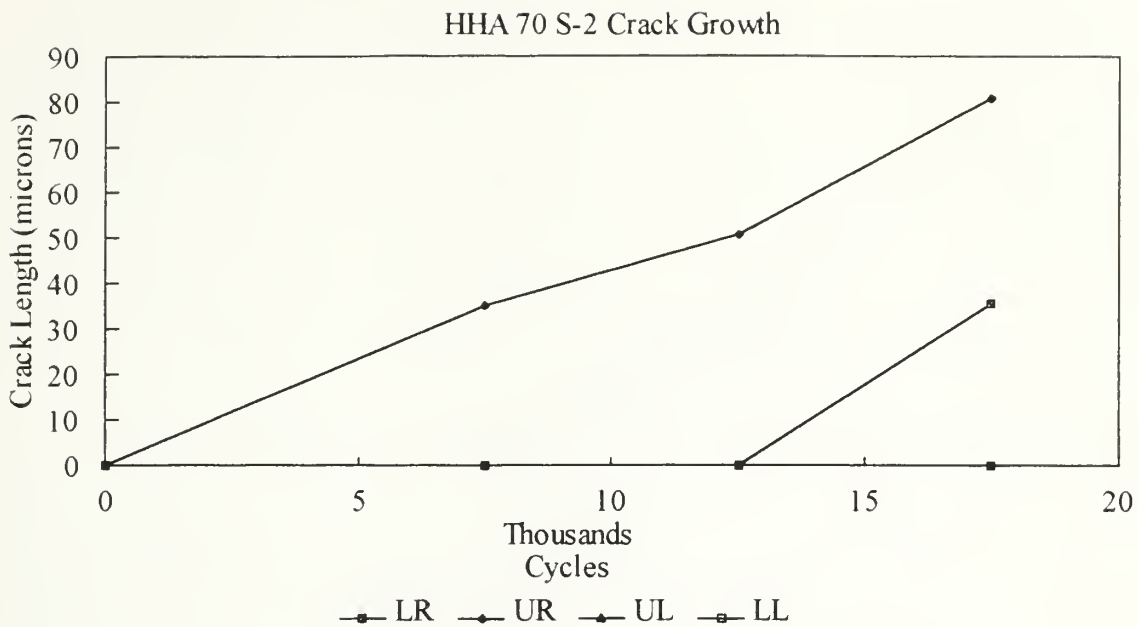


Figure 36: HHA 70 S-2 Crack Growth

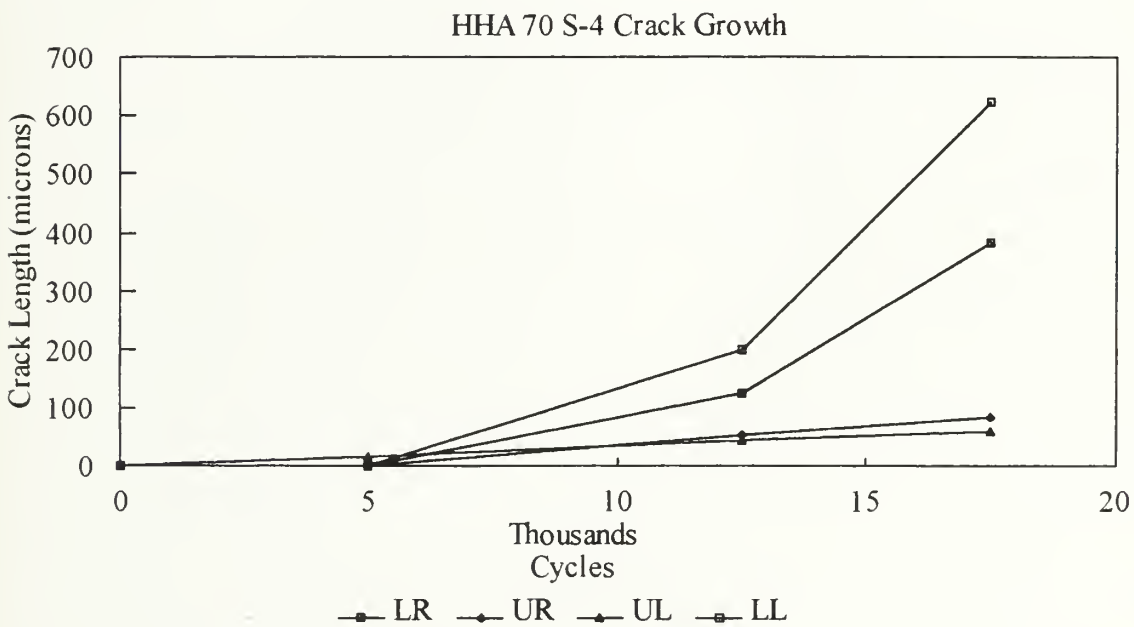


Figure 37: HHA 70 S-4 Crack Growth

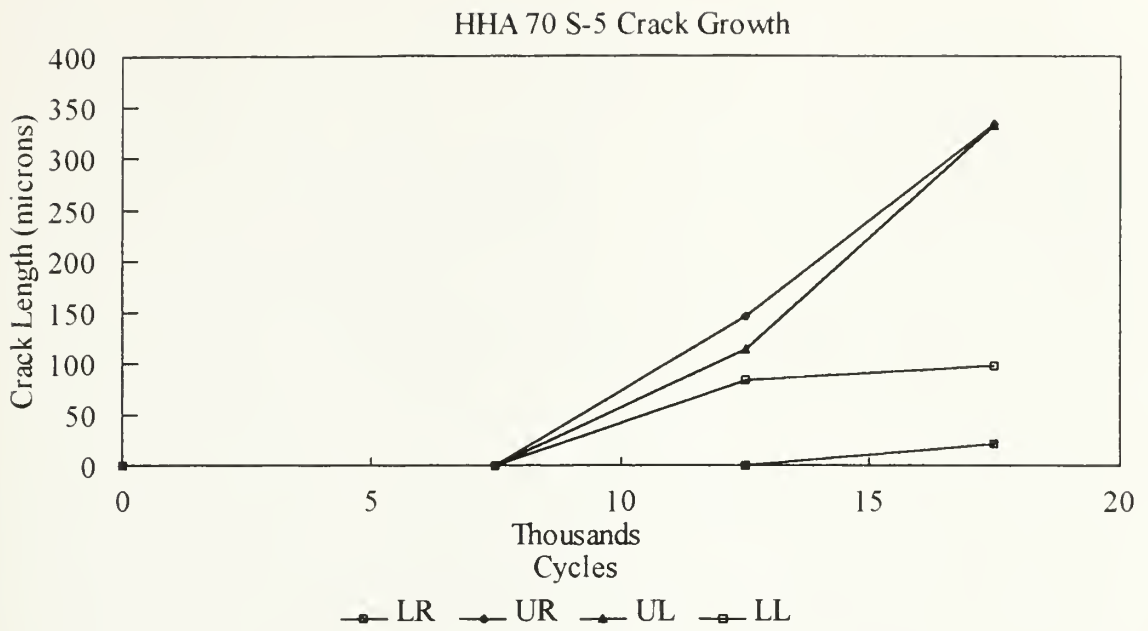


Figure 38: HHA 70 S-5 Crack Growth

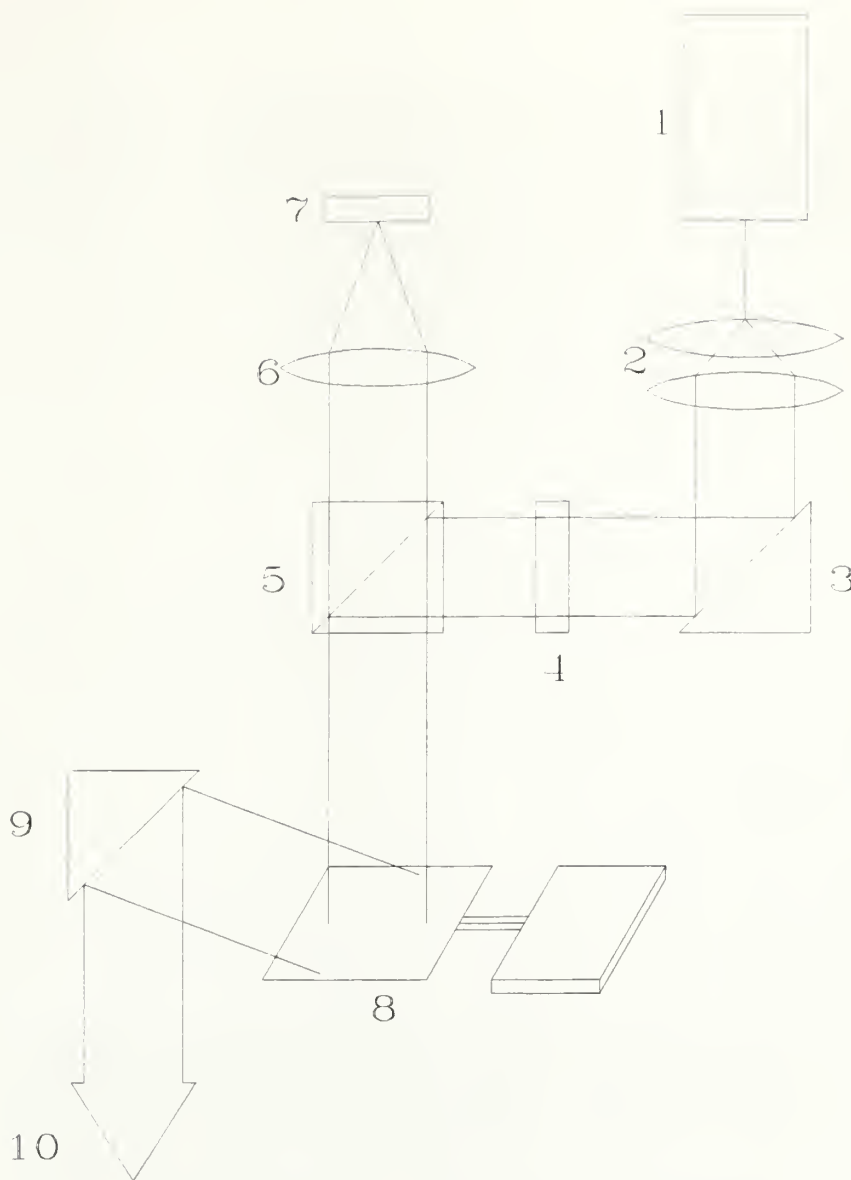


Figure 39: CSLM Optics Arrangement

1. Helium-Neon Laser
2. Beam Expander Lenses, Two
3. Mirror
4. Acousto-Optic Deflector: horizontal scanning
5. Polarized Beam Splitter
6. Lens
7. CCD Image Sensor: detects reflected light
8. Motor Driven Galvano Mirror: controls vertical scanning
9. Mirror
10. Laser Beam to Microscope

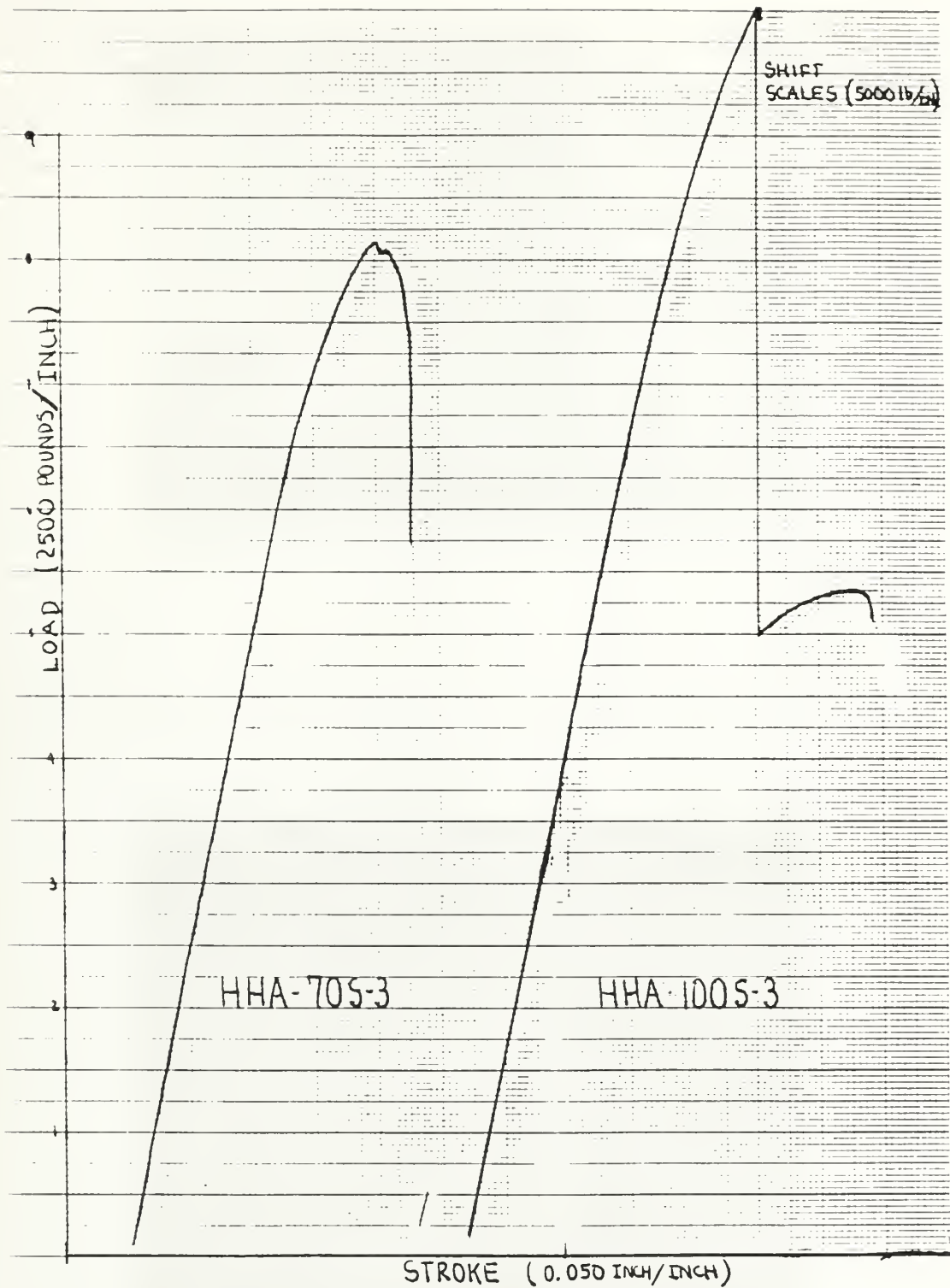


Figure 40: HHA 70 and HHA 100 Stress Strain Diagram

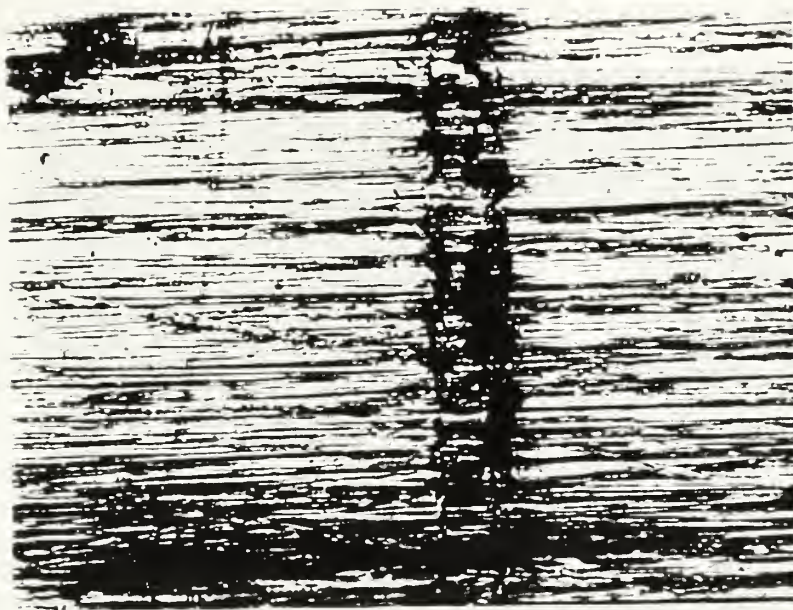


Figure 41 Image of 100 O/M-1 Fusion Zone, 100X Objective

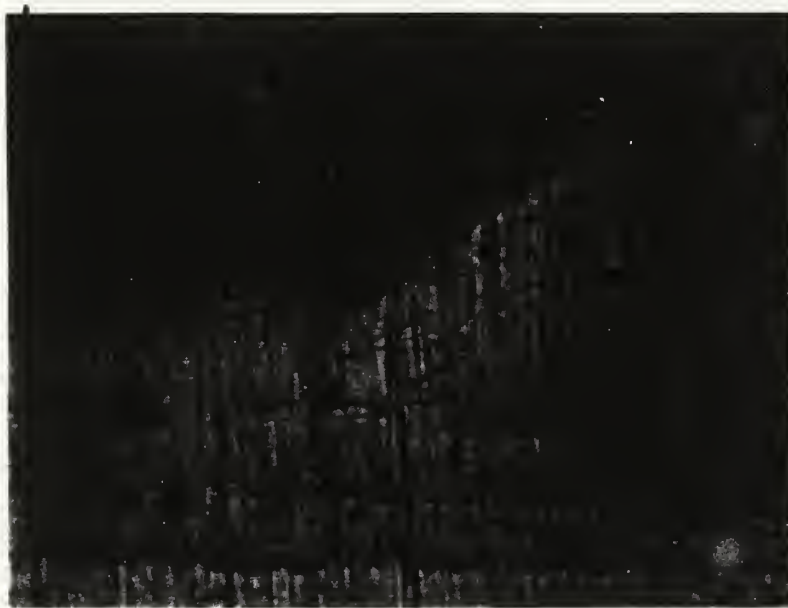


Figure 42 Image of 80 O/M-2 UR Crack at 2,500 Cycles, 40X Objective



Figure 43 Image of 100 U/M-2 UL Crack at 2,500 Cycles, 40X Objective



Figure 44 Image of 80 U/M-2 LR Crack at 2,500 Cycles, 40X Objective



Figure 45 Image of 80 Virgin Base Plate LR, 2,500 Cycles, 100X Objective



Figure 46 Image of 100 O/M-1 UL Crack at 3,000 Cycles, 20X Objective



Figure 47 Image of 80 Virgin Base Plate L.L. 7,500 Cycles. 20X Objective

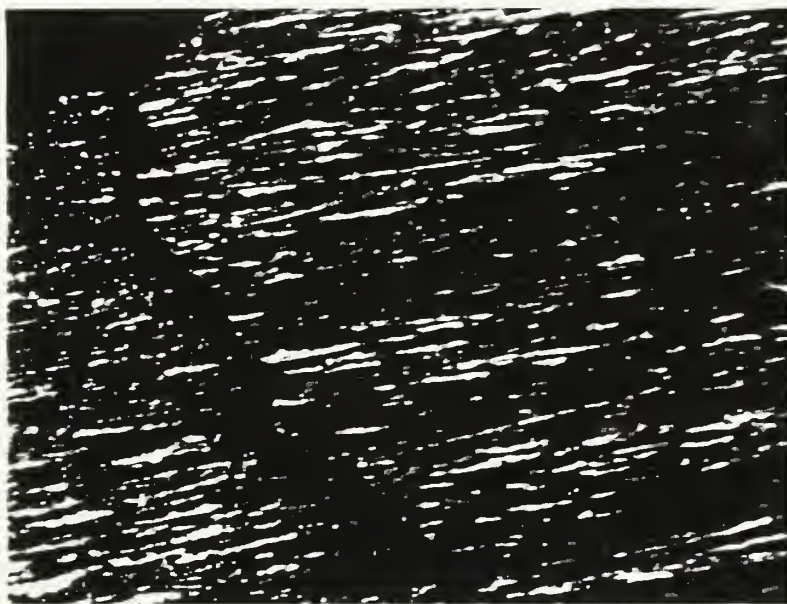


Figure 48 Image of 100 O/M-2 UR Crack at 8,000 Cycles. 100X Objective

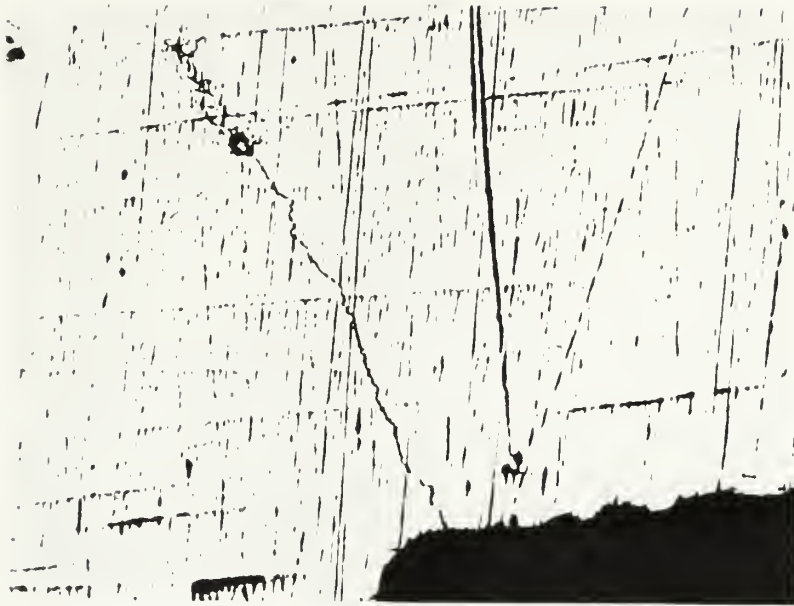


Figure 49 Image of 100 O/M-2 UR Crack at 9,730 Cycles, 10X Objective

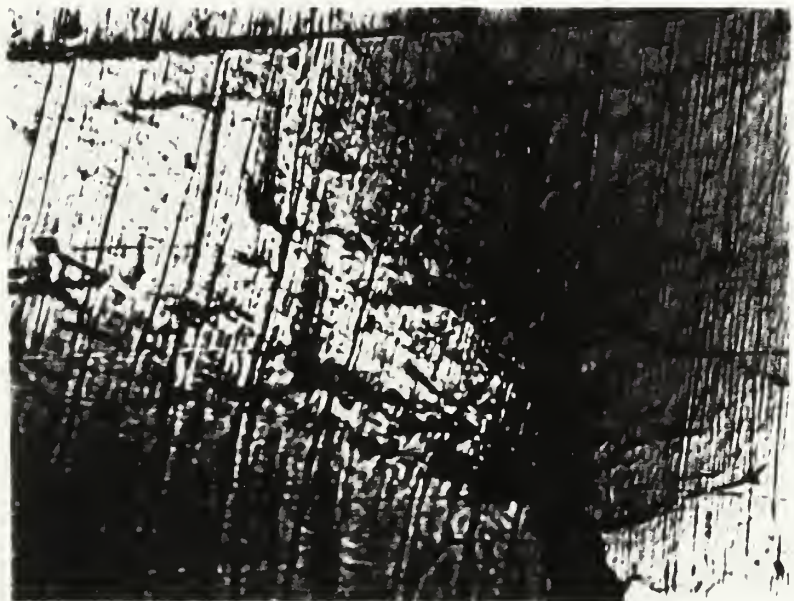


Figure 50 Image of 80 U/M-4 LL Crack at 11,130 Cycles, 10X Objective

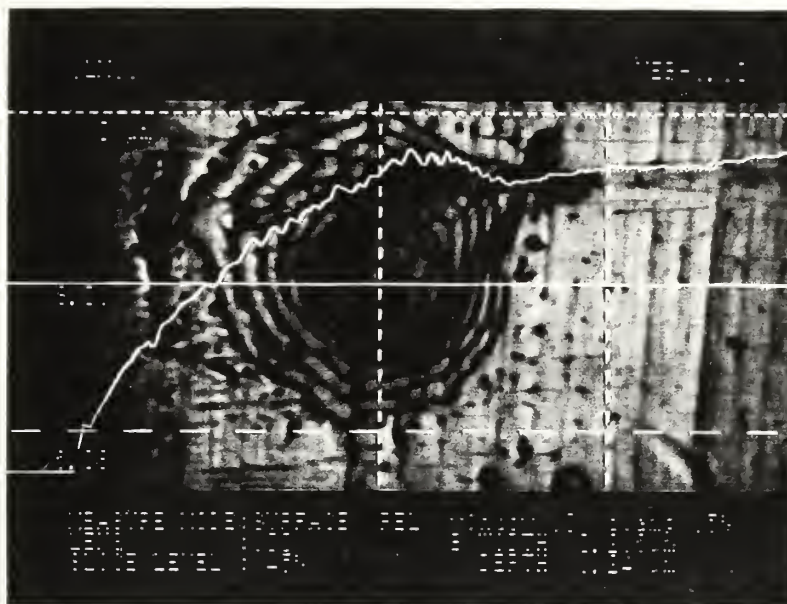


Figure 51 Image of 100 O/M-2 Asperity Profile, 11,730 Cycles, 100X Objective

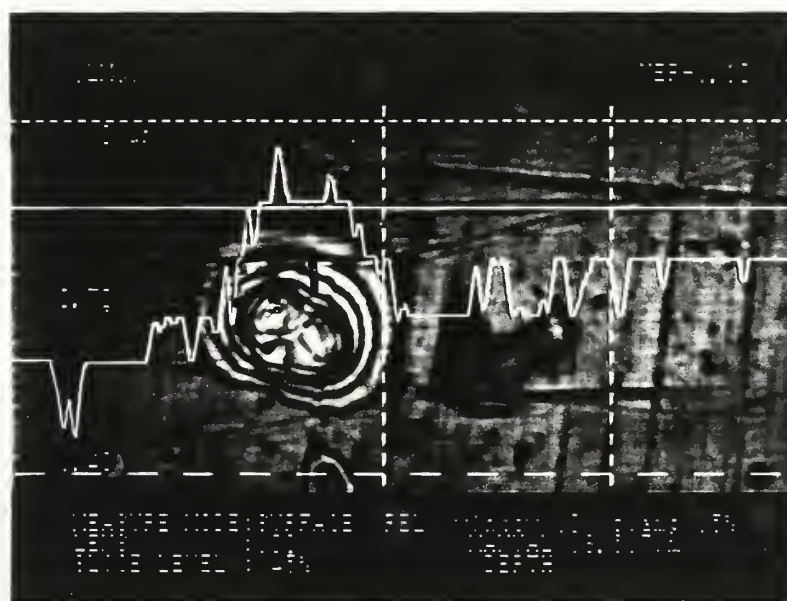


Figure 52 Image of 100 O/M-2 Asperity Profile, 11,730 Cycles, 100X Objective



Figure 53 Image of 100 O/M-3 LL Profile at 10,000 Cycles, 40X Objective

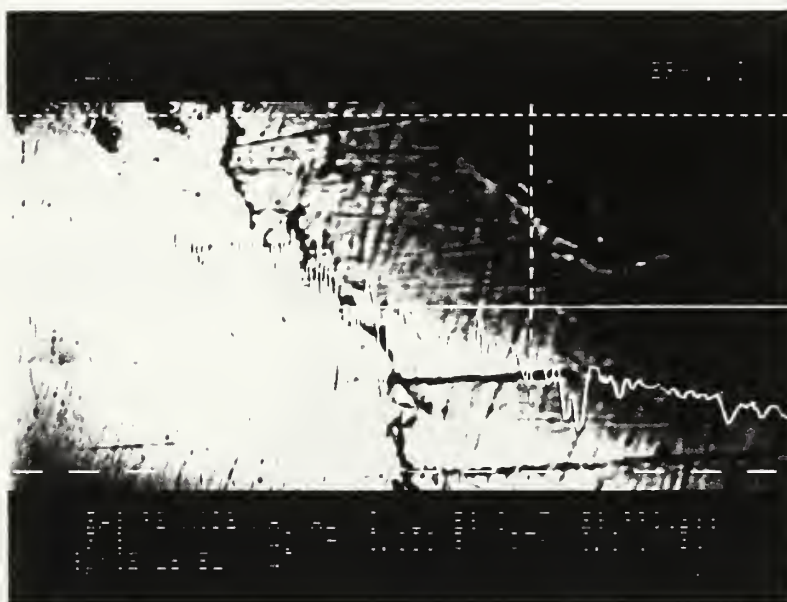


Figure 54 Image of 100 O/M-3 UL at 17,500 Cycles, 10X Objective



Figure 55 Image of 80 Virgin LR Plastic Zone at 18,500 Cycles, 10X Objective

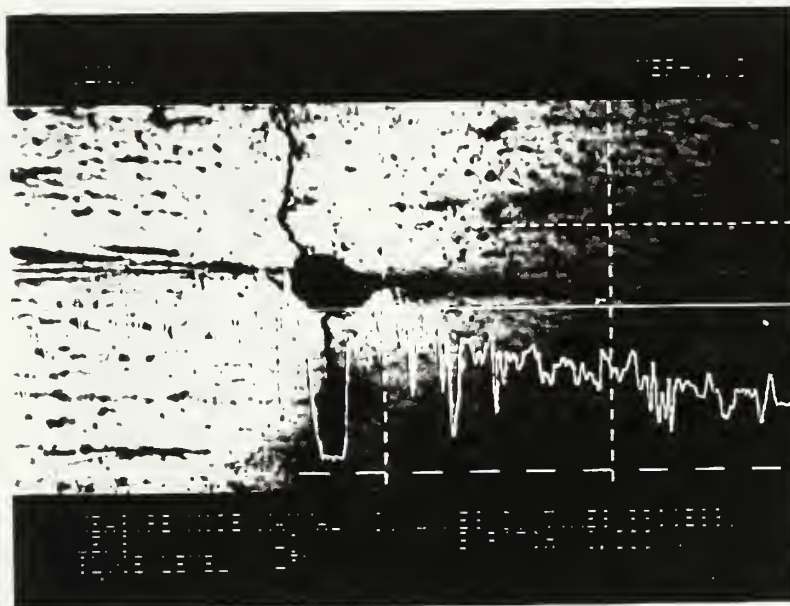


Figure 56 Image of HHA 100 S-4 UL Crack at 2,500 Cycles, 40X Objective



Figure 57 Image of HHA 100 S-4 UL Profile at 10,000 Cycles, 40X Objective

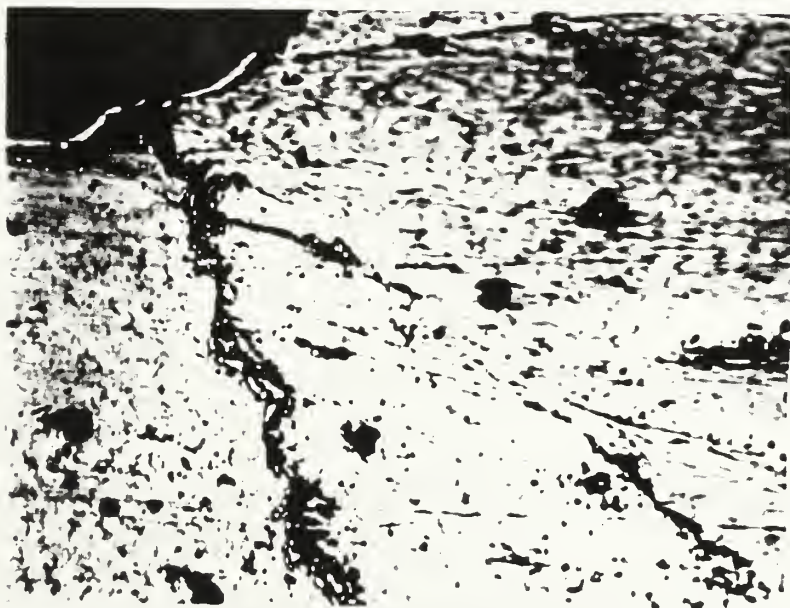


Figure 58 Image of HHA 70 S-4 LI Crack Forking at 12,500 Cycles, 40X Objective

References

Blackburn, J. M., Franke, G. L., "Cooling Rate Analysis of HY-100 Welds in Support of SSN-21 Construction", Carderock Division Naval Surface Warfare Center Report, CDNSWC-SME-92/16, February 1992.

Broek, D., Elementary Engineering Fracture Mechanics, Kluwer Academic Publishers, 1991.

Czyryka, E. J., and Werchniak, W., "Low Cycle Fatigue Performance of Matching and Undermatching Yield Strength HY-130 Steel Weldments", David Taylor Research Center Report, DTRC-SME-90/45, July 1991.

Czyryka, E. J., Juers, R. L., Werchniak, W., "Low Cycle Fatigue Crack Initiation Studies of HY-130 Industrial Base Verification Program", David Taylor Research Center Report, DTRC-SME-91/45, August 1991.

DeLoach, J. J., and Franke, G. L., "Microstructural Features Controlling Transition Behavior in Martensitic, High Strength Steel Weld Metals", Institute for Industrial Technology Transfer, 1989.

Dziubinski, J., and Adamiec, P., and Brunne, W., "A Welded Microstructure Effect on Low Cycle Fatigue", Paper presented to Structural Steel Conference, 1987.

Flinn, Richard A., and Trojan, Paul K., Engineering Materials and Their Applications, Second Edition, Houghton Mifflin Company, Boston, 1981.

Gregor, V., "Growth of Fatigue Cracks from Weldment Defects at Low Cycle Fatigue", Welding Research Institute Bratislava paper, 1987.

Goodwin, G. M., "Hot Cracking: Measurement, Mechanisms and Modeling", Welding Journal, February 1990.

Hatanaka, K., and Fujimitsu, T., "Growth of Small Cracks and an Evaluation of Low Cycle Fatigue Life", ASTM STP 942, 1988.

Iwanowicz, S. E., Study of Residual Stresses and Microcracks in High Strength Steels Weldments, MIT Master's Thesis, 1992.

Kirk, Mark T., "The Effect of Weld Metal Strength Mismatch on the Deformation and Fracture Behavior of Steel Butt Weldments", David Taylor Research Center Ship Materials Engineering Department Research and Development Report DTRC-SME-91/06, January 1991.

Kirk, Mark T. and Dodds, Robert H. Jr., "Effect of Weld Strength Mismatch on Elastic-Plastic Fracture Parameters", PhD Thesis, Department of Civil Engineering at University of Illinois, August 1992.

Lee, M. M. K. and Luxmoore, A. R., "An Experimental Study of the Elastic-Plastic Deformation of Double 'V' Butt Welds", Journal of Strain Analysis Vol 24, No 4 1990.

Masubuchi, K., Analysis of Welded Structures, Pergamon Press, 1980.

Masubuchi, K., "Design and Fabrication of Welded Ships", Paper presented at MIT under the Industrial Liaison Program (ILP), 1968.

Masubuchi, K., "Welding for Ocean Engineers", 13.17J Class Notes, Chapter 5, Fatigue Fracture, Fall 1991.

National Materials Advisory Board (NMAB), Commission on Engineering and Technical Systems National Research Council, "Effective Use of Weld Metal Yield Strength for HY-Steels", Report NMAB-380, January 1983.

Ohta, A., and Yoshio, M., and Suzuki, N., "Effect of Yield Strength on the Basic Fatigue Strength of Welded Joints", Paper submitted to Fatigue and Fracture of Engineering Materials and Structures, October 1992.

Oldland, P. T., Ramsay, C. W., Matlock, D. K., Olson, D. L., "Effects of Heat Input and Molybdenum Content on the Microstructures and Mechanical Properties of High Strength Steel Weld Metal", Center for Welding and Joining Research, Colorado School of Mines report, T-3599, July 1988.

Rolfe, S. T., Haak, R. P., Imhof, E. J., "Low Cycle Fatigue Of Experimental HY-130/150 and HY-180/210 Steels and Weldments", Technical Report 40.018-001(37) by United States Steel, December 1964.

Scoonover, T. M., "Heat-Affected Zone Toughness and Tensile Properties in ASTM A710 Steel Weldments", David Taylor Research Center Report, DTRC/SME-88-18, September 1988.

Shigley, Joseph E., and Mitchell, Larry D., Mechanical Engineering Design, Fourth Edition, McGraw-Hill, 1983.

Appendix A

The Confocal Scanning Laser Microscope

The Confocal Scanning Laser Microscope (CSLM) was developed by Lasertec Corporation. Table 34 outlines selected CSLM operating parameters and data. The CSLM is a conventional optical microscope with a scanning He-Ne laser for specimen illumination. The system also includes a confocal imaging system and an image processing unit. Unlike a standard microscope, observations of highly textured surfaces are possible through the use of an extended focus memory feature. This feature creates images that are the integration of many focused layers. The layers are superimposed to form a single image with apparent infinite depth of field. A 12 inch video monitor displays output from the image processing unit. Video recording and still shot photography is also possible. Specimen manipulation and initial focusing is similar to a standard microscope. An adjustable stage allows for two dimensional lateral movement (X and Y axis) of the specimen while the microscope can be focused by movement in the third dimension (Z-axis).

CSLM Optics and Image Magnification

The optical microscope is a Nikon model 1LM11. The objective turret allows for up to five objective lenses with an available range of 1X to 200X. The most commonly used objectives for this project were in the range of 10X to 40X. The image displayed on the 12 inch video monitor is further magnified by a factor of 60X. Video scan frequency is

nominally 0.033 s^{-1} and is adjustable to enhance image quality. Table 35 lists CSLM image display information.

The fixed He-Ne laser source is combined with an Acoustic Optical Device (AOD), galvano mirror and respective drive units. The AOD and galvano mirror provide the scanning motion of the fixed laser. Specifically, the AOD performs horizontal scanning (X axis) while the galvano mirror provides vertical (Y axis) scanning. Figure 39 shows the CSLM optical arrangement.

Confocal Imaging System

When using the Optiphot 100x 0.925NA objective lens, high resolution imaging on the order of $0.25 \mu\text{m}$ is possible. This high degree of resolution and the accompanying scan line density allows the confocal imaging system to quickly determine if a point of interest is in focus. The laser beam is focused onto the surface of the specimen and a portion of the light is reflected back into the objective lens. These reflected rays are then deflected by a beam splitter and focused through a pinhole opening onto the confocal point detector. When the surface is out of focus, the reflected rays form a cone of light at the pinhole opening. Therefore, less light passes through to the confocal point detector when an image is out of focus. Peak light intensities coincide with areas that are in focus. The image processing unit determines when the peaks occur in constructing sharply focused images, making it unnecessary to ascertain if an image is blurry. The image processing unit supports the following special capabilities of the CSLM:

- ♦ Extended Focus
- ♦ Surface Profilometry
- ♦ Lateral Surface Measurements

Extended Focus

This enables the processing unit to compose an image with a virtually infinite depth of field. This is a necessary feature when viewing specimens with a relatively large height dimension. Standard optical equipment are very limited in this sense because of finite focal planes. The CSLM scans finite layers and stores the information. The image processor identifies the light intensity of each pixel of the specimen. The final image is the integration of each of the layer's peak light intensities, forming a single focused view with apparent unlimited depth of field.

Surface Profilometry

This feature allows the viewing of a "cross section" of the specimen. Differences in elevation and slopes of the specimen can be observed and quantified. With the processor selected for Measurement Screen Mode, a solid horizontal crosshair is positioned along the region of desired profile. The Z-Axis Controller is then used (manually or automatically) to select the heighthwise region of interest. The initial or zero reference setting on the screen must be carefully observed to determine if it is a "hill" or "valley". Once this initial positioning is established, the image processor coordinates all peak intensities with the Z coordinate of the microscope. Raw data is processed with a

smoothing algorithm and an altitude profile is constructed. Elevations can then be measured with the processor unit controls.

Lateral surface measurements

This feature allows for lateral measurements of the specimen when the Measurement Screen Mode is selected on the processor. A set of dashed vertical crosshairs can be moved and adjusted to measure lengths to 0.25 μm .

Some other important features of the system are:

- ◆ Critical dimension (CD) measurement. Repeatability of 3σ or 0.03 μm .
- ◆ Real time television refresh rate imaging. Observation, search and focusing of a moving sample is essentially real time because of the high frequency refresh rate.
- ◆ High magnification, high resolution imaging by confocal optics.
- ◆ Low intensity monochromatic illumination precludes thermal damage to specimens.
- ◆ Sample preparation is not required. The sample only needs to be clean and dry.
- ◆ Light emitting objects may be viewed.
- ◆ Slow scan function allows observation of specimens with low reflectivity. The laser scan speed can be slowed to increase the memory storage time of the optical sensor. Sensitivity is inversely proportional to scan time, therefore lower scan rates are best as reflectivity decreases. There are eleven possible scan speed settings available.
- ◆ Optimization of signal source for various image processing capabilities.
- ◆ Output Signal Recording allows the video output signal to be recorded on tape with a standard Video Cassette Recorder (VCR). Visual signals may also be enhanced with an external image processing unit.
- ◆ Gamma Function selection adjusts the viewing quality by varying the correlation between the amount of optical sensor light input and the video signal output. Three gamma function profiles are available; linear, increasing, and decreasing. Normally the linear or constant slope gamma function is used. The decreasing slope gamma function causes dark portions of the image to be lightened and light portions to be

darkened. This is helpful in increasing contrast of dark areas of low reflectivity specimens. The positive gamma function performs the opposite, light areas are lightened more and dark areas are further darkened. This change in contrast allows better imaging of the lighter areas of a specimen.

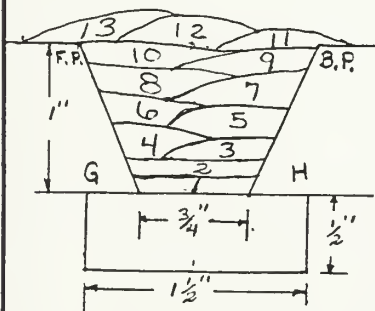
Appendix B

HY Steel Welding Data Sheets

[illegible]

Plate No.: PD2035	Position: Flat		Description: HY-80 UNDERMATCH								
Date: 3-15-93	Task No.:		Task Title: MIT/USN FATIGUE PLATES								
Wire Dia. & Type: 1/16 / 1005-1		Heat No.: 195254			Control No.: 10W0955			Spool No.:			
Shielding Gas Type: C-5		Cylinder No: 758269			Actual Composition:						
Bead No.	1	2	3	4	5	6	7	8	9	10	11
Cup Size (in.)	#8-1/2" OAL	#8	#8	#8	1/16, 5/8"	5/8"	5/8"	5/8"	5/8"	5/8"	5/8"
Flow Rate (cfh)	35	35	35	35	45	45	45	45"	45"	45	45
Cup to Work (in.)	1/2"	1/2"	1/2"	1/2"	5/8"	5/8"	1/2"	1/2"	1/2"	1/2"	1/2"
Tip to Work (in.)	5/8"	5/8"	5/8"	5/8"	3/4"	3/4"	5/8"	5/8"	5/8"	5/8"	5/8"
Current Type/Pol.	DCRP	DCRP									DCRP
PH/IP Temp. (F)	400°	400°	400°	400°	400°	400°	400°	400°	400°	400°	400°
WFS (ipm)	164	166	169	167	182	184	178	177	178	181	183
OCV (V)	32	32	31.5	31.5	31.5	32	31.5	31.5	31.5	31.5	31.5
Current (A)	340	340	340	340	340	335	340	340	340	340	340
Voltage (V)	25.5	25.5	25.5	25.5	25.5	26	25.5	25.5	25.5	25.5	25.5
Travel Speed (ipm)	4.73	4.75	4.7	4.75	4.76	4.77	4.75	4.74	4.77	4.74	4.75
Heat Input (kJ/in)	110.0	109.5	110.7	109.5	108.8	109.6	109.5	109.7	109.1	109.7	109.5
Osc. Width (in.)	9/16"	5/8"	5/8"	9/16"	9/16"	9/16"	5/8"	5/8"	5/8"	5/8"	1/16"
Osc. Speed (pot)	48	42	42	48	48	48	42	36	36	36	40
Dwell L/R (pot)	01 / 01	02 / 01	01 / 02	03 / 01	01 / 03	03 / 01	01 / 03	03 / 02	02 / 03	02 / 01	02 / 02

PLATE - 30" Long
HY-80 BASE MAT'L



Process: Spray GMAW Power Supply: GILLILAND (CVL60) #G24

Instrumentation: V.O.M. #NC36554, Amp #NC39708

WIRE SAMPLE - After Bead #5

Bead #6 - new T.P.

PLATES - #G + #H

3-16-93

9:50 A.M.

DRY BULB = 70

WET BULB = 51

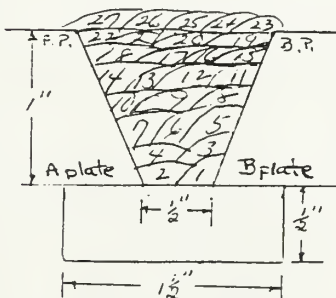
R.H. = 22%

Approx 6" CUT FROM START END FOR AWT

[illegible]

Plate No.: PD20326	Position: FLAT			Description: HY-100 OVERMATCH							
Date: 3/22/93	Task No.:			Task Title: MIT/USN FATIGUE PLATES							
Wire Dia. & Type: C-5/120S-1			Heat No.: 120029			Control No.: 01230			Spec'd No.: 0167		
Shielding Gas Type: C-5			Cylinder No: 634102			Actual Composition:					
Bead No.	1	2	3	4	5	6	7	8	9	10	11
Cup Size (in.)	#8 1/2	1/2	1/2	1/2	1/2	1/2	1/2	1/2	1/2	1/2	1/2
Flow Rate (cfh)	35	35	35	35	35	35	35	35	35	35	35
Cup to Work (in)	1/2	1/2	1/2	1/2	1/2	1/2	1/2	1/2	1/2	1/2	1/2
Tip to Work (in.)	5/8	5/8	5/8	5/8	5/8	5/8	5/8	5/8	5/8	5/8	5/8
Current Type/F	DCRP										DCRP
PH/IP Temp. (F)	200/200										200/200
WFS (ipm)	314	316	320	321	319	318	322	320	320	321	320
OCV (V)	30.5	30.5	30.5	30.5	30.5	30.5	30.5	30.5	30.5	30.5	30.5
Current (A)	250	280	280	280	280	280	280	280	280	280	250
Voltage (V)	25	25	25	25	25	25	25	25	25	25	25
Travel Speed (ipm)	13.53	13.43	13.84	14.29	14.29	14.4	14.17	14.06	14.06	13.95	13.95
Heat Input (kJ/in)	31.0	31.3	30.4	29.4	29.4	29.2	29.6	29.9	29.9	30.1	30.1
Osc. Width (in.)	—										
Osc. Speed (pot)	—										
Dwell L/R (pot)	—										

HY100 TEST PLATE - 30" LONG



Process: Spray GMAW | Power Supply: GILLILAND (CV600) #G24

Instrumentation: V.C.M. #NC 36554 Amp #NC 3970E

PLATE #A + #B

AFTER BEAD 11 SOAKED AT 350° FOR 12 HRS

3-23-93

WIRE SAMPLE AFTER BEAD #11 AT (7:40 A.M.)

DRY BULB = 69

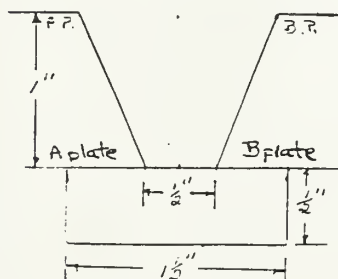
WET BULB = 49

R.H. = 13%

* AFTER FINISHED - SOAKED AT 350° FOR 12 HOURS

Plate No.: PD20366	Position: FLAT	Description: HY-100 OVERMATCH									
Date: 3/22/93	Task No.:	Task Title: MIT/USN FATIGUE PLATES									
Wire Dia. & Type: C-5/1205-1	Heat No.: 120029	Control No.: 01230					Spool No.: 0167				
Shielding Gas Type: C-5 Cylinder No: 634102 Actual Composition:											
Bead No.	23	24	25	26	27						
Cup Size (in.)	5/8	5/8	5/8	5/8	5/8						
Flow Rate (cfh)	45	45	45	45	45						
Cup to Work (in)	1/2	1/2	1/2	1/2	1/2						
Tip to Work (in)	5/8	5/8	5/8	5/8	5/8						
Current Type/P	DCRP										DCRP
PH/IP Temp. (F)	200										200
WFS (ipm)	325	324	318	321	323						
OCV (V)	30.5	30.5	30.5	30.5	30.5						
Current (A)	280	280	280	280	280						
Voltage (V)	25	25	25	25	25						
Travel Speed (ipm)	13.84	13.95	14.17	14.06	13.95						
Heat Input (kJ/in)	30.4	30.1	29.6	29.9	30.1						
Osc. Width (in.)	—	—	—								
Osc. Speed (pot)	—	—	—								
Dwell L/R (pot)	—	—	—								

HY100 TEST PLATE - 30" Long



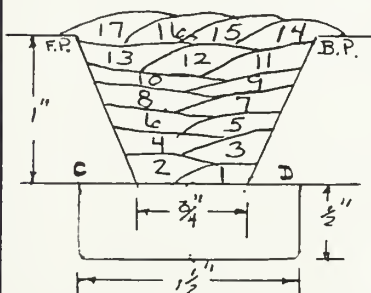
Process: Spray GMAW | Power Supply: GILLILAND (CV600) #G 24

Instrumentation: VCM #NC. 36554 Amp #NC 3970E

PLATE #A + #B

Plate No.: PD20307	Position: FLAT		Description: HY-100 UNDERMATCH								
Date: 3-17-93	Task No.:		Task Title: MIT / USN FATIGUE PLATES								
Wire Dia. & Type: .045/100S-1			Heat No.: 195245			Control No.: 11V21\$9			Spool No.:		
Shielding Gas Type: C-5			Cylinder No: 758269			Actual Composition:					
Bead No.	1	2	3	4	5	6	7	8	9	10	11
Cup Size (in.)	6-1/2"	1/2"	1/2"	1/2"	10 5/8"	10-5/8"	5/8"	5/8"	5/8"	5/8"	5/8"
Flow Rate (cfh)	35	35	35	35	45	45	45	45	45	45	45
Cup to Work (in.)	1/2"	5/8"	1/2"	1/2"	1/2"	5/8"	5/8"	5/8"	1/2"	1/2"	1/2"
Tip to Work (in.)	5/8"	3/4"	5/8"	5/8"	5/8"	3/4"	3/4"	3/4"	5/8"	5/8"	5/8"
Current Type/Pol.	DCRP										DCRP
PH/IP Temp. (F)	275/300										275/300
WFS (ipm)	282	306	304	305	303	323	312	311	299	302	300
OCV (V)	31	31	31	31	31	31	31	31	31	31	31
Current (A)	280	280	280	280	280	280	280	280	280	280	280
Voltage (V)	25.5	25.5	25.5	25.5	25.5	25.5	25.5	25.5	25.5	25.5	25.5
Travel Speed (ipm)	6.55	6.52	6.52	6.62	6.59	6.55	6.55	6.55	6.55	6.57	6.55
Heat Input (kJ/in)	65.4	65.7	65.7	64.7	65.0	65.4	65.4	65.4	65.4	65.2	65.4
Osc. Width (in.)	1/2"	1/16"	1/16"	1/16"	1/2"	1/2"	1/2"	1/2"	5/16"	5/16"	1/2"
Osc. Speed (pot)	56	52	52	52	44	40	40	36	40	40	44
Dwell L/R (pot)	C1 C3	C3 C2	C2 C3	C3 C2	C1 C3	C3 C2	C3 C3	C4 C3	C3 C3	C4 C2	C2 C4

PLATE - 30" LONG
HY 100 BASE MAT'L



Process: Spray GMAW | Power Supply: GILLILAND (CV600) #G 24

Instrumentation: v.o.m. # NC 36554, Amp # NC 39708

PLATE # C + #D

WIRE SAMPLE AFTER BEAD # 7 at 11:05 ^{A.M. DRY Bulb = 71}
_{WET Bulb = 56}
R.H. = 37%

Approx 6" cut from start end for AWT

GENERAL DYNAMICS
Electric Boat Division

D341 LABORATORY SERVICES SECTION QUANTITATIVE ANALYSIS REPORT

2 of 2

64-00-1663 (10-64) REV/591

TO: <i>R.W. Price, D341, Div 10 68544</i>		CHARGE - TO NUMBER <i>3304-106</i>	DATE <i>4-15-93</i>	
ITEM	HEAT NO.	DESCRIPTION	SPECIFICATION	REMARKS
1	<i>P020306</i>	<i>.045" after heat 11</i>		<i>01230, 12029</i>
2				
3				
4				
5				
6				
7				
8				
9				
10	SPEC REQ'T Mil-1205-1 wire Mil-E-23765/20 (modified)			

ITEM	C	S	P	Si	Mn	Fe	Ti	Cr	N	Cu	Mo	Cb	V	Al	Sn	Pb	02 ppm	N2 ppm
1	<i>0.051</i>	<i>0.003</i>	<i>0.004</i>	<i>0.30</i>	<i>1.61</i>	<i>0.019</i>	<i>0.27</i>	<i>2.27</i>	<i>0.030</i>	<i>0.48</i>			<i>0.019</i>	<i>0.002</i>			<i>97</i>	<i>40</i>
2																		
3																		
4																		
5																		
6																		
7																		
8																		
9																		
10	<i>0.130</i>	<i>0.008</i>	<i>0.012</i>	<i>0.25</i>	<i>1.40</i>	<i>0.100</i>	<i>0.60</i>	<i>1.00</i>	<i>info</i>	<i>0.30</i>			<i>0.100</i>	<i>0.030</i>			<i>info</i>	<i>info</i>

CHEMIST	DATE	APPROVED	DATE	APPROVED
		<i>Wm H Kelly</i>	<i>4/15/93</i>	

172
D341 LABORATORY SERVICES SECTION QUANTITATIVE ANALYSIS REPORT

TO: R.W. Perschke, D341, DWID 68544	CHARGE - TO NUMBER 3324-106	DATE 4-11-93
-------------------------------------	--------------------------------	-----------------

ITEM		ANAL. NO.	DESCRIPTION		SPECIFICATION		REMARKS												
1	PD 20304		.045", after head 10				11V2159, 195245												
2	PD 20305		1/16", after head 5				10W0955, 195254												
3	PD 20307		.045", after head 7				11V2159, 195245												
4																			
5																			
6																			
7																			
8																			
9																			
10	SPEC REQ'T		Mil-1005-1 wire			Mil-E-23765/2D (mod)													
ITEM	C	S	P	SI	Mn	Fe	Li	Cr	Ni	Cu	Mo	Co	Fe	V	Al	Sn	Pb	N2	N2
1	0.045	0.003	0.003	0.30	1.57	0.020	0.09	1.73	0.016	0.30	0.011	0.002	0.010	185	73				
2	0.056	0.003	0.007	0.28	1.61	0.016	0.09	1.62	0.038	0.32	0.014	0.003	0.015	129	38				
3	0.044	0.003	0.005	0.32	1.59	0.021	0.09	1.73	0.017	0.33	0.015	0.001	0.011	187	82				
4																			
5																			
6																			
7																			
8																			
9	0.080	0.008	0.012	0.20	1.25	0.100	0.30	1.40	0.010	0.35	0.100	0.010	0.100	185	73				
10	0.080	0.008	0.012	0.20	1.25	0.100	0.30	1.40	0.010	0.35	0.100	0.010	0.100	185	73				
CHEMIST		DATE		APPROVED		DATE		APPROVED		DATE		APPROVED		DATE					

Electric Boat Division

DATE 3-30-93

LOG: 2m 49.1 d 102 + 104

LAB. REF: L3745 DW0 68543

	% R
1	11

[illegible]

APPROVED

TECHNOLIAN

TECHNICIAN
Gary Carter

DATE 3-10-93

LAB. REF: 13745 DWL 68528 (5253) CHARGE-TO NO.: 3324-106

[illegible]

04 00 2498 14EV 1/11

Electric Boat Division

LABORATORY SERVICES

MECHANICAL PROPERTIES TEST REPORT

DATE _____

3/24/93

TO: Mr. H. H. Mitchell dept 341

LOG: Lm 491 p 97

LAB. REF. 63745 DW0 68524 (5269)

CHARGE-TO NO.: 3324-106.

[illegible]

APPROVED

W. H. D. Logan
11/1/73

2025 RELEASE UNDER E.O. 14176

my wife,

Appendix C

High Hardness Armor Performance Data Sheets



REPLY TO
THE ATTENTION OF

DEPARTMENT OF THE ARMY
U.S. ARMY RESEARCH LABORATORY
ARSENAL STREET
WATERTOWN, MASSACHUSETTS 02172-0001



AMSRL-MA-MB (930415-HH)

15 April 1993

Lt. Edward Olson
Engineering Duty Officer
USN 13A Graduate Program
Massachusetts Institute of Technology
Department Of Ocean Engineering
Cambridge, MA 02139

SUBJECT: Weldment Specimens To MIT.

Per your request, I am submitting weldment specimens to aid you with your graduate studies involving HAZ crack growth. The base metal is MIL-A-46100 armor steel and the filler metal is ER100S-1 and ER70S-6. The specimens are as follows:

1. (5) 12"x 1.5"x 0.25" transverse GMAW weldments using ER100S-1 filler metal.
2. (5) 12"x 1.5"x 0.25" transverse GMAW weldments using ER70S-6 filler metal.
3. (2) 8"x 1.5"x 0.25" virgin base metal.
4. (1) 8"x 1.5"x 0.25" virgin base metal with an arc strike in the center of the plate.

If you need any additional information please call me at (617) 923-5185.

Sincerely,

Thomas G. Melvin
Welding Engineer
Processing Research Group

encl: Weldment specimens.

CF Mr. C. Hickey Jr., Chief, MPB
Mr. J. Nunes, Chief, PRG

Composition (wt%)	6.31 mm (1/4 in.)	7.31 mm (9/32 in.)	7.31 mm (Extra Hard)	9.71 mm (3/8 in.)
C	0.29	0.31	0.31	0.31
Mn	0.83	0.87	0.87	0.96
Ni	0.90	1.16	1.16	1.10
Cr	0.47	0.54	0.54	0.52
Mo	0.53	0.55	0.55	0.55
Si	0.38	0.43	0.43	0.39
Al	0.030	0.036	0.036	0.025
P	0.015	0.010	0.010	0.015
S	0.001	0.002	0.002	0.003
HRC	48	50	51	48
Plate Dimensions (in.)	65 x 165	65 x 220	65 x 220	72 x 100

NOTE: The heat treatment was as follows:

Austenitizing	1660°F (904°C)	~ 20 min
Spray Water (Roller Quench)		
Tempering	400°F (204°C)	~ 50 min for 3 plates 30 min for the extra hard (XH) plate

Table 4. TENSILE PROPERTIES OF HIGH HARD ARMOR AT ROOM TEMPERATURE

Specimen	UTS (ksi)	0.2% YS (ksi)	Elong. (%)	RA (%)
6.31 mm LT	252.2	202.7	10.4	44.5
6.31 mm LT	251.6	208.6	10.2	42.6
6.31 mm TL	249.7	200.8	10.5	44.2
6.31 mm TL	244.5	201.1	10.1	43.2
7.31 mm LT	259.2	209.3	10.0	46.1
7.31 mm LT	253.4	205.6	11.0	45.2
7.31 mm TL	254.7	206.7	10.3	48.0
7.31 mm TL	251.1	207.6	9.4	43.1
7.31 mm XH LT	265.8	207.0	9.8	41.5
7.31 mm XH LT	263.7	208.9	10.0	42.1
7.31 mm XH TL	266.4	209.5	11.3	36.1
7.31 mm XH TL	263.2	207.2	9.2	39.7
9.71 mm LT	250.0	197.7	12.0	48.8
9.71 mm LT	248.2	198.1	10.1	41.7
9.71 mm TL	249.7	204.1	9.0	48.4
9.71 mm TL	255.0	205.3	10.5	33.6

NOTE: LT = Longitudinal
TL = Transverse

Table 5. TENSILE PROPERTIES OF HIGH HARD ARMOR AT -40°F

Specimen	UTS (ksi)	0.2% YS (ksi)	Elong. (%)	RA (%)
6.31 mm TL	235.7	193.3	9.1	54.2
6.31 mm TL	255.0	209.9	11.2	50.1
7.31 mm TL	257.7	210.3	9.7	51.5
7.31 mm TL	258.5	209.4	9.7	51.2
7.31 mm XH TL	266.5	205.8	9.4	48.3
7.31 mm XH TL	266.0	205.3	10.2	47.9
9.71 mm TL	263.6	213.0	9.9	43.9
9.71 mm TL	263.0	219.1	9.7	47.1

NOTE: TL = Transverse

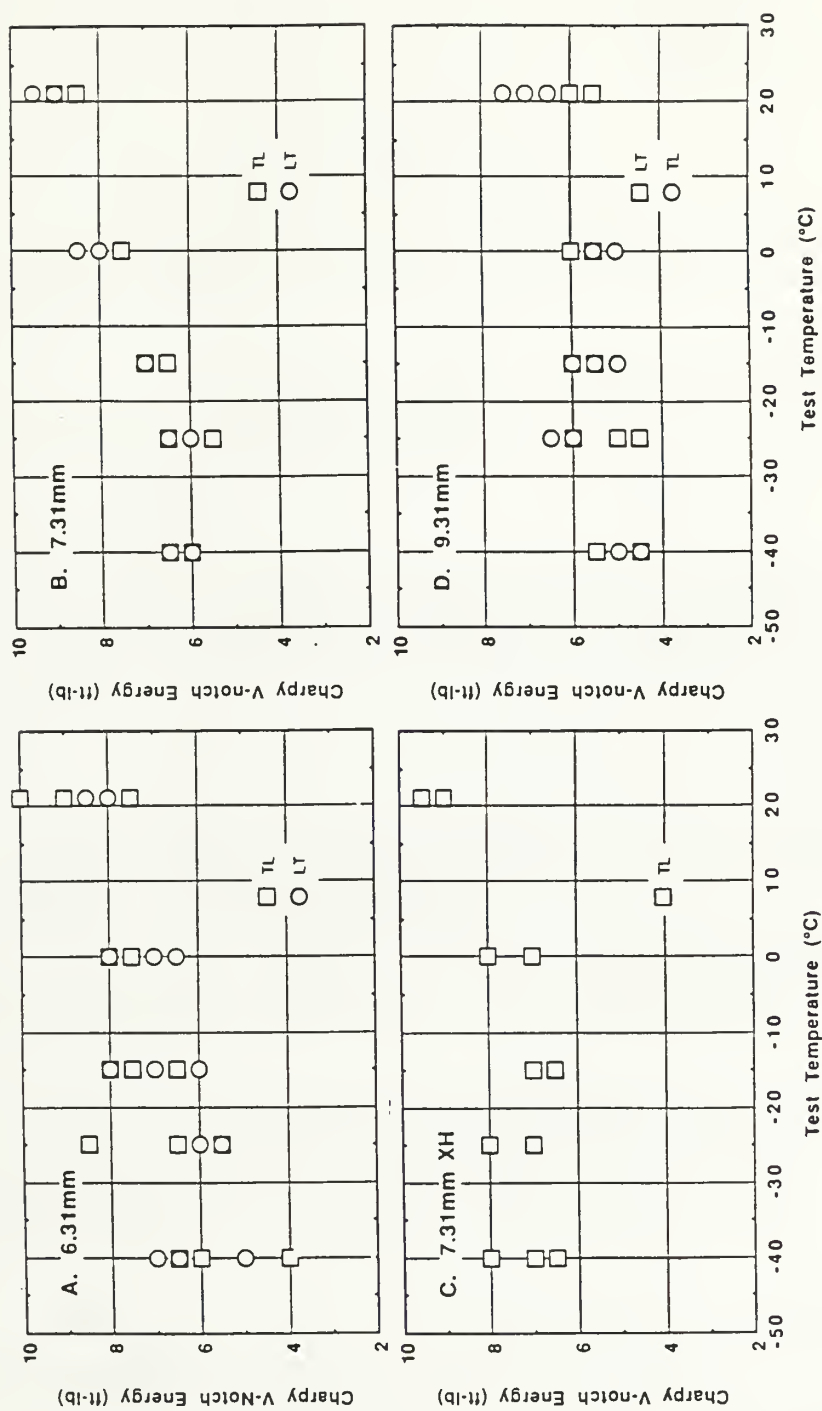


Figure 9. Charpy Impact energy (1/2 size specimens) versus temperature for (a) 6.31-mm plate, (b) 7.31-mm plate, (c) 7.31-mm XH plate, and (d) 9.71-mm plate

MIL-A-46100D(MR)
16 May 1988
SUPERSEDING
MIL-A-46100C
13 June 1983
AMENDMENT 2
20 October 1986

MILITARY SPECIFICATION

ARMOR PLATE, STEEL, WROUGHT, HIGH-HARDNESS

This specification is approved for use within the Department of the Army, and is available for use by all Departments and Agencies of the Department of Defense.

1. SCOPE

1.1 Scope. This specification covers quenched and tempered high-hardness wrought steel armor plate for lightweight armor applications for recommended thickness up to 2 inches inclusive (see 6.1 and 6.3).

2. APPLICABLE DOCUMENTS

2.1 Government documents.

2.1.1 Specifications and standards. Unless otherwise specified (see 6.2), the following specifications and standards of the issue listed in that issue of the Department of Defense Index of Specifications and Standards (DODISS) specified in the solicitation, form a part of this specification to the extent specified herein.

STANDARDS

MILITARY

MIL-STD-129 - Marking for Shipment and Storage
MIL-STD-163 - Steel Mill Products Preparation for Shipment and Storage
MIL-STD-367 - Armor Test Data Reporting
MIL-STD-1185 - Welding High Hardness Armor

(Copies of specifications, standards, handbooks, drawings, and publications required by manufacturers in connection with specific acquisition functions should be obtained from the contracting activity or as directed by the contracting officer.)

Beneficial comments (recommendations, additions, deletions) and any pertinent data which may be of use in improving this document should be addressed to: Director, US Army Laboratory Command, Materials Technology Laboratory, ATTN: SLCMT-MEE, Watertown, MA 02172-0001 by using the Standardization Document Improvement Proposal (DD Form 1426) appearing at the end of this document or by letter.

AMSC No. A4388

/FSC 9515/

DISTRIBUTION STATEMENT A Approved for public release; distribution unlimited.

2.1.2 Other Government documents, drawings, and publications. The following other Government documents, drawings, and publications form a part of this specification to the extent specified herein.

USATECOM TOP 2-2-710 - Ballistic Tests of Armor Materials
QSTAG 335 - Certification of Personnel for Ultrasonic Inspection

(Application for copies should be addressed to the Director, Defense Technical Information Center, Attn: DDR, Cameron Station, Alexandria, VA 22314)

2.2 Other publications. The following document(s) form a part of this specification to the extent specified herein. The issues of the documents which are indicated as DoD adopted shall be the issue listed in the current DODISS and the supplement thereto, if applicable.

ASTM

ASTM A578 - Specification for Straight-Beam Ultrasonic Examination of Plain and Clad Steel Plates for Special Applications
ASTM A751 - Methods, Practices, and Definitions for Chemical Analysis of Steel Products
ASTM E10 - Brinell Hardness of Metallic Materials
ASTM E18 - Rockwell Hardness and Rockwell Superficial Hardness of Metallic Materials
ASTM E23 - Notched Bar Impact Testing of Metallic Materials
ASTM E109 - Dry Powder Magnetic Particle Inspection
ASTM E290 - Semi-Guided Bend Test for Ductility of Metallic Materials

(Application for copies should be addressed to ASTM, 1916 Race Street, Philadelphia, PA 19103.)

Technical society and technical association specifications and standards are generally available for reference from libraries. They are also distributed among technical groups and using Federal agencies.

2.3 Order of precedence. In the event of a conflict between the text of this specification and the references cited herein, the text of this specification shall take precedence.

3. REQUIREMENTS

3.1 First article. When specified in the contract or purchase order (see 4.2.1.1.2, 6.2, 6.4, and 6.9), a sample or samples of the specified item shall be made available to the contracting officer or his authorized representative for approval in accordance with 4.2.1.1. The approval of the first article samples authorizes the commencement of shipment but does not relieve the supplier of responsibility for compliance with all applicable provisions of this specification. The first article samples and test plates shall be manufactured by the process proposed for use on production armor. The manufacturer's declared chemical analysis must be submitted to the contracting agency and to the ballistic test agency. The ballistic test agency will record the first article ballistic test plates submitted, showing the dates tested. Requests from the procuring activity to the ballistic test agency as

to prior conformance with first article tests must be accompanied by copies of the first article test firing records. Any deviation(s) noticed by the ballistic agency will be brought to the attention of the contracting activity and to the manufacturer.

3.1.1 First time producer. First time producers wishing to qualify to this specification should follow the instructions of 6.7.

TABLE I. Chemical composition (product analysis). 1/ 5/

Element	Maximum Range Percent	Maximum Limit Percent
CARBON	0.10	0.32
MANGANESE: Up to 1.00% incl	0.30	-
Over 1.00%	0.40	-
PHOSPHORUS	-	0.020 2/
SULFUR	-	0.010 2/
SILICON: Up to 0.60% incl	0.20	-
Over 0.60% to 1.00% incl	0.30	-
NICKEL	0.50	-
CHROMIUM: Up to 1.25% incl	0.30	-
Over 1.25%	0.40	-
MOLYBDENUM: Up to 0.20% incl	0.07	-
Over 0.20%	0.15	-
VANADIUM	0.15	-
BORON	-	- 3/
COPPER	-	0.25 4/
TITANIUM	-	0.10 4/
ZIRCONIUM	-	0.10 4/
ALUMINUM	-	0.10 4/
LEAD	-	0.01 4/
TIN	-	0.02 4/
ANTIMONY	-	0.02 4/
ARSENIC	-	0.02 4/

1/ This table lists the maximum range for elements of the manufacturer's established chemical composition.

2/ Phosphorus and sulfur should be controlled to the lowest attainable levels but in no case should the combined phosphorus and sulfur content exceed 0.025 percent.

3/ When the amount of boron is specified in the alloy, its content so determined by heat analysis shall not exceed 0.003%.

- 4/ When the amount of an element is less than 0.02% the analysis may be reported as 0.02%.
- 5/ Elements not listed in table, but intentionally added, shall be reported.

3.2 Acceptance requirements.

3.2.1 Chemical composition. The product produced to this specification shall meet the analysis of table I unless otherwise agreed upon between the steel supplier and the purchaser. All limits as specified in table I (including any deviations negotiated) shall be submitted in advance to the purchaser. The purchaser may establish and submit separate limits for each thickness of plate to be furnished (see 6.5). A statement showing the heat analysis of each melt and one product analysis of each lot and complete details of the heat treatment of each lot shall be furnished for the files of the purchaser at no cost. All elements of the chemical composition specified in table I shall be shown in the statement. When specified in the contract or order, armor material test reports shall be prepared in accordance with MIL-STD-367 to report the chemical composition range established by the producer and the chemical analysis of the material submitted (see 6.2.2 and 6.6).

3.2.2 Heat treatment. All plates in each lot, including samples, shall receive the same heat treatment except for such variations in tempering temperature as may be necessary to produce the prescribed hardness. Unless otherwise specified, local or general heating shall not be performed after the final heat treating operation (see 6.2). This does not include preheating for welding or flame cutting, as long as the tempering temperature is not exceeded. Unless otherwise specified (see 6.2) all plates shall be tempered for a minimum of 30 minutes after the centerline of the plate thickness has reached a temperature of at least 350°F, or shall be tempered for a minimum of one hour for each inch of thickness after the plate surface has reached a temperature of at least 350°F. For plates under one inch thick the tempering process shall be carried out according to the time schedule listed below, after the plate surface has reached a minimum temperature of 350°F:

1.00 inch	1 hour minimum
0.75 inch	3/4 hour minimum
0.50 inch	1/2 hour minimum
0.25 inch	1/2 hour minimum

The tempering operation should be done as soon as possible after quenching. It is recommended that the delay after quenching be no greater than 24 hours.

3.2.3 Condition. Unless otherwise specified (see 6.2), plates shall be in the as-heat treated condition; surfaces shall not be pickled.

3.2.4 Mechanical properties.

3.2.4.1 Hardness. The surface hardness of each plate, including first article samples, shall be within the range of HB 477 - HB 534. The diameters of Brinell hardness impressions on any individual plate shall not vary by more than 0.15 mm (see 4.6.2).

3.2.4.2 Impact resistance. The minimum Charpy V-notch impact resistance requirement of the armor plate shall be as shown in table II. The Charpy V-notch specimens shall be obtained in both the TL orientation (i.e., transverse to the major direction of rolling with the notch perpendicular to the plate surface so that the crack will propagate in the longitudinal direction) and the LT orientation (i.e., parallel to the major direction of rolling).

TABLE II. Minimum Charpy V-notch impact resistance requirements at -40° + 2°P.

Specimen orientation	Impact resistance for standard depth specimens (Average of 2 or more specimens), ft. lbs.			
	Standard width	3/4 width	1/2 width	1/4 width
Transverse (T-L)	10.0	7.5	5.0	2.5
Longitudinal (L-T)	12.0	9.0	6.0	3.0

3.2.5 Bend test. All bend test samples from that lot shall be capable of being bent to the requirements below without cracking as determined by either penetrant inspection per MIL-STD-6866 or magnetic particle inspection per MIL-STD-1949. Two bend test samples shall be tested in the transverse direction per ASTM E290, transverse bend test, at room temperature through an included angle of 90° (unrestrained) to the inside radii shown below. After bending, samples shall be free of cracks as determined by either penetrant inspection per MIL-STD-6866 or magnetic particle inspection per MIL-STD-1949.

<u>PLATE THICKNESS (T)</u>	<u>INSIDE RADIUS</u>
1/8 to 5/16	4T
Over 5/16 to 1/2	6T
Over 1/2 to 3/4	8T
Over 3/4 to 1	10T
Over 1 to 2	12T

NOTE: The bend test on material thicker than 1/2 inch shall be negotiated between the steel supplier and contractor if bending is required. Dimensions for thickness over 1/2 inch are listed for information purposes only.

3.2.6 Ballistic requirements. Ballistic requirements shall be in accordance with the appendix of this specification.

3.2.7 Dimensions and tolerances.

3.2.7.1 Dimensions. Plates shall comply with the dimensions specified in the applicable drawings or in the contract or order (see 6.2).

3.2.7.2 Thickness. The thickness tolerance of each plate, after final treatment, shall be in accordance with table III for the thickness specified.

3.2.7.3 Flatness. Unless otherwise specified in the contract or order, the flatness tolerance of each plate shall be within the requirements specified in

table IV. Tighter tolerance requirements may be specified in the contract or order and shall be as agreed upon between the contractor and the procuring activity.

3.2.7.4 Waviness. Unless otherwise specified in the contract or order, the waviness tolerance of each plate shall be within the requirements of table V.

TABLE III. Thickness tolerances for ordered thickness 1/
inches (over and under) 2/.

		Tolerances over and under ordered thickness for widths given						
Specified Thickness	To	60" to 72"	72 to 84"	84 to 96"	96 to 108"	108 to 120"	120 to 132"	132 to 144"
Inches	60"	excl.	excl.	excl.	excl.	excl.	excl.	incl.
1/8	2/	.016	.016	.019	.019	.023	----	----
3/16	2/	.016	.016	.019	.019	.023	----	----
1/4	2/	.016	.016	.019	.019	.023	----	----
5/16	2/	.016	.019	.019	.019	.023	.026	----
3/8	2/	.016	.019	.019	.023	.023	.026	----
7/16	2/	.016	.019	.019	.023	.026	.026	.031
1/2	2/	.016	.019	.019	.023	.026	.026	.031
9/16	2/	.019	.019	.019	.023	.026	.031	.031
5/8	2/	.019	.019	.019	.023	.026	.031	.031
11/16	2/	.019	.019	.019	.023	.026	.031	.031
3/4	2/	.019	.019	.023	.023	.026	.031	.039
13/16	2/	.023	.023	.023	.026	.031	.031	.039
7/8	2/	.023	.023	.026	.026	.031	.031	.039
15/16	2/	.023	.023	.026	.026	.031	.036	.043
1	2/	.026	.026	.026	.026	.031	.036	.043
1-1/16	2/	.026	.026	.026	.031	.031	.036	.043
1-1/8	2/	.026	.026	.026	.031	.031	.039	.043
1-3/16	2/	.031	.031	.031	.031	.036	.043	.048
1-1/4	2/	.031	.031	.031	.036	.036	.043	.048
1-5/16	2/	.031	.031	.031	.036	.036	.043	.053
1-3/8	2/	.031	.031	.031	.036	.039	.048	.053
1-7/16	2/	.036	.036	.036	.036	.043	.048	.058
1-1/2	2/	.036	.036	.036	.039	.043	.048	.058
1-9/16	2/	.036	.036	.036	.039	.043	.058	.058
1-5/8	2/	.036	.036	.036	.043	.048	.058	.063
1-11/16	2/	.039	.039	.039	.043	.048	.058	.063
1-3/4	2/	.039	.039	.039	.043	.048	.058	.068
1-13/16	2/	.043	.043	.043	.048	.053	.058	.068
1-7/8	2/	.043	.043	.043	.048	.053	.063	.068
1-15/16	2/	.043	.043	.043	.048	.053	.063	.076
2	2/	.043	.043	.043	.048	.053	.063	.076

1/ For intermediate thickness, the tolerance of the closer specified gage shall apply. In case of mid-point, the tolerance for lower gage or interpolated value shall apply.

2/ When plates under 60" are rolled double width, the equivalent wider plate tolerance shall apply.

TABLE IV. Permissible variations from flatness.

Specified Thickness, in.	Variations from a flat surface for specified widths, in.									
	Over 8 to 36 excl.	36 to 48 excl.	48 to 60 excl.	60 to 72 excl.	72 to 84 excl.	84 to 96 excl.	96 to 108 excl.	108 to 120 excl.	120 to 144 incl.	144 to 160 incl.
Up to 1/4, excl.	13/16	1-1/8	1-3/8	1-7/8	2	2-1/4	2-3/8	2-5/8	2-3/4	
1/4 to 3/8, excl.	3/4	15/16	1-1/8	1-3/8	1-3/4	1-7/8	2	2-1/4	2-3/8	
3/8 to 1/2, excl.	3/4	7/8	15/16	15/16	1-1/8	1-5/16	1-1/2	1-5/8	1-7/8	
1/2 to 3/4, excl.	5/8	3/4	13/16	7/8	1	1-1/8	1-1/4	1-3/8	1-5/8	
3/4 to 1, excl.	5/8	3/4	7/8	7/8	14/15	1	1-1/8	1-5/16	1-1/2	
1 to 2, excl.	9/16	5/8	3/4	13/16	7/8	15/16	1	1	1	

Note 1 - Flatness tolerances for length - The longer dimension specified in considered the length, and variations from a flat surface along the length should not exceed the tabular amount for the specified width in plates up to 12 ft. in length, or in any 12 ft. or longer plates.

Note 2 - Flatness tolerances for width - The flatness variations across the width should not exceed the tabular amount for the specified width.

Note 3 - When the longer dimension is under 36 in., the variation should not exceed 3/8 in. When the larger dimension is from 36 to 72 in., incl., the variation should not exceed 75% of the tabular amount for the specified width."

TABLE V. Waviness tolerances for plates.

Flatness tolerance from table IV	When number of waves in 12 ft is:						
	1	2	3	4	5	6	7
3/8	3/8	5/16	3/16	3/16	1/8	1/16	1/16
7/16	7/16	5/16	1/4	3/16	1/8	1/8	1/16
1/2	1/2	3/8	5/16	3/16	3/16	1/8	1/16
9/16	9/16	7/16	5/16	1/4	3/16	1/8	1/8
5/8	5/8	1/2	3/8	1/4	3/16	1/8	1/8
11/16	11/16	1/2	3/8	5/16	3/16	3/16	1/8
3/4	3/4	9/16	7/16	5/16	1/4	3/16	1/8
13/16	13/16	5/8	7/16	5/16	1/4	3/16	1/8
7/8	7/8	11/16	1/2	3/8	1/4	3/16	1/8
15/16	15/16	11/16	1/2	3/8	5/16	1/4	3/16
1	1	3/4	9/16	7/16	5/16	1/4	3/16
1-1/8	1-1/8	7/8	5/8	1/2	3/8	1/4	3/16
1-1/4	1-1/4	15/16	11/16	1/2	3/8	5/16	1/4
1-3/8	1-3/8	1-1/16	3/4	9/16	7/16	5/16	1/4
1-1/2	1-1/2	1-1/8	7/8	5/8	1/2	3/8	1/4
1-5/8	1-5/8	1-1/4	15/16	11/16	1/2	3/8	5/16
1-3/4	1-3/4	1-5/16	1	3/4	9/16	7/16	5/16
1-7/8	1-7/8	1-7/16	1-1/16	13/16	5/8	1/2	3/8
2	2	1-1/2	1-1/8	7/8	5/8	1/2	3/8
2-1/4	2-1/4	1-11/16	1-1/4	15/16	11/16	9/16	3/8
2-3/8	2-3/8	1-13/16	1-5/16	1	3/4	9/16	7/16
2-5/8	2-5/8	2	1-1/2	1-1/8	13/16	5/8	7/16
2-3/4	2-3/4	2-1/16	1-9/16	1-1/8	7/8	5/8	1/2

NOTES:

NOTE 1 Waviness denotes the deviation of the top or bottom surface from a horizontal line, when the plate is resting on a flat surface, as measured in an increment of less than 12 ft of length. The waviness tolerance is a function of the flatness tolerance as obtained from table IV.

NOTE 2 When the flatness tolerance is 5/8 inch or less for plates 1/2 inch or less in thickness, the waviness tolerance shall not apply.

3.2.8 Identification marking. Identification marking shall be legibly painted and records shall be such as to ensure positive identification of all plates, including test samples and specimens, with the lot and corresponding heat from which they were produced. Marking shall be approximately six inches in from the edge of the plate. The key to identification symbols shall be furnished to the inspector prior to submittal for inspection. First article and acceptance ballistic test plates shall also be marked with the manufacturer's name or trademark, the number of this specification, and the ordered plate thickness in inches. First article plates shall be marked "PRE", acceptance plates "ACC", and retest plates will be marked "R1" and "R2". If a second set of retest plates are submitted they shall be marked "RR1" and "RR2". The primary plate rolling direction should be identified.

3.2.9 Workmanship.

3.2.9.1 Surface condition. The top and bottom surface of each plate shall be free from the following surface defects: slivers, laps, checks, seams, blisters, snakes, cold shuts, cracks, burning, mechanical seams, mechanical gouges and laminations (see 6.10). The surface of each plate shall be such that mill scale or oxidation product shall not interfere with determination of acceptability. Imperfections listed above, which are of such a nature as to affect the fabrication of the materials, are rejectable.

3.2.9.1.1 Depth of imperfections. The depth of rolled-in scale, scale pitting or snakes shall not exceed 0.015 inch and shall not reduce the steel thickness below the allowable minimum. Isolated individual pits over 0.015 inch deep but not over 0.03 inch deep and not within 6 inches of each other and which do not violate the minimum allowable thickness, as specified in the applicable drawings and fabrication documents, are acceptable.

3.2.9.2 Edge preparation. Thermal cutting shall be permitted after final heat treatment provided the procedure, which may include grinding after thermal cutting, is such that no cracks develop on any thermally cut edge whether detected by nondestructive inspection, or as agreed upon in the contract. To reduce the potential for plate cracking, plates shall not be cut by cold shearing after final heat treatment. The heat affected zone of thermally cut plates (up to and including 1/2-inch in thickness) shall not exceed 1.2 times the plates thickness from the cut edge. For plates over 1/2-inch thick, the heat affected zone shall not exceed 5/8-inch from the cut edge. In order to have the heat affected zone exceed these limits approval shall be obtained from the procuring activity.

3.2.9.3 Edge condition. Plate edge on plates delivered after heat treatment shall be free of cracks. The supplier shall practice such necessary process controls to prevent this condition.

3.2.9.4 Edge quality. For all plates the steel supplier shall institute such necessary controls such that any cut parts shall comply with the requirements of 3.2.9.4.1, whether detected by magnetic particle inspection, or liquid penetrant inspection.

3.2.9.4.1 Acceptance criteria.

3.2.9.4.1.1 Single linear indications. In any four inches of length a single linear indication shall not exceed twice the plate thickness.

3.2.9.4.1.2 Multiple linear indications. Multiple linear indications shall not exceed 1-1/2 times the plate thickness if two or more lie in the same plane. The total length of indications in one plane, in any four inch length, shall not exceed twice the plate thickness. No more than ten indications, whether in one plane or multiple planes, are permitted in any four inch length.

3.2.9.4.1.3 Cracks. All cracks are rejectable.

3.2.9.4.1.4 Removal of large indications. Large indications shall be removed by the manufacturer or processor by grinding, provided the resulting cavity does not exceed 1/4 inch.

4. QUALITY ASSURANCE PROVISIONS

4.1 Responsibility for inspection. Unless otherwise specified in the contract or purchase order (see 6.2), the contractor is responsible for the performance of all inspection requirements as specified herein. Except as otherwise specified in the contract or order, the contractor may use his own or any other facility suitable for the performance of the inspection requirements specified herein, unless disapproved by the Government. The Government reserves the right to perform any of the inspections set forth in the specifications where such inspections are deemed necessary to assure that supplies and services conform to prescribed requirements.

4.1.1 Responsibility for compliance. All items must meet all requirements of sections 3 and 5. The inspection set forth in this specification shall become a part of the contractor's overall inspection system or quality program. The absence of any inspection requirements in the specification shall not relieve the contractor of the responsibility of assuring that all products or supplies submitted to the Government for acceptance comply with all requirements of the contract. Sampling in quality conformance does not authorize submission of known defective material, either indicated or actual, nor does it commit the Government to acceptance of defective material.

4.2 Classification.

4.2.1 Classification of inspection. The inspection requirements specified herein are classified as follows:

1. First article inspection (see 4.2.1.1).
2. Quality conformance inspection (see 4.2.1.2).

4.2.1.1 First article inspection. When required (see 6.2), the first article samples submitted in accordance with 3.1, shall be examined for all the provisions of this specification applicable to end item examination.

4.2.1.1.1 First article tests. First article tests shall consist of all the tests specified in 4.6 (see 6.2.2).

4.2.1.1.2 First article ballistic test. Unless otherwise specified (see 3.1, 6.2 and 6.4), the first article ballistic test shall not be required provided (a) the manufacturer, within 37 months, has produced acceptable plates within the same nominal thickness ranges of table VI and (b) his production conditions are the same as for previously accepted plates. A supplier who has previously met the first article requirements will furnish the procuring activity with the pertinent data relative to compliance with first article test.

4.2.1.2 Quality conformance (acceptance) inspection. The acceptance examination under 4.5 and the tests under 4.6 shall serve as a basis for the acceptance of individual production lots.

4.3 Lot. A lot shall consist of all production and ballistic test plates of the same melt of steel, of the same thickness, having the same treatment, and heat-treated with the same thermal cycle in the same production furnace(s) in the same facility. When specified (see 4.3.1 and 6.2), production and

ballistic test plates may be allowed to be heat-treated separately. The test plate shall be heat-treated in a production furnace.

4.3.1 Separately heat treated ballistic test plate. When a ballistic test plate is allowed to be heat-treated separately from the production plates it represents, the production plates shall remain in the non-heat treated condition (as rolled condition only) until the results are received from the testing activity showing that the ballistic test plate has passed (see 6.15). Note: If the ballistic test plate is separately heat-treated it will be so stated in the data to be supplied in accordance with MIL-STD-367.

4.4 Sampling.

4.4.1 For first article.

4.4.1.1 Chemical analysis samples. One sample for chemical analysis shall be taken from each plate submitted.

4.4.1.2 Impact samples. At least two impact test specimens shall be taken from each test plate submitted for ballistic testing.

4.4.1.3 Ballistic samples. Two ballistic test plates of the same ordered thickness for each nominal thickness range shown in table VI below shall be submitted for ballistic testing and shall represent any other thickness in the range. One sample shall be taken from the first plate heat treated and one from the last plate heat treated in the initial lot produced. When only one plate is heat treated, a sample shall be taken from each end of the plate. The ballistic test plates shall be 12 inches by 36 inches.

TABLE VI. Thickness ranges and corresponding test projectiles for first article testing (a).

Nominal thickness range (inches)	Obliquity (degrees)	Test Projectile
0.125 to 0.300 incl.	30	Cal .30 AP, M2
0.301 to 0.590 incl.	30	Cal .50 AP, M2
0.591 to 0.765 incl.	30	14.5 mm API, B32
0.766 to 1.065 incl.	30	14.5 mm API, BS41
1.066 to 2.000 incl.	0	20 mm API-T, M602

(a) Minimum required ballistic limits are tabulated in tables VII through X of the Appendix. The plates are tested at 30° obliquity.

4.4.1.4 Bend test samples. Unless otherwise specified (see 6.2), two samples shall be taken from each submitted test plate and shall be tested in accordance with 4.6.4 and shall meet the requirements of 3.2.5.

4.4.2 Sampling for quality conformance inspection.

4.4.2.1 For chemical analysis. At least one sample for chemical analysis shall be taken from each heat in accordance with the applicable method specified in ASTM A751 (see 6.5).

4.4.2.2 For hardness tests. The Brinell hardness of each plate, as heat-treated, shall be measured in two places, one at each end of a diagonal on one surface of the plate.

4.4.2.3 For Charpy V-notch impact tests. A sample shall be taken from a plate representing each lot for Charpy V-notch impact tests. The sample shall be the same thickness as the plate it represents and large enough to obtain at least four specimens from the sample in accordance with 4.6.3.

4.4.2.4 For ballistic acceptance testing. One plate, of each thickness to be supplied on the contract, shall be randomly taken from each lot for ballistic testing. In the event that two ordered thicknesses that are 0.010 inches or less apart, are to be made from the same lot, then only one of the ordered thicknesses need be submitted for acceptance testing. The other ordered thickness, however, shall be included on the applicable reporting form in accordance with MIL-STD-367, with the words indicating that it is represented by the sample to be tested. However, if the two ordered thicknesses are such that each thickness requires testing with a different type projectile as shown in table VI, then each of the ordered thicknesses shall be ballistically tested. Unless otherwise specified, the plates shall be 12 inches by 36 inches. Test projectiles will be as specified in table VI.

4.4.2.5 Bend test samples. Unless otherwise specified (see 6.2), two samples shall be randomly taken from each lot for these tests representing the entire lot of material; however, when an entire heat represents only one lot the samples shall be taken from the first and last usable portion of the heat. Testing shall be conducted in accordance with 4.6.4 and shall meet the requirements of 3.2.5.

4.4.2.6 Thermally cut plates. For plates thermally cut after heat treatment, one sample plate per thickness shall be sampled and tested for hardness at two (2) locations perpendicular to the cut edge in accordance with 3.2.9.2. Plates not meeting the minimum requirement of 3.2.4.1 shall be rejected. In addition, the edges of the plates shall be examined nondestructively for cracks after cutting.

4.4.2.7 Ultrasonic inspection. All plates 1/2-inch and greater in thickness shall be inspected ultrasonically for soundness in accordance with 4.6.6.

4.5 Examination.

4.5.1 Visual. All steel plate shall be subject to visual inspection for compliance with the requirements for identification marking (see 3.2.3) and for workmanship (see 3.2.9).

4.5.2 Dimensional. All steel plate shall be subject to inspection for compliance with dimensional and tolerance requirements (see 3.2.7).

4.5.3 Preparation for shipment. Examination shall be made to determine compliance with the requirements for preparation for shipment (see section 5).

4.6. Tests.

4.6.1 Chemical analysis. Chemical analysis shall be conducted in accordance with the applicable method specified in ASTM A751 (see 6.5). The analysis shall comply with the declared composition established in accordance with the requirements of table I (see 3.2.1).

4.6.2 Hardness tests. Brinell hardness tests (HB) shall be conducted in accordance with ASTM E10, using a 10mm carbide ball and a 3000 kilogram load. Surface scale and decarburization shall be removed from the areas where the tests are to be made. However, no more than 0.060" shall be removed from the test area. Hardness tests may be made on the surfaces of pieces cut from the plate after heat treatment.

4.6.2.1 Rockwell hardness tests. For plates less than 3/16 inch in thickness, Rockwell - C hardness tests (HRC) shall be substituted for HB tests. Tests shall be conducted in accordance with ASTM E18 and the readings shall be converted to HB.

4.6.3 Charpy V-notch impact tests. At least four Charpy V-notch impact test specimens shall be taken from the sample and shall be prepared and tested in accordance with ASTM E23. Charpy V-notch impact test specimens shall be taken in both the TL orientation and in the LT orientation from locations midway between the top and bottom surfaces of the plate and at least 4 inches or 2T, whichever is less, from any quenched edge as well as outside the heat affected zone of any oxygen-cut edge. The largest attainable subsize Charpy V-notch impact specimens shown in figure 7 of ASTM E23 shall be used.

4.6.4 Bend test: The bend test shall be conducted in accordance with ASTM E290 using method Arrangement C.

4.6.5 Ballistic tests. Ballistic testing of armor plate shall be conducted at a Government test facility specified in the contract or order (see 6.2). Testing shall be conducted in accordance with the requirements of the appendix of this specification.

4.6.6 Ultrasonic examination.

4.6.6.1 Inspection equipment. The ultrasonic soundness inspection equipment shall conform to ASTM A578.

4.6.6.2 Procedure. Unless otherwise specified (see 6.2) the ultrasonic examination shall be carried out in accordance with ASTM A578 with the following exceptions.

- (a) Scanning shall be continuous over 100% of the plate surface.
- (b) Scanning rate shall be at a speed where recordable discontinuities can be detected.
- (c) The testing frequency shall be a minimum of 2-1/4 megahertz (MHz).
- (d) Any area within a plate where a discontinuity produces a continuous total loss of back reflection accompanied by continuous indications on the same plane that cannot be encompassed within a circle whose diameter is 1-in. shall be cause for rejection of that plate. All discontinuities will be evaluated using a frequency of 2-1/4 megahertz (MHz).

4.6.6.3 Certification of inspection personnel. Unless otherwise specified (see 6.2), personnel performing ultrasonic inspection shall comply with the qualification requirements of MIL-STD-410, level II, or equivalent, as determined by QSTAG 335 (see 6.11).

4.7 Reduced testing. At the discretion of the procuring activity, the amount of testing may be reduced provided the results on consecutive lots indicate that a satisfactory uniform product meeting the testing requirements is being produced (see 6.2). Reduced testing shall be in accordance with a system previously approved or established by the procuring activity involved.

4.8 Rejection and retest.

4.8.1 Rejection. Unless otherwise specified in the contract or order (see 6.2), failure of the first article samples to meet the requirements of this specification shall be cause for rejection of the process, failure of the acceptance samples to meet the requirements of this specification shall be cause for rejection of the lot (see 4.8.2).

4.8.2 Retest. Unless specific retest procedure is specified in the contract or order (see 6.2), two retest samples shall be submitted for each failed sample. Failure of either of the retest samples (plates) shall be cause for rejection of the material. First article retests shall not be permitted until the supplier has made the necessary corrections in the processing of the material to the satisfaction of the procuring activity.

5. PACKAGING

5.1 Preservation and packaging. Preservation and packaging shall be level A or C as specified (see 6.2).

5.1.1 Level A. Cleaning, drying, preservation, and packaging shall be in accordance with MIL-STD-163.

5.1.2 Level C. Cleaning, drying, preservation, and packaging shall be in accordance with manufacturer's commercial practice.

5.2 Packing. Packing shall be level A or level C as specified (see 6.2).

5.2.1 Level A. Packing shall be in accordance with MIL-STD-163.

5.2.2 Level C. Packing shall be in accordance with commercial practice adequate to ensure acceptance and safe delivery by the carrier for the mode of transportation employed.

5.3 Marking. In addition to any special marking specified in the contract or order, shipments shall be marked in accordance with the requirements of MIL-STD-129.

6. NOTES

6.1 Intended use. The steel armor covered by this specification is intended for lightweight applications where resistance to ball and armor piercing types of ammunition and multiple hit capability are required.

6.2 Ordering data.

6.2.1 Procurement requirements. Procurement documents should specify the following:

- a. Title, number and date of this specification
- b. If first article samples are to be made available (see 3.1).
- c. If additional heat treatment may be performed (see 3.2).
- d. If plates may be furnished in a condition other than in 3.2.2.
- e. Dimensions (see 3.2.7).
- f. Name of inspection agency when inspection shall be performed by other than the contractor (see 4.1).
- g. If first article testing is required (see 4.2.1.1).
- h. When a special first article ballistic tested is required (see 3.1, 4.2.1.1.2 and 6.9).
- i. If lot is different than 4.3.
- j. Production sampling if other than in 4.4.2.5.
- k. If different certification of inspection personnel is required (see 4.6.6.3).
- l. Where ballistic testing is to be conducted (see 4.6.5).
- m. The reduced testing plan when applicable (see 4.7).
- n. If rejection and retest differ from 4.8.
- o. Preparation for delivery requirements (see section 5).
- p. If different ultrasonic test procedures are required (see 4.6.6.2).

6.2.2 Data requirements. When this specification is used in an acquisition and data are required to be delivered, the data requirements identified below shall be developed as specified by an approved Data Item Description (DD Form 1664) and delivered in accordance with the approved Contract Data Requirements List (CDRL), incorporated into the contract. When the provisions of DOD FAR supplement, Part 27, Sub-Part 27.475-1 (DDForm 1423) are invoked and the DD Form 1423 is not used, the data specified below shall be delivered by the contractor in accordance with the contract or purchase order requirements. Deliverable data required by this specification are cited in the following paragraphs.

<u>Paragraph No.</u>	<u>Data Requirement Title</u>	<u>Applicable DID No.</u>	<u>Option</u>
3.1, 4.2.1.1.1	Report, First Article Test	UDI-T-23790	
3.2.1	Armor Material Test Reports	DI-MISC-80073	Format I

(Copies of DID's required by contractors in connection with specific acquisition functions should be obtained from the Naval Publication and Forms Center or as directed by the contracting officer.)

6.3 Fabrication. The armor plate covered by this specification is subject to fabrication involving cutting, drilling, forming, and welding. It is intended that selection and control of chemical composition, cleanliness, and plate processing will be such that the armor will be suitable for fabrication under procedures and controls such as specified in MIL-STD-1185, Welding High Hardness Armor.

6.3.1 Plate Cutting. To reduce the potential for plate cracking, it is important that plates should not be cut by cold shearing after final heat treatment.

6.4 Special First Article ballistic test. Special first article ballistic tests are required when the manufacturer changes either the heat treatment or the declared chemistry of the armor.

6.5 Chemical analysis. Suggested ASTM instrumental methods that can be used for chemical analysis are E415, E282, E484 and E322. ASTM A751 should be consulted for a complete list of methods.

6.6 MIL-STD-367. MIL-STD-367 replaces Form MIL 46100 and TAC Form 3983.

6.7 Potential suppliers. Potential suppliers who have not previously supplied armor plate to MIL-A-46100 and wish to have their material ballistically tested, may do so at their own expense. It is recommended that inquiries for such testing be directed to Commander, US Army CSTA, ATTN: AMSTE-TO-O, Aberdeen Proving Ground, MD 21005.

6.8 Metric units. When metric dimensions are required, units for inch, foot, foot-pounds and feet per second may be converted to the metric equivalent by multiplying them by the following conversion factors:

English	Multiply by	Equals	Metric SI unit
inch	0.0254	=	meter (m)
foot	0.3048	=	meter (m)
foot-lb	1.3558	=	joule (J)
feet/sec	0.3048	=	meter per second (m/s)

Note: Conversion factors can be associated with ASTM E380 entitled "Metric Practice Guide."

6.9 New contracts sponsored by government agencies. At the time that a new contract is initiated for the production of combat vehicles, the contractor's supplier is to estimate the number, size and delivery schedule of the ballistic test plates which are to be submitted for first article or acceptance testing (see 6.2). A lead time of 60 days after the contract has been signed is to be allowed prior to shipment of the first ballistic test(s) to APG to insure that all administrative functions for the establishment of a new CSTA project have been completed in preparation for the test. The contracting government activity is to initiate the new project through a letter to Commander, US Army CSTA, ATTN: AMSTE-TO-O, Aberdeen Proving Ground, MD 21005-5059 requesting a cost estimate for the ballistic testing of the applicable number and sizes of plates. In the case of increases in scope of existing projects, similar correspondence is needed.

6.10 Definitions.

6.10.1 Slivers. An imperfection consisting of a very thin elongated piece of metal attached by only one end to the parent metal into whose surface it has been worked.

6.10.2 Laps. A surface imperfection with the appearance of a seam, caused by hot metal, fins or sharp corners being folded over and thus being forged or rolled into the surface but without being welded.

6.10.3 Checks. Numerous very fine cracks at the surface of a metal part. Checks may appear during processing or during service and are most often associated with thermal cycling or thermal treatment. Also called check marks, checking, heat checks.

6.10.4 Seams. An unwelded fold or lap that appears as a crack, usually resulting from a discontinuity on a metal surface.

6.10.5 Blisters. A raised area, often dome shaped, resulting from delamination under pressure of expanding gas trapped in metal in a near sub-surface zone. Very small blisters may be called pinhead blisters or pepper blisters.

6.10.6 Snakes. Any crooked surface imperfection in a metal plate, resembling a snake.

6.10.7 Cold shuts. A lap on the surface of a forging or billet that was closed without fusion during deformation.

6.10.8 Burning. Permanently damaged metal due to overheating enough to cause incipient melting or intergranular oxidations. Note: This condition is usually obscured by normal cleaning methods and would require deep pickling and/or metallography to note the continuous oxidation (chicken wire effect) of the enlarged grain boundaries. This defect is usually not limited to the surface and may be sub-surface or at interior locations when associated with heavy mechanical working. Metal with these conditions shall be scrapped.

6.10.9 Laminations. A type of discontinuity with separation or weakness generally aligned parallel to direction of the worked surface of the metal and may be the result of pipe blisters, seams, inclusions, or segregation elongated and made directional by working.

6.10.10 Linear indication. For nondestructive examination purposes, a linear indication is evidence of a discontinuity that requires interpretation to determine its significance.

6.11 Quadripartite standardization agreement (QSTAG). QSTAG 335, pertaining to the certification of personnel for ultrasonic inspection, states that level I of Canadian Government specification Board Standard 48-GP-7M is equivalent to MIL-STD-410, level II.

6.12 Certain provisions of this specification (see 6.11) are the subject of international standardization agreement (QSTAG 335). When amendment, revision, or cancellation of this specification is proposed which will modify the international agreement concerned, the preparing activity will take appropriate action through international standardization channels including departmental standardizational offices to change the agreement or make other appropriate accommodations.

6.13 Plates in the as-rolled condition. When the fabricator performs the final quench and temper of plates, it shall be his responsibility that the mechanical and ballistic requirements of the plates, meet this specification.

6.14 Subject term (key word) listing.

Armor - lightweight	Heat-treated armor plates
Ballistic testing	Wrought steel, high-hardness

6.15 Caution for production plates. Material made to this specification has a tendency to develop stress cracks if not tempered as soon as possible after austenizing. To avoid this situation where plates may be left in the austenized condition and in the untempered state while waiting to receive the results of the ballistic test plate representing the lot, all the plates in the lot shall be left in the as-rolled (unheat-treated) condition.

Custodian:
Army - MR

Preparing activity:
Army - MR

Review activities:
Army - AT, EA, AR, TE
DLA - IS

Project 9515-A002

(WP# ID-2901A/DISC-0393A. FOR MTL USE ONLY)

APPENDIX

BALLISTIC TESTING OF ARMOR PLATE, STEEL, WROUGHT
HIGH HARDNESS

10. SCOPE

10.1 This appendix covers the requirements for ballistic testing of high hardness steel armor plate.

20. DEFINITIONS

20.1 Fair impact. A fair impact is an impact resulting from the striking of the test plate by a projectile in normal flight (no yawing or tumbling) and separated from another impact or the edge of the plate, hole, crack, or spalled area by an undisturbed area of at least two test projectile diameters.

20.2 Witness sheet. A witness sheet is normally a 0.014 inch thick sheet of 5052 H36 aluminum alloy (or a 0.020 inch thick sheet of 2024-T3 aluminum alloy) placed 6 inches (+1/2 inch) behind and parallel to the test plate or other ballistic sample.

20.3 Complete penetration, protection, CP(P). A protection complete penetration is a penetration in which the projectile or one or more fragments of the projectile or plate pass beyond the back of the test plate and perforates the witness plate.

20.4 Partial penetration, protection, PP(P). A partial penetration is any impact that is not a complete penetration.

20.5 Gap. The difference in velocity between the high partial penetration velocity and the low complete penetration velocity used in computing the ballistic limit where the high partial penetration velocity is lower than the low complete penetration velocity..

20.6 V₅₀ protection ballistic limit, BL(P). The protection V₅₀ ballistic limit is defined as the average of 6 fair impact velocities comprising the three lowest velocities resulting in complete penetration and the three highest velocities resulting in partial penetration. A maximum spread of 150 feet per second shall be permitted between the lowest and highest velocities employed in determination of ballistic limits. In only those cases where the lowest complete penetration velocity is lower than the highest partial penetration velocity by more than 150 fps will the ballistic limit be based on 10 velocities (the 5 lowest velocities that resulted in complete penetration and the 5 highest velocities that resulted in partial penetrations). When the 10-round excessive spread, ballistic limit is used, the velocity spread will be reduced to the lowest partial level (as close to 150 fps as possible). When a 10-round ballistic limit is used, this will be noted in all reports. The normal up-and-down firing method will be used in the determination of all BL(P)'s, all velocities being corrected to striking velocity. In the event that the ballistic limit computed is less than 30 fps above the minimum required and if a gap (high partial penetration velocity below the low complete penetration velocity) of 30 fps or more exists, firing will continue as needed to reduce this gap to 25 fps or less. (This procedure will insure better evaluation of the steel when the ballistic limit is near the minimum required.)

20.7 Thickness, impact area. The thickness of ballistic test plates used for determining ballistic limits shall be that of the area subjected to the ballistic testing.

30. REQUIREMENTS

30.1 Resistance to penetration. The minimum ballistic limits shall be in accordance with the values shown in tables VII, VIII, IX, X or XI as applicable.

30.2 Resistance to cracking. Ballistic test plates when visually examined after testing shall not develop any through-crack greater in length than five calibers of the projectile.

40. TESTS

40.1 Ballistic tests. V_{50} ballistic tests shall be performed in accordance with USATECOM TOP 2-2-170, Ballistic Tests of Armor Materials to determine compliance with the requirements of tables VII through XI.

40.1.1 Plate thickness as measured by the ballistic test agency shall be used to determine the required ballistic limit for the plate. Individual thickness measurements are to be read from a micrometer to the nearest 0.001 inch and the average of these readings reported to the nearest 0.001 inch. At least one measurement shall be taken along each edge of the plate at a distance of at least one inch from the edge, but preferably in the area which will be impacted. The average of the measurements to the nearest 0.001 inch will be used to determine the minimum ballistic limit requirements in the appropriate tables (tables VII through XI). The required ballistic limit will be determined by interpolation, if necessary, in the tables in the appendix.

40.1.2 Rejection and retest of ballistic plates.

40.1.2.1 First article tests (rejection). Unless noted otherwise in the contract or order, failure of either of the first article test plates to meet the minimum ballistic requirements as specified in the appendix to this specification indicates failure of the product and process.

40.1.2.2 First article (retests). Resubmission of ballistic retest plates shall not be made until the manufacturer has made the necessary corrections in the processing of the material to the satisfaction of the procuring activity. Two retest plates must be submitted for first article testing and both must pass.

40.1.2.3 Acceptance tests (rejection). Unless otherwise noted in the contract or order, failure of a test plate to meet the ballistic requirements indicates failure of the lot, however, the final decision will depend on the outcome of retests, if submitted.

40.1.2.4 Acceptance tests (retests). If a test plate representing a lot fails to meet the ballistic requirements, the manufacturer has the following options: Immediately upon notification of the failure, he may:

(1) At his own expense submit two additional test plates from the same lot for ballistic retest, or

(2) He may first re-heat-treat (quenching and tempering) the lot and then submit a test plate from the re-treated lot, or

(3) He may scrap the lot and submit a plate representing a new lot for acceptance.

If he chooses any one of these options and the ballistic retest plate (or plates) meet the requirements, then the lot represented is acceptable. If he chooses option (1) and one or both of the retest plates fail, the manufacturer may re-heat-treat the lot and submit a test plate from the retreated lot. If this plate fails, the lot is rejected. If he chooses option (3) and the test plate fails, he may again resort to any one of the three options. The manufacturer shall report the processing used on the failed plates.

40.1.3 Disposition of ballistic test plates.

40.1.3.1 First article test plates. Upon request of the applicant within 15 days after ballistic testing, first article plates will be returned "as is" to the applicant, at his expense, unless the plates were destroyed in testing.

40.1.3.2 Acceptance test plates. Acceptance test plates that comply with the requirements of this specification are considered as part of the lot of steel they represent and ownership of them passes to the Government with the acceptance of that lot. Acceptance test plates that fail to comply with the requirements of this specification are considered as part of the lot they represent and remain the property of the producer just as the rejectable lot does. The failed plates will be returned, upon request, as in 40.1.3.1.

TABLE VII. Minimum required ballistic limits - Caliber .30
AP M2 Projectile at 30 degrees Obliquity.

Thickness inches	Required BL(P) FPS	Thickness inches	Required BL(P) FPS	Thickness inches	Required BL(P) FPS
0.100	994	0.185	1799	0.265	2328
0.105	1057	0.190	1836	0.270	2357
0.110	1116	0.195	1872	0.275	2386
0.115	1172	0.200	1908	0.280	2415
0.120	1226	0.205	1943	0.285	2443
<u>1/</u> 0.125	1279	0.210	1978	0.290	2471
0.130	1329	0.215	2012	0.295	2499
0.135	1378	0.220	2046	0.300	2526
0.140	1425	0.225	2079	0.305	2554
0.145	1471	0.230	2111	0.310	2581
0.150	1515	0.235	2144	<u>2/</u> 0.315	2607
0.155	1558	0.240	2175	0.320	2634
0.160	1601	0.245	2207	0.325	2660
0.165	1642	0.250	2237	0.330	2686
0.170	1682	0.255	2268	0.335	2711
0.175	1722	0.260	2298	0.340	2737
0.180	1761				

1/ Specification requirements begin for this ordered thickness.

2/ Specification requirements end for this ordered thickness.

Note: Numbers above and below upper and lower limits are requirements for within the tolerance limits.

TABLE VIII. Minimum required ballistic limits - Caliber .50
AP M2 Projectile at 30 degrees Obliquity.

Thickness inches	Required BL(P) FPS	Thickness inches	Required BL(P) FPS	Thickness inches	Required BL(P) FPS
0.290	1783	0.400	2151	0.515	2481
0.295	1801	0.405	2166	0.520	2494
0.300	1820	0.410	2182	0.525	2508
0.305	1837	0.415	2197	0.530	2521
0.310	1855	0.420	2212	0.535	2534
0.315	1873	0.425	2227	0.540	2547
<u>1/</u> 0.316	1876	0.430	2242	0.545	2560
0.320	1890	0.435	2256	0.550	2573
0.325	1907	0.440	2271	0.555	2586
0.330	1925	0.445	2286	0.560	2599
0.335	1942	0.450	2300	0.565	2612
0.340	1958	0.455	2314	0.570	2625
0.345	1975	0.460	2329	0.575	2638
0.350	1992	0.465	2343	0.580	2650
0.355	2008	0.470	2357	0.585	2663
0.360	2025	0.475	2371	<u>2/</u> 0.590	2675
0.365	2041	0.480	2385	0.595	2688
0.370	2057	0.485	2399	0.600	2700
0.375	2073	0.490	2413	0.605	2713
0.380	2089	0.495	2427	0.610	2725
0.385	2104	0.500	2440	0.615	2737
0.390 -	2120	0.505	2454	0.620	2750
0.395	2136	0.510	2468	0.625	2762

1/ Specification requirements begin for this ordered thickness.

2/ Specification requirements end for this ordered thickness.

Note: Numbers above and below upper and lower limits are requirements for within the tolerance limits.

TABLE IX. Minimum required ballistic limits - 14.5 mm
API B 32 Projectile at 30 degrees Obliquity.

Thickness inches	Required BL(P) FPS	Thickness inches	Required BL(P) FPS	Thickness inches	Required BL(P) FPS
0.575	2320	0.645	2469	0.720	2621
0.580	2331	0.650	2480	0.725	2630
0.585	2342	0.655	2490	0.730	2640
0.590	2353	0.660	2500	0.735	2650
<u>1/</u> 0.591	2355	0.665	2511	0.740	2659
0.595	2364	0.670	2521	0.745	2669
0.600	2374	0.675	2531	0.750	2679
0.605	2385	0.680	2541	0.755	2688
0.610	2396	0.685	2551	0.760	2698
0.615	2407	0.690	2561	<u>2/</u> 0.765	2707
0.620	2417	0.695	2571	0.770	2717
0.625	2428	0.700	2581	0.775	2726
0.630	2438	0.705	2591	0.780	2736
0.635	2449	0.710	2601	0.785	2745
0.640	2459	0.715	2611	0.790	2754

1/ Specification requirements begin for this ordered thickness.

2/ Specification requirements end for this ordered thickness.

Note: Numbers above and below upper and lower limits are requirements for
within the tolerance limits.

TABLE X. Minimum required ballistic limits - 14.5 mm
API BS41 Projectile at 30 degrees Obliquity.

Thickness inches	Required BL(P) FPS	Thickness inches	Required BL(P) FPS	Thickness inches	Required BL(P) FPS
0.740	2212	0.855	2505	0.975	2779
0.745	2225	0.860	2517	0.980	2790
0.750	2239	0.865	2529	0.985	2800
0.755	2252	0.870	2540	0.990	2811
0.760	2265	0.875	2552	0.995	2822
0.765	2278	0.880	2564	1.000	2822
<u>1/</u> 0.766	2281	0.885	2576	1.005	2843
0.770	2292	0.890	2588	1.010	2854
0.775	2305	0.895	2599	1.015	2865
0.780	2318	0.900	2611	1.020	2875
0.785	2331	0.905	2622	1.025	2886
0.790	2343	0.910	2634	1.030	2896
0.795	2356	0.915	2645	1.035	2907
0.800	2369	0.920	2657	1.040	2917
0.805	2382	0.925	2668	1.045	2927
0.810	2394	0.930	2679	1.050	2938
0.815	2407	0.935	2690	1.055	2948
0.820	2419	0.940	2702	1.060	2958
0.825	2431	0.945	2713	<u>2/</u> 1.065	2968
0.830	2444	0.950	2724	1.070	2979
0.835	2456	0.955	2735	1.075	2989
0.840	2468	0.960	2746	1.080	2999
0.845	2481	0.965	2757	1.085	3009
0.850	2493	0.970	2768	1.090	3019

1/ Specification requirements begin for this ordered thickness.2/ Specification requirements end for this ordered thickness.

Note: Numbers above and below upper and lower limits are requirements for within the tolerance limits.

TABLE XI. Minimum required ballistic limits - 20 mm
API-T, M502 Projectile at 0 degrees Obliquity.

Thickness inches	Required BL(P) FPS	Thickness inches	Required BL(P) FPS	Thickness inches	Required BL(P) FPS
1.020	1758	1.215	2088	1.415	2382
1.025	1767	1.220	2096	1.420	2389
1.030	1776	1.225	2104	1.425	2396
1.035	1785	1.230	2112	1.430	2402
1.040	1794	1.235	2120	1.435	2409
1.045	1804	1.240	2127	1.440	2416
1.050	1813	1.245	2135	1.445	2423
1.055	1821	1.250	2143	1.450	2430
1.060	1830	1.255	2150	1.455	2436
1.065	1839	1.260	2158	1.460	2443
<u>1</u> / 1.066	1841	1.265	2165	1.465	2450
1.070	1848	1.270	2173	1.470	2457
1.075	1857	1.275	2180	1.475	2463
1.080	1866	1.280	2188	1.480	2470
1.085	1874	1.285	2195	1.485	2477
1.090	1883	1.290	2203	1.490	2483
1.095	1892	1.295	2210	1.495	2490
1.100	1900	1.300	2218	1.500	2496
1.105	1909	1.305	2225	1.505	2503
1.110	1917	1.310	2232	1.510	2510
1.115	1926	1.315	2240	1.515	2516
1.120	1934	1.320	2247	1.520	2523
1.125	1943	1.325	2254	1.525	2529
1.130	1951	1.330	2262	1.530	2536
1.135	1959	1.335	2269	1.535	2542
1.140	1968	1.340	2276	1.540	2549
1.145	1976	1.345	2283	1.545	2555
1.150	1984	1.350	2290	1.550	2561
1.155	1992	1.355	2298	1.555	2568
1.160	2001	1.360	2305	1.560	2574
1.165	2009	1.365	2312	1.565	2581
1.170	2017	1.370	2319	1.570	2587
1.175	2025	1.375	2326	1.575	2593
1.180	2033	1.380	2333	1.580	2600
1.185	2041	1.385	2340	1.585	2606
1.190	2049	1.390	2347	1.590	2612
1.195	2057	1.395	2354	1.595	2619
1.200	2065	1.400	2361	1.600	2625
1.205	2073	1.405	2368	1.605	2631
1.210	2081	1.410	2375	1.610	2637

TABLE XI. Minimum required ballistic limits - 20 mm
API-T, M602 Projectile at 0 degrees Obliquity. (Continued)

Thickness inches	Required BL(P) FPS	Thickness inches	Required BL(P) FPS	Thickness inches	Required BL(P) FPS
1.615	2644	1.805	2871	1.995	3082
1.620	2650	1.810	2877	2.000	3088
1.625	2656	1.815	2883	2.005	3093
1.630	2662	1.820	2888	2.010	3098
1.635	2669	1.825	2894	2.015	3104
1.640	2675	1.830	2900	2.020	3109
1.645	2681	1.835	2905	2.025	3114
1.650	2687	1.840	2911	2.030	3120
1.655	2693	1.845	2917	2.035	3125
1.660	2699	1.850	2922	2.040	3130
1.665	2705	1.855	2928	2.045	3135
1.670	2711	1.860	2934	2.050	3141
1.675	2718	1.865	2939	2.055	3146
1.680	2724	1.870	2945	2.060	3151
1.685	2730	1.875	2951	2.065	3156
1.690	2736	1.880	2956	2.070	3162
1.695	2742	1.885	2962	2.075	3167
1.700	2748	1.890	2967	2.080	3172
1.705	2754	1.895	2973	2.085	3177
1.710	2760	1.900	2978	2.090	3183
1.715	2766	1.905	2984	2.095	3188
1.720	2772	1.910	2990	2/ 2.100	3193
1.725	2778	1.915	2995	2.105	3198
1.730	2784	1.920	3001	2.110	3203
1.735	2789	1.925	3006	2.115	3208
1.740	2795	1.930	3012	2.120	3214
1.745	2801	1.935	3017	2.125	3219
1.750	2807	1.940	3023	2.130	3224
1.755	2813	1.945	3028	2.135	3229
1.760	2819	1.950	3033	2.140	3234
1.765	2825	1.955	3039	2.145	3239
1.770	2831	1.960	3044	2.150	3244
1.775	2836	1.965	3050	2.155	3250
1.780	2842	1.970	3055	2.160	3255
1.785	2848	1.975	3061	2.165	3260
1.790	2854	1.980	3066	2.170	3265
1.795	2860	1.985	3071	2.175	3270
1.800	2865	1.990	3077		

1/ Specification requirements begin for this ordered thickness.

2/ Specification requirements end for this ordered thickness.

Note: Tabulated values on either side of the specification requirements are for interpolation of BL(P) requirements on undersize or oversize plates.

GAYLORD S



DUDLEY KNOX LIBRARY



3 2768 00036268 5